THE HONG KONG
POLYTECHNIC UNIVERSITY
香港理工大學
Pao Yue-kong Library
包玉剛圖書館

Copyright Undertaking

This thesis is protected by copyright, with all rights reserved.

By reading and using the thesis, the reader understands and agrees to the following terms:

1. The reader will abide by the rules and legal ordinances governing copyright regarding the use of the thesis.
2. The reader will use the thesis for the purpose of research or private study only and not for distribution or further reproduction or any other purpose.
3. The reader agrees to indemnify and hold the University harmless from and against any loss, damage, cost, liability or expenses arising from copyright infringement or unauthorized usage.

IMPORTANT

If you have reasons to believe that any materials in this thesis are deemed not suitable to be distributed in this form, or a copyright owner having difficulty with the material being included in our database, please contact lbsys@polyu.edu.hk providing details. The Library will look into your claim and consider taking remedial action upon receipt of the written requests.

Pao Yue-kong Library, The Hong Kong Polytechnic University, Hung Hom, Kowloon, Hong Kong

http://www.lib.polyu.edu.hk

This thesis in electronic version is provided to the Library by the author. In the case where its contents is different from the printed version, the printed version shall prevail.

High-intensity ultrasound for extraction and controlled degradation of high molecular weight polysaccharides from medicinal mushrooms: process characteristics and product properties

CHEUNG YI CHING

Ph.D.

The Hong Kong Polytechnic University

2014

THE HONG KONG
POLYTECHNIC UNIVERSITY
香港理工大學

Department of Applied Biology & Chemical Technology

High-intensity ultrasound for extraction and controlled degradation of high molecular weight polysaccharides from medicinal mushrooms: process characteristics and product properties

CHEUNG YI CHING

A thesis submitted in partial fulfillment of the requirements
for the degree of Doctor Philosophy

August, 2013

CERTIFICATE OF ORIGINALITY

I hereby declare that this thesis is my own work and that, to the best of my knowledge and belief, it reproduces no material previously published or written, nor material that has been accepted for the award of any other degree or diploma, except where due acknowledgement has been made in the text.

Cheung Yi Ching

30th August 2013

Abstract

Polysaccharides (PS) and polysaccharide-protein complexes (PSPs) from edible/medicinal fungi or mushrooms have attracted increasing research and commercial interests for nutraceutical and pharmaceutical uses. The aim of this research project is at a comprehensive study on the application of an innovative food processing technique, high-power ultrasound (US), for the processing and modification of bioactive polysaccharides from several important medicinal fungi. Ultrasound-assisted extraction (UAE) has been widely evaluated as a more favourable and efficient process than the traditional hot water extraction (HWE) for isolation and recovery of food and medicinal products. On the other hand, high power ultrasound (US) is an interesting mechanical means for partial and controlled degradation of high molecular weight (MW) polysaccharides to improve the solution properties for desirable clinical applications.

UAE was evaluated in comparison with HWE in several important edible/medicinal fungi in mushroom fruit body and mycelial form, including *Cordyceps sinensis* (Chinese caterpillar fungus Dong Chong Xia Cao), *Grifola frondosa* (Maitake), *Coriolus versicolor* (Yunzhi) and *Lentinus edodes* (Shiitake), and *Ganoderma lucidum* (Linzhi) for extraction of water soluble products and isolation of PSPs. Compared with those by HWE, the yield of PSP

by UAE was similar on *G. frondosa*, notably higher on *L. edodes* and lower on *C. versicolor*, and the extraction rate of UAE was notably higher with *G. frondosa* and *L. edodes* but much lower with *C. versicolor*. The PSPs from all three mushrooms by UAE (1) had higher protein but lower carbohydrate contents (2) exhibited an overall shift to lower MW (3) contained distinct protein bands between 10-130 kDa on SDS-PAGE than those by HWE. This suggested that UAE at low temperature can retain the protein constituents, avoiding the denaturation by HWE. The antioxidant activities of PSPs from the three mushrooms by UAE were generally higher than those by HWE.

Further study was performed on the kinetics and process parameters for UAE of water-soluble components and PS from these fungal materials. At a fixed power and a temperature below 50℃, the experimental data were fitted to several kinetic models by linear regression. More detailed kinetic study was performed on UAE of the *Cordyceps sinensis* Cs-HK1 fungal mycelium with four process variables (factors) at different levels, ultrasound intensity (2.44 - 44.1 W/cm^2), temperature (40-70 ^{o}C), solid particle size (156.5-750 μm), and solid-to-liquid ratio (1/30-1/70 g/mL). The experimental data of yields versus time in most cases were fitted closely to two empirical kinetic models for solid-liquid extraction, parabolic diffusion equation ($y = y_o + y_1 t^{1/2}$) and power law ($y = \beta t^n$) with high correlation coefficients (R^2) of 0.95-0.99 for total extract yield, and 0.90-0.96 for PS yield. Reducing the particle size and increasing the extraction temperature led to a higher yield and extraction rate;

increasing the solid-to-liquid ratio (or decreasing the liquid volume) increased the PS yield and extraction rate but had little influence on the total extract. Significant correlations were found between extraction rate (*dy/dt*) and ultrasound power density (*P/V*), and between extract yield (*y*) and energy density (*Pt/V*).

High-intensity ultrasound (20 kHz) was applied to the degradation of a high-MW PS extracted from *C. sinensis* Cs-HK1. With US applied at selected power intensities (10-50 W/cm^2), the intrinsic viscosity (correlated to the MW) of the polysaccharide decreased rapidly in the initial period (~10 min) and attained steady level gradually. The degradation rate was increased with US power and PS initial MW. The US treatment also shifted the particle size distribution of the PS in aqueous solution from large to small particle size range (40-50 nm). Transmission electron microscopy (TEM) of the PS particles suggested that US at a relatively low intensity (e.g. 10.6 W/cm^2) was mainly effective to disperse the polysaccharide aggregates, and US at a high intensity (e.g. 48.4 W/cm^2) caused the change in the particle morphology from globular to longitudinal shape. From the study on a PS of known-structure, curdlan from *Alcaligenes faecalis*, the degradation kinetics by US was established. The US of degradation of studied for curdlan in 0.1M and 0.3M NaOH, which molecules were in triple-helix and random coil conformation, respectively. Degradation rate constant *k* (mol/g·min) was determined based on the kinetic model: $\frac{1}{M_t} - \frac{1}{M_0} = kt$ (with R^2 values > 0.91). The value of *k* in 0.3M was higher than that for in 0.1M, which suggested that

the random coil conformation of curdlan molecules in 0.3M NaOH was more liable to to degradation than the rigid rod conformation in 0.1M NaOH. A test was performed to detect the existence of single helix structures in both original and US-degraded curdlan, and the amount of single-helix-structured molecules was increased by US treatment.

High-intensity US was also applied to facilitate the extraction of both intracellular and extracellular PS from the viscous mycelial broth of a medicinal fungus *C. sinensis* Cs-HK1. The results showed that high-intensity US irradiation of the Cs-HK1 mycelial broth caused mycelium fragmentation and fungal cell disintegration, and a dramatic reduction of the apparent broth viscosity and the release of intracellular products into the liquid medium. Statistic experimental design and response surface methodology were applied to evaluate and optimize the major factors affecting the ultrasonic extraction yields of total water soluble product and PS (PS), including time (5-25 min), US intensity (10-30 W/cm^2) and concentration of mycelial broth (0.25-1). The kinetics of total water-soluble product release (yield y versus time t) as a result of mycelium disruption by US at various power intensities was well represented by the Elovich model $y = y_o + y_1 \ln t$ with a high regression coefficient $R^2 \approx 0.99$, while that of PS yield was close fit to the parabolic morel $y = y_o + y_1 t^{1/2}$ ($R^2 > 0.85$). The US treatment also appeared to improve the antioxidant activity of PS recovered from the broth with a stronger cytoprotective effect against H_2O_2 induced cell death.

Overall the results from this project have shown that high power US is an efficient and versatile means for extraction, processing and controlled degradation of bioactive PS from edible/medicinal fungi. The kinetic models and process parameters derived from the project will be useful for design and operation of the ultrasonic processes.

List of publications

Journal Papers

1. Wang, Z.M., **Cheung, Y.C.**, Leung, P.H., Wu, J.Y. (2010) Ultrasonic treatment for improved solution properties of a high-molecular weight exopolysaccharide produced by a medicinal fungus. *Bioresource Technology*, 101, 5517-5522.

2. **Cheung, Y.C.**, Siu, K.C., Liu, Y.S., Wu, J.Y. (2012) Molecular properties and antioxidant activities of polysaccharide–protein complexes from selected mushrooms by ultrasound-assisted extraction. *Process Biochemistry*, 47, 892-895.

3. **Cheung, Y.C.**, Siu, K.C., Liu, Y.S., Wu, J.Y. (2013) Kinetic Models for Ultrasound-Assisted Extraction of Water-Soluble Components and Polysaccharides from Medicinal Fungi. *Food and Bioprocess Technology,* (DOI) 10.1007/s11947-012-0929-z.

4. Huang, Q.L., Siu, K.C., Wang, W.Q., **Cheung, Y.C.**, Wu, J.Y. (2013) Fractionation, characterization and antioxidant activity of exopolysaccharides from fermentation broth of a *Cordyceps sinensis* fungus. *Process Biochemistry*, 48, 380-386.

5. **Cheung, Y.C.**, Wu, J.Y. (2013) Kinetic models and process parameters for ultrasound-assisted extraction of water-soluble components and polysaccharides from a medicinal fungus. *Biochemical Engineering Journal*, 79, 214-220.

Conference presentations and posters (International)

1. **Cheung, Y.C.**, Wu, J.Y.. (2010) Ultrasonic-assisted Extraction of Biopolymers from Medicinal Mushroom: *Grifola frondosa* & *Cordyceps sinensis*. The 6th Hong Kong – Macau Postgraduate Symposium on Chinese Medicine. Hong Kong.

2. **Cheung, Y.C.**, Wu, J.Y.. (2010) Ultrasonic-assisted Extraction of Polysaccharides and Proteins from Medicinal Mushroom *Grifola frondosa* & *Cordyceps sinensis*. The 4th FHH International Symposium of research of herbs and herbal product. Hong Kong.

3. **Cheung, Y.C.**, Wu, J.Y. (2010) Antitumor activities of cultivated *Cordyceps sinensis* Cs-HK1 fungal mycelia. The 4th FHH International Symposium of research of herbs and herbal product. Hong Kong.

4. **Cheung, Y.C.**, Siu, K.C., Wu, J.Y.. (2011) Characteristics and antioxidant activities of polysaccharides extracted by ultrasound from medicinal mushrooms. The 7th International Postgraduate Symposium on Chinese Medicine. Hong Kong.

5. **Cheung, Y.C.**, Siu, K.C., Wu, J.Y.. (2012) Application of empirical models for ultrasound-assisted extraction of water-soluble components from medicinal fungi. The 8th International Postgraduate Symposium on Chinese Medicine. Hong Kong.

6. **Cheung, Y.C.**, Siu, K.C., Wu, J.Y.. (2013) Optimization and kinetic modeling of polysaccharide extraction by ultrasonic disruption of a medicinal fungal mycelia in fermentation broth. 2nd Runner-up of Graduate Student Poster Competition (International Individual Division) of IFT13 Annual Meeting & Food Expo, Chicago, USA.

7. **Cheung, Y.C.**, Siu, K.C., Chen, Xia, Wu, J.Y.. (2013) High-intensity ultrasound for degradation and modification of a high-molecular weight polysaccharide complex isolated from a medicinal fungus. IFT13 Annual Meeting & Food Expo, Chicago, USA

Conference presentations and posters (Local)

1. **Cheung, Y.C.**, Wu, J.Y. (2010) Ultrasonic-assisted Extraction of Biopolymers from Medicinal Mushroom *Grifola frondosa*. The 17th Symposium on Chemistry Postgraduate Research in Hong Kong.

2. **Cheung, Y.C.**, Siu, K.C., Wu, J.Y. (2011) Properties and antioxidant activities of polysaccharides from medicinal mushrooms by ultrasound-assisted extraction. The 18th Symposium on Chemistry Postgraduate Research in Hong Kong.

3. **Cheung, Y.C.**, Siu, K.C., Wu, J.Y. (2012) Kinetic models for ultrasound-assisted extraction of water-soluble components and polysaccharides from medicinal fungi. The 19th Symposium on Chemistry Postgraduate Research in Hong Kong.

4. **Cheung, Y.C.**, Siu, K.C., Chen, X., Wu, J.Y. (2013) Effect of processing factors on the kinetic parameters of ultrasound-assisted extraction of water-soluble components from a medicinal fungus. The 20th Symposium on Chemistry Postgraduate Research in Hong Kong.

Acknowledgements

I would like to thank my chief supervisor, Dr. Jian-yong Wu, for all his guidance, professional advice and encouragement throughout this project as well as his comments on this thesis and all the publications.

Meanwhile I would also like to thank the Department of Applied Biology and Chemical Technology of The Hong Kong Polytechnic University, all the technicians and staff, and my lab mates in Dr. JY Wu's group for their valuable suggestions and technical support in the past 4 years.

I am especially thankful to Prof. Georges M. Halpern for his language help and comments on this thesis.

Last but not least, I am indebted to my family members (particularly my fiancé Mr Wu Kit Ho) for their constant encouragement during the course of this work particularly in the hard times.

Table of Contents

List of figures

List of tables

List of abbreviations and symbols

EPS	Exopolysaccharides
HWE	Hot water extraction
IPS	Intracellular polysaccharides
MW	Molecular weight
PS	Polysaccharides
PSP	Polysaccharide-protein complex
SEM	Scanning electronic microscopy
TEM	Transmitted electron microscopy
UAE	Ultrasound-assisted extraction
US	Ultrasound

Part I

Introduction, Objectives and Literature Review

Chapter 1 Introduction

Mushrooms (edible) are favourite foods in our daily diet, many having tonic effects and medicinal properties. Polysaccharides (PS) are the major bioactive constituents of medicinal mushrooms and useful components of health foods and dietary supplements (Halpern, 2006). Because of their strong antitumor and immumodulatory activities, a number of the purified β-glucans and PS-protein complexes (PSPs) from mushrooms have found clinical applications for immunotherapy and cancer treatment (Wasser, 2010; Halpern, 2013), such as Lentinans from *Lentinus* (*Lentinula) edodes* (Hobbs, 2000; Halpern, 2006), polysaccharide D-fraction and MD-fraction from *Grifola frondosa* (Zhang et al., 2007; Boh & Berovic, 2007), and PSPs from *Coriolus (Trametes) versicolor* (Hobbs, 2000; Cui, 2003). In both commercial processes and research studies, the first and an essential step in the isolation of bioactive natural products and PS from the source plant and microbial materials is extraction (liquid–solid), which can strongly affect the quantity (yield and composition) and quality (bioactivities) of the isolated products. Many of the bioactive PS are water-soluble and isolated from mushroom fruiting bodies or fungal mycelium through hot-water extraction (Zhang et al., 2007; Yang & Zhang, 2009). Hot-water extraction (HWE) is also a common method for the preparation of herbal decoctions in Chinese and other folk medicines and for the isolation of water-soluble bioactive compounds from natural materials. However, a major

concern with the application of HWE to separation of natural products is thermal destruction of temperature-sensitive components such as the protein constituents of PSPs from mushrooms. Another disadvantage of HWE is the low process efficiency because of a slow extraction rate. High power ultrasound (US) and known as or ultrasound-assisted extraction (UAE) is one of the most widely explored processes for more efficient extraction of bioactive products at lower temperatures than those for hot water or hot solvent extraction (Chemat et al., 2008; Glisic et al., 2011). UAE has been reported to improve the extraction of natural products in various sources and organisms (Patist & Bates, 2008). Compared with other extraction processes, UAE has potential advantages like the simple and convenient processing equipment, the low-temperature and hazard-free operation and a high process efficiency. Several recent researchers studied UAE of PS from medicinal plants and fungi or mushrooms were mostly about the low molecular weight compounds and few recent studies have been focused on the polysaccharides from plants (Ebringerová & Hromádková 2010; Vankar & Srivastava 2010; Xia et al. 2011) and medicinal fungi (Chen et al. 2010), which demonstrated the feasibility and potential advantages of UAE.

Polysaccharides are complex natural products with high-molecular weight (MW) and variable structures, and their structure-activity relationships are more difficult to characterize than small molecules. Many of the high-MW PS have poor solubility, high viscosity and unstable physicochemical properties, which are unfavourable for clinical uses. It is desirable

and imperative to improve the solubility and reduce the viscosity of polysaccharides in water by modification of the polysaccharide molecules. A direct and effective approach is partial depolymerization of the large PS molecules by chemical and enzymatic hydrolysis, and various radiation means of γ-ray, ultraviolet light, microwave and power ultrasound (Vodeničarová et al., 2006). A chief advantage of physical over chemical or biochemical methods of degradation is that few or no chemicals need to be added to the PS solutions and the degraded products are easier to recover and purify. Ultrasonic treatment is regarded as a simpler, safer and more convenient means than other radiation means. In addition to degradation of soluble polymers, the application of power US may also be effective to split and disperse aggregates formed by large polymers (Montalbo-Lomboy et al., 2010; Zhang et al., 2007). Power US has been applied to biomolecules in solution to modify the molecular structures and improve the solution properties (Suslick, 1988; Mason & Lorimer, 2002; Zhao et al., 2009).

The various effects of high power US are mostly attributed to the hydrodynamic activities of acoustic cavitation. Ultrasonic irradiation of a liquid causes oscillation of the liquid elements, leading to alternate regions of compression and rarefaction, and the formation of cavities or micro-bubbles in the rarefaction region under a negative pressure. The bubbles grow to a large size and eventually collapse, generating shock waves and high shear force. For enhancing the extraction, the hydrodynamic forces can cause the disruption

of cell walls and reduce the resistance to the transport of molecules through the solid molecules and into the liquid. (Mason & Lorimer 2002; Chemat et al. 2008). Besides, the strong forces together with the induced high temperature (up to 5000K), pressure (about 1000 atm) and liquid turbulence are also responsible for the ultrasonic effects on the polymer molecules in the system, which includes the covalent bond-breaking process (Mason & Lorimer, 2002; Güzey 2002; Soria & Villamiel, 2010). However, studies on various US processes have been mostly concerned with the ultrasound effects on a specific material (Patist & Bates, 2008; Soria & Villamiel, 2010) and seldom on the effects of material properties on the US processing. Therefore, there is a need to put more research effort to understand the relationship of US effects to the properties of material being processed. Because of the limited supply and high price of natural or wide mushrooms, mycelial fermentation has been widely applied for commercial production of fungal biomass and polysaccharides of medicinal fungi. The mycelial fermentation broths of filamentous fungi containing high-MW exopolysaccharides (EPS) are highly viscous and difficult to be processed by filtration or centrifugation for solid (biomass)-liquid (medium) separation. High-intensity US has also been widely applied to disintegration of live cells and microorganisms for extraction and recovery of intracellular products (Piyasena et al., 2003; Geciova et al., 2002). In addition to product release, US disruption of filamentous fungi (fungal mycelia) can lead to alteration of the mycelial morphology and broth rheology in

liquid fermentation (Kwiatkowska et al., 2011). *Cordyceps sinensis*, generally known as the Chinese caterpillar fungus or Cordyceps in short, is a renowned and precious medicinal fungus in China with a broad range of health effects to human (Halpern, 1999; Li & Tsim, 2004). Because natural Cordyceps is very rare and cannot meet the increasing demand in recent years, mycelial fermentation is increasingly applied for production of Cordyceps components such as polysaccharides. Cs-HK1 is a fungus isolated from a natural *C. sinensis* fruit body in our lab and its mycelial culture has been established and applied to liquid fermentation for production of mycelial biomass and EPS as health food ingredients (Leung et al., 2006; Leung et al., 2009; Yan et al., 2011). We propose to apply power US to disintegrate the mycelia and to lower the broth viscosity.

Chapter 2 Objectives and significance

2.1 Objectives

This research project is aimed to gain a better understanding of the effects and mechanisms of high power ultrasound (US) on extraction and degradation of bioactive polysaccharides (PS), and on the physiochemical properties and bioactivities of PS, and to quantify the process kinetics in relation to the material properties and major process factors. These are attained through the following studies:

1. Examination of the effects of US on the yield, chemical composition, molecular properties and antioxidant activities of PS (and PSPs) isolated from selected edible/medicinal mushroom fruit bodies and fungal mycelia in comparison with water extraction (WE).
2. Evaluation of the suitable kinetic models for ultrasound-assisted extraction (UAE) of water-soluble constituents and PS from the mushrooms and fungal mycelia; and the relationship between UAE kinetics and the major process factors.
3. Investigation of the US effects on the molecular structures and physicochemical properties of the PS in various treatment conditions and US powers.

4. Characterization of US degradation effects on the structures and conformation of high MW PS in different alkaline solutions.
5. Evaluation of the use of high-intensity US to facilitate the extraction and recovery of mycelial biomass and EPS from the viscous mycelial fermentation broth of *Cordyceps sinensis* Cs-HK1 fungus, the US-induced changes in the mycelium morphology, broth rheology, and the kinetics of US-induced release of intracellular products and PS from the mycelia.

2.2 Significance

High-intensity US is regarded as an innovative, versatile and promising means for processing of food and medicinal products. However, US has not been widely applied to extraction or degradation of high MW PS from edible and medicinal fungi. This research project provided new and interesting results on the two major processes and the relationships between the processing efficiency, product quality and the process conditions. These results from this project are most useful for further development, improvement and application of these ultrasonic processes. In particular, the process kinetics and relationships with the processing factors to be established will be useful for optimal design and efficient operation of these processes.

Cordyceps (*Cordyceps sinensis*) is a rare and precious medicinal fungus. Mycelial fermentation has become the most viable process for mass production of fungal biomass and bioactive polysaccharides. Application of power US to the Cs-HK1 mycelial fermentation broth is an innovative and promising strategy for efficient product recovery and processing from fermentation systems of medicinal fungi.

Chapter 3 Literature Review

3.1 Polysaccharides from medicinal mushrooms

Mushroom is defined as a macro-fungus with distinctive fruiting body that can be observed by naked eyes and picked up by hands (Chang & Miles, 1992). In addition to their wide application as a tasty and nutritious food, many mushroom species have proven and notable medicinal properties. Polysaccharides (PS) are recognized as a major class of the mushroom constituents with significant antitumor and immunomodulating activities. The medicinal value of mushrooms have stimulated wide research studies on the isolation process, characterization of structures and various medicinal properties of PS from edible and medicinal mushrooms (Zhang et al., 2007; Yang & Zhang, 2009; Wasser, 2010). In Asian countries, *Cordyceps sinensis* (Dong Chong Xia Cao), *Ganoderma lucidum* (Lingzhi), *Lentinus edodes* (Shiitake), *Coriolus versicolor* (Yunzhi) and *Grifola frondosa* (Maitake) are among the most common and important mushrooms under investigation. Several polysaccharides and polysaccharide-protein conjugates from some of the mushroom species have been applied to clinical cancer therapy (Halpern, 2006; Zhang et al., 2007). Some common polysaccharide extracts from these five mushrooms with their main bioactivities were summarized and shown in Table 3-1. The bioactive polysaccharides are mainly glucans

in linear or branched molecules with backbone composed of either α- or β-linked glucose unit. The exact molecular structure of the polysaccharide is generally identified by standard methods, which include enzyme digestion, methylation analysis and NMR spectroscopy. Based on the molecular parameters and together with the further analysis by x-ray diffraction or atomic force microscopy, the conformation of polysaccharide is confirmed in either random coil or helix structure (Zhang et al., 2007; Yang & Zhang, 2009). In addition to the antitumor activity, mushroom polysaccharides also exhibited other biological activities; include immunomodulation, antioxidant, antiviral, anti-inflammatory, anti-hyperglycemia. It is believed that the bioactivities of polysaccharides are related to the relative structural conformation. Molecular structure with (1→3)-β-linkages as the main chain with (1→6)-β-branch chain is indicated as an significant factor for the polysaccharide to exhibit a notably antitumor activities (Mizuno et al., 1995; Zhang et al., 2007; Halpern, 2013). Besides, (1→3)-β-glucans in triple helical conformation are also identified as an important structural features for the immune-stimulating activities. The representative polysaccharides are schizophyllan (Kashiwagi et al., 1981), lentinan and curdlan (Saito et al., 1990).

Fig. 3-1. Fruit bodies of some common medicinal mushrooms (a) *Coriolus versicolor* (b) *Grifola frondosa* (c) *Lentinus edodes* (d) *Ganoderma lucidum* (e) *Cordyceps sinensis*

Table 3-1. Some common polysaccharides with their main bioactivities from populated mushrooms found in Asia.

Fungi source	Polysaccharide	Main bioactivities	Reference
Grifola frondosa (Fruiting body)	Proteoglycan, Glucan, Galatomannan, Heteroglycan, Grifolan Fucomannogalactan	Immunomodulating, antitumor, antiviral, hepatoprotective	Zhuang et al., 1993; Cun et al., 1994; Zhuang et al., 1994; Mizuno & Zhuang, 1995
Lentinus edodes (Fruiting body, culture broth)	Mannoglucan, Polysaccharide-protein complex, Glucan, Lentinan	Immunomodulating, antitumor, antiviral	Chihara, 1969; Chihara et al., 1970 Mizuno, 1997 Hobbs, 2000
Ganoderma lucidum (Fruiting body, culture broth)	Heteroglycan, Mannoglucan, Glycopeptide	Hyperglycemia, immunomodulating, antitumor, antioxidative, anti-decrepitude	Miyazaki & Nishijima,1981; Mizuno, 1997
Coriolus versicolor (Fruiting body, mycelium, culture broth)	Polysaccharide-peptide /protein complex	Antitumor, immunomodulating	Cui & Chisti, 2003
Cordyceps sinensis (Fruiting body, mycelium, culture broth)	Glucan, heteroglycan	Antitumor, immunomodulating, heperglycemia, antioxidative	Leung et al., 2006 Leung et al., 2009 Yan et al., 2011

3.2 Ultrasound physics

3.2.1 Acoustic cavitation

Sound is a form of energy transmitted in waves. In human, certain ranges of waves can be heard and that range is called audible frequency which ranges from 20 Hz to 20 kHz. Ultrasound refers to the frequency region beyond audible frequency. Therefore frequencies used for sonochemistry are in the range of kHz. The range beyond 20 kHz to megahertz is regarded as ultrasound (Fig. 3-2).

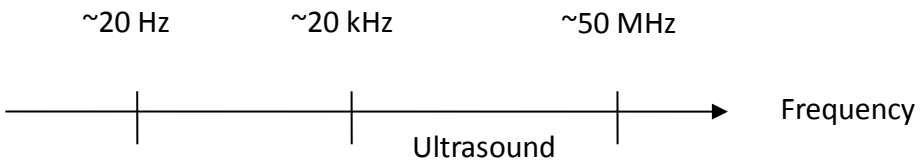

Fig. 3-2. Frequency spectrum of ultrasound.

The ultrasound working principle originated from cavitation. As shown in Fig. 3-3, when high-intensity US waves are propagated in a liquid, microbubbles are formed at the point where the US power is high enough so that the rarefaction cycle of ultrasound wave exceeds the attractive forces of the liquid molecules. The bubbles grow in size by cycles and eventually collapse when they have reached an unstable large size. Shear forces with strong

energy are induced from such rapid bubbles implosion to release energy for chemical and mechanical effect. Such strong forces together with the induced high temperature (up to 5000K), pressure (about 1000 atm) and liquid turbulence are responsible for the ultrasonic effects on the chemical molecules in the system, such as covalent bond-breaking process (Mason & Lorimer, 2002; Güzey 2002; Soria & Villamiel, 2010).

The various ultrasonic effects mainly depend on the extent of cavitation, which depends on US frequency, sample concentration, temperature of treatment, solvent nature, energy (kWh/L), intensity (W/cm^2) and even sonication density (W/cm^3) (Patist & Bates, 2008; Soria & Villamiel, 2010).

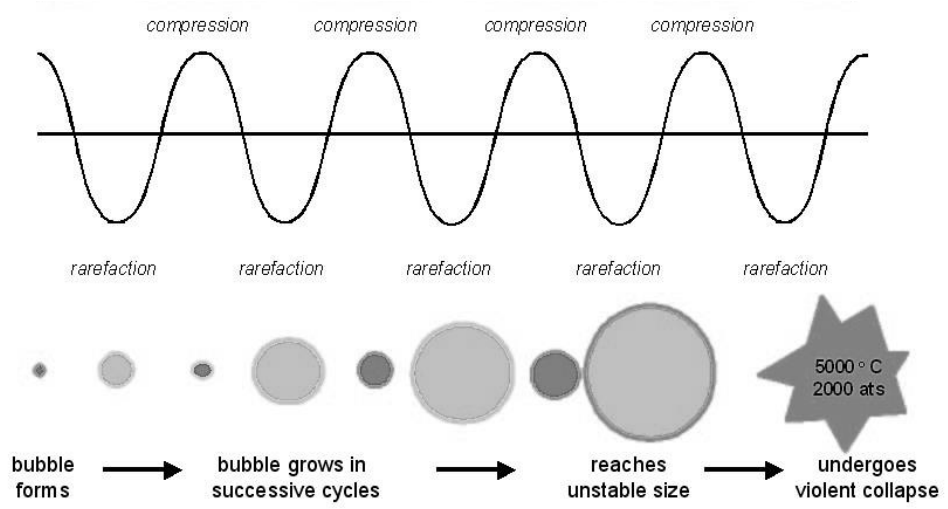

Fig. 3-3. Schematic diagram for acoustic caviation (Mason & Peters, 2002).

3.2.2 Parameters affecting sonochemistry

When applied frequency increases in the sonication process, the rarefaction phase is

shortened and hence the cavitation energy is less. To maintain the same cavitation energy, amplitude needs to increase. Sample concentration affects viscosity. The viscosity can be regarded as the resistance of shear and it hinders the cavitation process. Therefore it is more difficult to produce microbubbles in a viscous liquid. Although a higher temperature can lead to easier cavitation, violence of bubble collapse is reduced and results in lower cavitation energy. Power intensity is directly proportional to the square of applied amplitude. Therefore, in general, an increase in intensity leads to an enhancement of sonochemical effects.

3.2.3 Homogeneous and heterogeneous liquid-phase reactions

Sonochemistry can be applied to different types of reactions. Homogeneous reaction is the most common one. The chemical and mechanical effects of cavitation can be described in three regions: reactions inside the bubble, reactions at/near the bubble-liquid interface and reactions in the liquid immediately surrounding the bubble (Fig. 3-3). Each bubble is a representation of energy. For a chemical to experience the energy during bubble collapse, it must carry a high energy enough so that can enter inside the bubble. During the sonication in water, OH and H radicals are produced and eventually form H_2O_2. Radicals are produced within bubble, migrate to the interface and undergo reactions in the bulk medium. There is a large shear force produced during the bubbles collapse. This force is capable to break the chemical bonding in some materials, like polymers, and this breaking of polymer is known as

polymer degradation (Suslick, 1988; Mason & Peters, 2002).

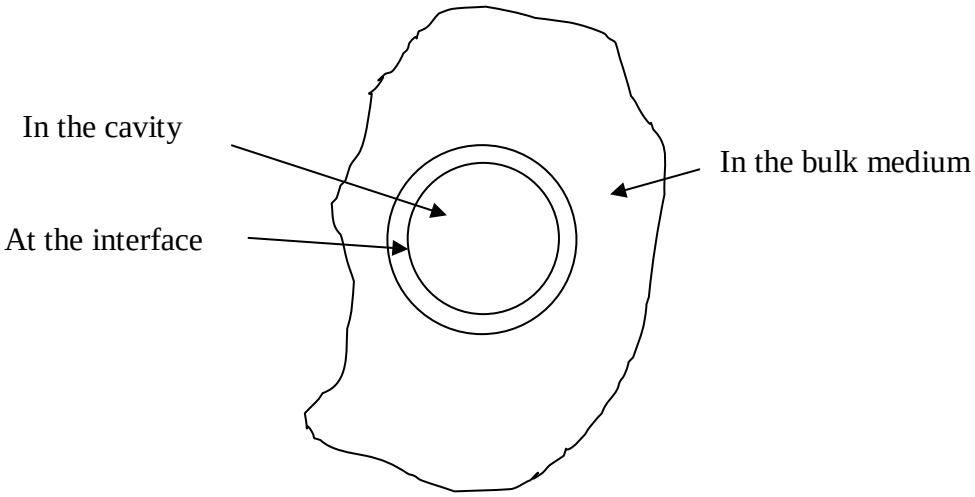

Fig. 3-4. Cavitation bubble collapse in a homogeneous medium (Mason, 1999).

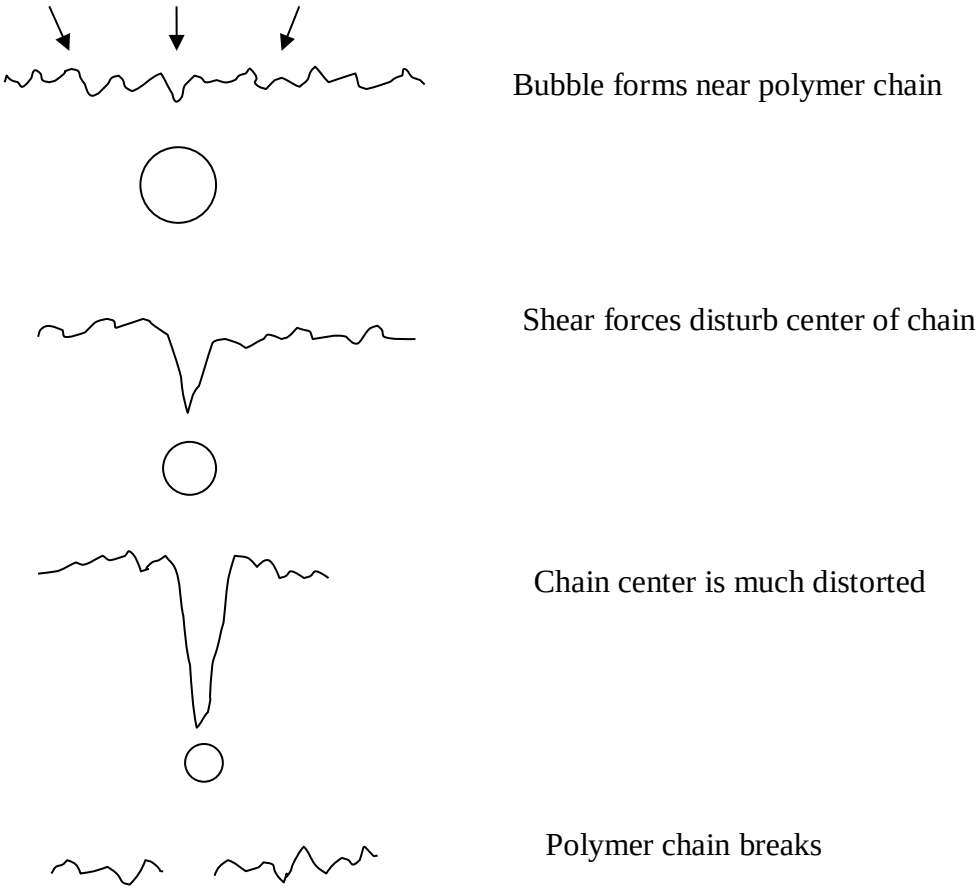

Fig. 3-5. Mechanical degradation of polymer (Mason, 1999).

Powders suspended in a liquid would be significantly affected by cavitation. Irregular surface could favor cavitation bubble formation on the surface and make the surface collapse. Thus shock waves at collapsed surface could break the particle apart. Cavitation bubble collapse in the liquid phase near the suspended particle can force it to mobilize. Particle mobilization leads to interparticle collisions and causes erosion, surface cleaning, wetting of the particles and particle size reduction (Mason & Peters, 2002).

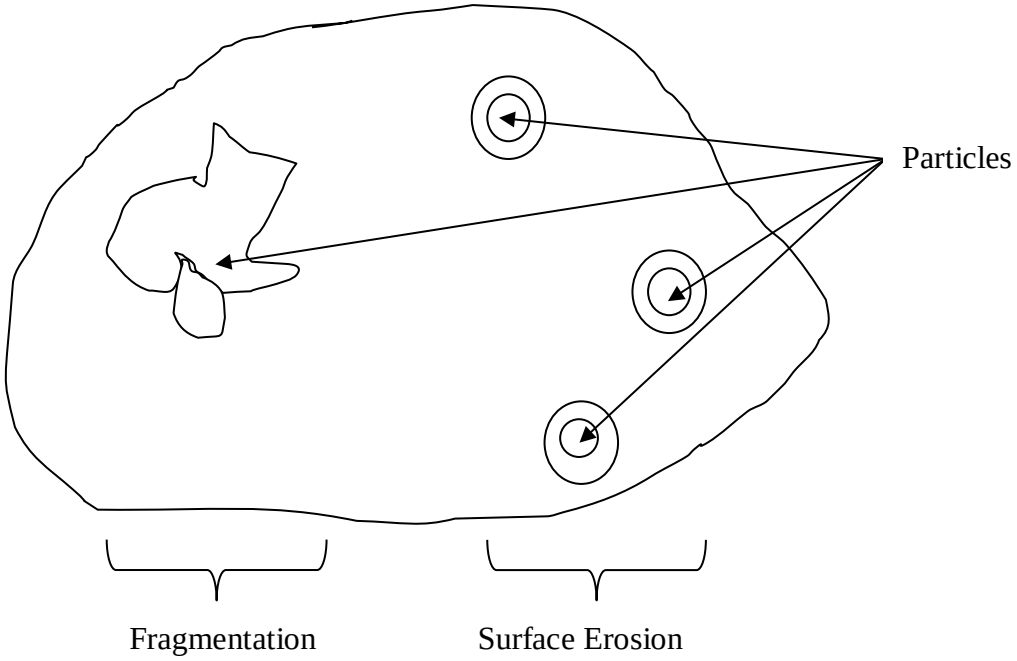

Fig. 3-6. Acoustic cavitation in suspended powder.

3.2.4 Ultrasonic system

The most common ultrasonic irradiation source in the laboratory is the ultrasonic bath for cleaning. Due to its convenience, previous research of sonochemistry was mainly based

on the use of the bath. The results of experiments and performance of the bath were sometimes disappointing and unpredictable. The advantages for using ultrasonic bath are cost (it is inexpensive), convenience, evenly acoustic field distribution and no need of special apparatus for reaction mixture. The disadvantages are low acoustic power density, energy input assessment before experiment, non-specified frequency used, poor temperature control and non-controllable amplitude output (Ebringerova & Hromadkova, 2010; Kwiatkowska et al., 2011).

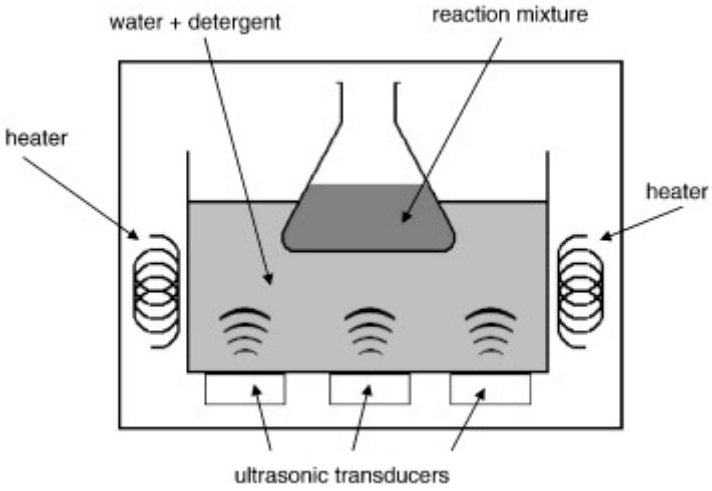

Fig. 3-7. Ultrasonic bath setup (Kwiatkowska et al., 2011).

Due to the low power and absence of absence of energy control, ultrasonic probes have been developed for sonochemistry. In a probe system, it is possible to delivery 100 times more energy than in a bath system. Compared with the ultrasonic bath, the ultrasonic probe system has the following advantages: precise power and energy output delivered to reaction mixture, and frequency regulation. These advantages increase the reproducibility of results.

But some drawbacks remain: energy dissipation by overtones production from the fundamental frequency, difficulties in temperature control, a non-uniform acoustic filed production, and tip erosion. Despite these drawbacks, the ultrasonic probe system is still the best choice for sonochemistry in laboratory scale. For the food industry, a combination of ultrasonic probing and bathing is recommended for higher extraction efficiency (Chemat et al., 2008; Ebringerova & Hromadkova, 2010).

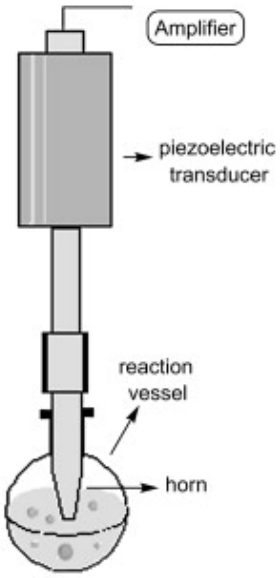

Fig. 3-8. Ultrasonic probe setup (Cellaa & Stefani, 2009).

3.3 Ultrasound-assisted extraction (UAE)

Extraction (solid–liquid) is the first key step for isolating natural products from plant and microbial materials. Solid-liquid extraction or leaching involves the contact of a liquid solvent with the solid through which the solute is transferred from the solid into the liquid through a series of steps (Aguilera and Stanley, 1999; Chemat et al., 2008). The mass transfer involves in the solid-liquid extraction process is stated in Fig. 3-8. The solvent first enters the solid matrix through its microstructure by internal diffusion. The targeted solute molecules are then dissolved in the solvent and being transferred to the exterior of the solid matrix by internal diffusion. During this process, the solvent may cause a breakdown of components in the solute which is generally called degradation. The extracted solute molecules will then migrate through the capillary pores on the external surface of the solid matrix into the bulk solution. Finally the solute is obtained by another separation process from the extract solution. The rate of extraction can be expressed as the mass of solute to be leached per unit of time, or the decrease of solute in the solid per unit of time (*dc/dt*). The extraction rate of each step may be different from each other, and the overall extraction rate is controlled by the slowest step, which is called the rate-determining step. Diffusion through the solid matrix should be the rate-determining step (Aguilera and Stanley, 1999; Bucić-Kojić et al., 2007). The microstructure of food solids plays an important role in the rate and quality of the extraction

process. Therefore it is necessary to clearly understand the relationship between the food microstructure and the extraction rate of the mass transfer process.

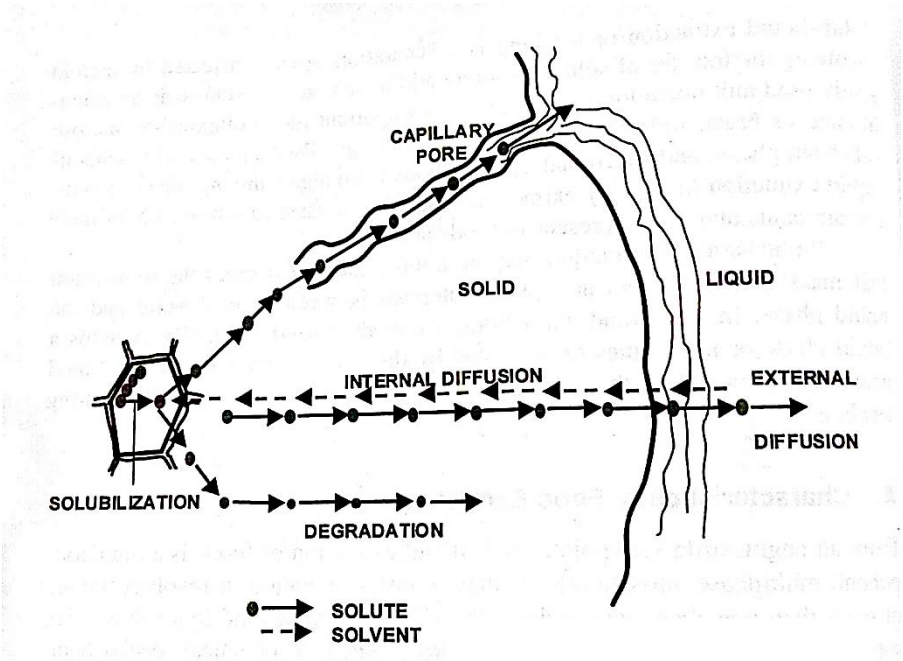

Fig. 3-9. Schematic diagram showing the key steps of the solvent extraction for solute through solid food particles (Aguilera and Stanley, 1999).

UAE can be defined as the application of power or high-intensity US to accelerate the extraction of a solid material in a liquid solvent. Ultrasonic enhancement of the solid–liquid extraction is mainly attributed to the hydrodynamic activities of acoustic cavitation. The hydrodynamic forces generated from cavitation can cause the disruption of cell walls and reduce the resistance to the transport of molecules through the solid particles and into the liquid, enhancing the extraction (Mason and Lorimer, 2002; Chemat et al., 2008). The extraction yield and efficiency of UAE result in much higher values than that of ordinary hot

water extraction. UAE is therefore highly recommended for industrial applications of mushroom extractions.

3.4 Ultrasonic degradation of polymers

Although the actual mechanism of ultrasonic degradation is still under investigation, it is believed that the effects of the ultrasonic degradation on the properties of polymers are related to a set of factors. Among the factors, the ultrasonic irradiation time and power, initial solution concentration and initial solution pH are the most common ones as it is believed that the ultrasonic degradation is mainly affected by these four factors (Mason & Lorimer, 2002).

Average molecular weight of a polymer depends on the chain length of the polymer. Viscosity of a polymer is related to the polymer chain length by the Flory-Fox equation (Nevell & Zeronian, 1985). Besides, viscosity is related to concentration of polymer solution. It was stated that, above a specific concentration, the dependence of viscosity on concentration was increased. The specific concentration was likely to be dependent on the intrinsic viscosity. Intrinsic viscosity can be found out according to the y-intercept of the Huggins plot from the Huggins equation (Carraher, 2003),

$$\frac{\eta_{sp}}{c} = [\eta] + k_1[\eta]^2 c \qquad \text{(Eq. 3-1)}$$

where $[\eta]$ is intrinsic viscosity η_{sp} is specific viscosity, k_1 is Huggins constant and c is concentration of solution. The specific viscosities of the polymer solution can be obtained by

using an Ubbelohde viscometer as shown in Fig. 3-9 at constant temperature, according to Carraher (2003), $\eta_{sp} = \frac{t - t_s}{t_s}$ where t is time of efflux of sample solution in second and t_s is time of efflux of solvent in second. The time of the efflux was measured from point **a** to point **b** (Fig. 3-9). After intrinsic viscosity was found, the viscosity-average molecular weight was found according to the Mark-Houwink equation (Carraher, 2003),

$$[\eta] = K\overline{M}^{\alpha} \qquad \text{(Eq. 3-2)}$$

where $[\eta]$ in L/g, K (in L/g) and α are constants for a system, and $\overline{M}$ is the viscosity-average molecular weight. As a result, in the studies of ultrasonic degradation, either viscosity (intrinsic or dynamic) or average molecular weight is, or both of them are, used as the analysis index of the ultrasonic effects (Zhou & Ma, 2006; Gronroos et al., 2008; Taghizadeh & Asadpour, 2009).

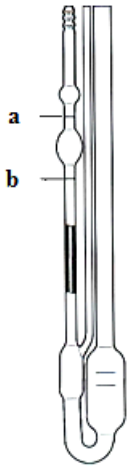

Fig. 3-10. Ubbelohde viscometer for intrinsic viscosity measurement.

The viscosity and average molecular weight of polymers were decreased with increasing ultrasonic irradiation time, and eventually reached a limiting value. The limiting values depended on the polymer samples and some sonication factors, like the irradiation power (Mason & Lorimer, 2002; Zhou & Ma, 2006; Gronroos et al., 2008; Taghizadeh & Asadpour, 2009). The effect of ultrasonic degradation was proved to be affected by the initial solution concentration (Mason & Lorimer, 2002; Gronroos et al., 2008; Taghizadeh & Asadpour, 2009). It was found that the ultrasonic degradation efficiency decreased with initial solution concentration. The limiting values of the viscosity and average molecular weight of the polymer sample were also increased (Mason & Lorimer, 2002; Taghizadeh & Asadpour, 2009). On the other hand, some have suggested that, instead of having a trend, there was an optimum initial solution concentration that gave the optimum efficiency of the ultrasonic degradation. The optimum concentration depended on the polymer sample (Mason & Lorimer, 2002). The study done by Machova et al. (1999) on a carboxymethylated chitin-glucan complex proved that the polymer sample followed a decreasing trend of the ultrasonic degradation efficiency when the initial concentration of sample increased (Machova et al., 1999). On the other hand, the study done by Gronroos et al. (2008) on carboxymethylcellulose showed that there was an optimum concentration. Zhou & Ma (2006) stated that the ultrasonic degradation efficiency was enhanced at lower initial solution pH. The limiting intrinsic viscosity of the degraded polymer sample was lower in the case of

lower initial solution pH.

The kinetics of ultrasonic degradation of polymers usually follows a first order model (Mason & Lorimer, 2002). The average molecular weight of the polymer was decreased sharply during the initial period of ultrasonic treatment. The rate of degradation was slowed upon an increase in the irradiation time and finally came to a constant, obtaining the limiting average molecular weight. The idea was also stated by Akyuz et al. (2008), and experimentally proven by Taghizadeh & Asadpour (2009) and Daraboina & Madras (2009). Daraboina & Madras (2009) also proved that the rate constant of ultrasonic degradation was increased with an increase in ultrasonic irradiation intensity and solvent viscosity. Besides, Taghizadeh & T. Asadpour (2009) experimentally proved that the ultrasonic degradation reaction constant was decreased with an increase in the initial solution concentration. The effect of initial solution pH on the reaction rate constant of ultrasonic degradation was not commonly studied.

3.5 Ultrasound in bioprocess

US has been applied to enhance the subsequent activities of the intracellular contents extracted from natural materials. Flosdorf & Chambers (1933) found that egg albumin was almost instantly coagulated at 30 °C when investigating the bactericidal action of audible sound. They further extended their work to report on the decreased antigenic activity and altered specificity of egg albumin coagulum after sonic radiation (Flosdorf & Chambers, 1935). Since that ultrasound was started to be used in different bioprocesses. Most previous studies on US disruption of microbial cells were dealing with bacteria and yeast cells with few on filamentous fungi, and not any on intracellular products and PSPs from mycelia broth of medicinal fungi.

3.5.1 Effects of US on enzymatic processes

US has the potential to influence the enzymatic processes activities by providing the energy input which is not able to disrupt the enzyme function. The low-power ultrasound increases growth in microbial cell cultures, while high power causes cell disruption and hence can be considered as microbicidal (Geciova et al., 2002). One evaluation of lipase activity under sonication reported that porcine pancreatic lipase was inactivated by US at 50 °C, while it was stable at or below 30 °C. It was found that sonication of lipase and olive oil for

less than a short period led to several times increment of free fatty acid production compared to the absence of US (Goodman & Dugan, 1970). In addition, Goodman & Dugan (1970) reported that the hydrolysis of tripalmitin was achieved by US and lipase. The effect of ultrasound (20 kHz) on the hydrolysis of corn, rice and wheat starch using alpha-amylase enzymes produced by *Bacillus species* and *Bacillus licheniformis* has been studied at 40 °C and at pH 6.5 (Apar et al., 2006). In some situations, sonication was found to have positive effects on starch hydrolysis with alpha-amylase at 40 and 50 °C; the control samples showed higher starch hydrolysis and lower residual enzyme activity.

3.5.2 Effects of US on microbial fermentations

Fermentation processes can also be beneficial by sonication. Immobilisation of yeast cells like *Saccharomyces cerevisiae* increases their stress tolerance by protective micro-environments creations (Kwiatkowska et al., 2011). US can be used to move and manipulate yeast cells prior to immobilisation. Low frequency ultrasound has shown its ability to stimulate production of riboflavin from *Ecemothecium ashbyii* which decreased the fermentation time and increased the production amount of riboflavin compared to controls (Chuanyun et al., 2003). Chuanyun et al., (2004) indicated that the optimal stimulation time was around 110 hours with the US (24 kHz, 28–30 °C) being applied every 1.5 h. Fermentation with *Aspergillus terreus* is used for cholesterol-lowering drug lovastatin

production. Herran et al. (2008) examined the effects of low (957Wm^{-3}), medium (2870Wm^{-3}) and high (4783Wm^{-3}) sonication energy on lovastatin production in a slurry bubble column sonobioreactor. Herran et al. (2008) indicated that sonication at any power of ultrasound did not affect biomass growth profiles but medium and high intensity reduced lovastatin production growth morphology modification and fungal pellets disruption which caused the biomass grow mainly as dispersed hyphae. The overall conclusion was that ultrasound could be used to alter morphology and broth rheology without affecting growth of filamentous fungi. Sonication appeared to influence primary and secondary growth metabolism differently depending on the conditions.

3.5.3 US and enzymatic hydrolysis of biopolymers

US together with enzymes was used to maximize the amount of glucose and hence ethanol production from cellulosic materials. Some processes enhanced fermentation while some increase the amount of available substrates from biopolymers. Yachmenev et al. (2009) reported that the combination of enzyme/ultrasound applying bioprocessing resulted in enhancing the enzyme macromolecules transfer to substrate surface by cavitation effects, opening up substrate surface for enzyme activity from mechanical impact of cavitation, enhancing cavitation effect in heterogeneous systems or achieving optimum enzyme temperature of 50 °C with maximum cavitation. Rolz (1986) showed that 20 kHz US during

enzymatic saccharification would double the rate and extent of reaction of US pretreated sugarcane bagasse. It was suggested that dynamic adsorption-desorption enzyme mechanism was influenced by acoustic streaming and local micro-turbulence.

3.5.4 US stimulation of enzymes in food science and technology

Mason et al. (1996) had reviewed US application in food industry and they describe its function as alternative non-thermal processing in freezing, sterilisation, extraction, and drying foods. Emulsification, dispersion and crystallisation processes also employed sonication but little report on US in bioprocesses in food science and technology. Toba et al. (1990) suggested the improvement of lactose-hydrolysed yogurt by sonication during the course of fermentation, which can add nutritional value for lactose-intolerant people. Nguyen et al. (2009) reported the effect of 20 kHz US between 30 °C and 40 °C on the fermentation of four strains of *Bifidobacterium* in milk. US under the applied conditions decreased the fermentation time for three of the four samples. The US caused ruptures of the probiotic cells and released β-galactosidase which led to lactose hydrolysis and trans-glycosylation. US also improved the growth of the remaining bacterial cells.

There are still many applications of US on various bioprocesses. Also much research has focused on microbial cell or enzymes. These results ensure that ultrasound in the range of 20–40 kHz is damaging to biological molecules both *in vivo* and *in vitro* through cavitation. But

still, there is little scientific reference on sonication effect on medicinal fungus culture or its fermentation broth.

Part II

Ultrasound-assisted extraction of water-soluble components from medicinal mushrooms

Chapter 4 General materials and methods of ultrasound-assisted extraction

4.1 Medicinal mushrooms

Several species of the most common and commercially important edible and medicinal mushrooms were chosen as experimental material for this project, originating either from mushroom fruiting body or as fungal mycelium. The dry mushroom material was ground into fine powder with an electric mill and screened through mesh sieves into selected particular sizes between 250 and 2000 μm. All dry mushroom material was stored in plastic bags, and kept at room temperature (20-25^{o}C) before use.

4.2 Extraction processes and conditions

4.2.1 Ultrasound-assisted extraction (UAE)

Ultrasound-assisted extraction experiments were performed with ultrasonic probe processors. Each batch (3 g of dry mushroom powder) was mixed with 90 ml of distilled water (1:30 solid-liquid ratio) in a 250-ml flat-bottom plastic centrifuge bottle. In experiments with variable solid-liquid ratio of extraction, the volume of water varied but the

solid mass was fixed at 3 g. The ultrasound probe tip was inserted into the sample liquid 2-3 cm deep for sonication. The UAE was performed at a selected ultrasound power for various periods of time. The extraction bottle was placed in an ice or a water bath to maintain a constant temperature during the UAE process.

4.2.2 Ultrasonic processors and power measurement

The UAE experiments were performed with two 20 kHz ultrasonic processors, one with a maximum output power of 130 W (Model VCX-130, Sonics & Materials Inc., Newton, USA) and the other of 900 W (Model CTXNW-2B, Hong Xiang Long Biotechnology Developing Co., Ltd., Beijing, China). A 12 mm-diameter probe was used with the former processor and a 15 mm-diameter probe for the latter. The power level in these ultrasonic processors was controlled by adjusting the amplitude (%). The actual power P (in W) transferred into the extraction liquid (water) at a given amplitude was determined by the calorimetric method (Mason et al., 1990). The measurement was performed in an insulated polycarbonate flask filled with 100 ml of water and sonicated with the probe horn for 15-20 min, during which water temperature was recorded. The actual power was derived from the following equation,

$$P = C_p W \left(\frac{dT}{dt}\right)_{t=0} \qquad \text{(Eq. 4-1)}$$

where C_p is the heat capacity (4.18 kJ/kg-^{o}C) and W the mass of water used for extraction (100 g), and $(dT/dt)_{t=0}$ the initial slope of temperature (T) versus time (t) plot. The plots of

temperature versus t within the initial 5-min period were close to linear for both processors. The actual power was roughly proportional to the amplitude shown in the processor panels. The ultrasound intensity I (in W/cm^2) is represented by the power per unit area of probe tip (= πr^2, where r is the radius of the tip surface),

$$I = \frac{P}{\pi r^2} \qquad \text{(Eq. 4-2)}$$

Fig. 4-1 and Table 4-1 showed the experimental results for calibration of the ultrasonic processors: from amplitude reading to actual power transferred into the extraction medium according to Eq. 4-1.

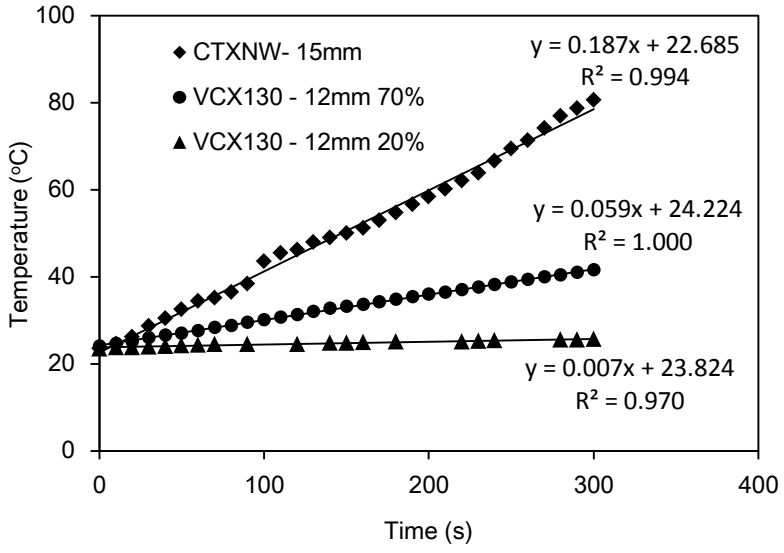

Fig. 4-1. Temperature (T) increase due to absorption of ultrasound energy from the probe horns of ultrasonic processors during the initial 5 min period of sonication.

Table 4-1. Actual ultrasound power and intensity transferred into the extraction liquid corresponding to the amplitude reading in ultrasonic processors (by Eq. 4-1 and Eq. 4-2).

Processor	Amplitude	Probe tip D (mm)	*dT/dt* ($^oC/s$)	Power, P (W)	Intensity, I (W/cm^2)	Power density, P/V (kW/m^3) [a]
VCX 130	70%	12	0.0586	24.5	21.7	272.2
	20%	12	0.0066	2.76	2.44	30.7
CTXNW-2B	20%	15	0.1865	77.9	44.1	865.6

[a] $I = P/\pi r^2 = P/\pi (0.6)^2$; $P/V = P/90 \times 10^3$ kW/m^3 (r = tip diameter/2 = 12 mm/2 = 0.6 cm; liquid volume of extraction V = 90 mL).

4.2.3 Hot water extraction (HWE)

Hot water extraction was performed for comparison with UAE. Mushroom powders were mixed with distilled water in the solid-to-liquid ratio of 1:30 (3 g sample powder in 90 ml of water). Each mixed sample solution was placed in a round-bottomed flask and substituted to under reflux for 2 hours.

4.3 Isolation of water-soluble PS

After UAE and HWE, the solid-liquid mixture was centrifuged at 6000 rpm for 10 minutes and the supernatant was collected as the liquid extract after further suction filtration.

The liquid extract was then mixed with 5 volumes of 95% ethanol (~80% v/v final concentration) and placed at 4^{o}C overnight for precipitation. The precipitates were separated from the liquid by centrifugation at 16,000 rpm for 15 min and lyophilized, yielding the crude PS fraction. The crude PS solid was stored in a sealed plastic bag and kept in a desiccator at room temperature (~20^{o}C) before use.

4.4 Composition contents and molecular properties of PS

4.4.1 Total carbohydrate and protein contents

The total carbohydrate content of crude PS was determined by the Anthrone test (Yemm & Willis, 1954). Diluted PS solution was reacted with Anthrone solution (98% v/v sulfuric acid, 2% w/v Anthrone) at room temperature for at least 45 minutes for complete acid degradation of PS molecules into monosaccharides. The sample solution was then heated in a boiling water bath for 10 minutes, with the color changing from yellow to green due to complex formation between monosaccharide and Anthrone. Glucose was used as a standard. Absorbance of standard solution (0 – 100 ppm) and reacted PS sample solution was measured under UV irradiation at 620nm wavelength.

Total protein content of crude PS was measured by the Lowery method (Lowery et al., 1951). Diluted PS solution was reacted with Lowery reagent for at least 1 hour. The resulted

solution was then reacted with Folin reagent for another 30 minutes, changing to blue or deep blue color. Bovine serum albumin (BSA) was used as a standard. Absorbance of the standard solutions (0-1000 ppm) and the reacted PS sample solutions was measured at 750nm wavelength.

4.4.2 Molecular weight distribution

The molecular weight (MW) profiles of PS were analyzed by high-pressure gel permeation chromatography (HPGPC) with two columns in a series, Ultrahydrogel 250 and Ultrahydrogel 2000 (both of 7.8 mm × 300 mm dimensions from Waters). Distilled water was used as a carrier liquid and the eluate was detected with a refractive index (RI) detector (Waters Co., Milford, MA, USA). The PS samples were dissolved in distilled water at 5 mg/ml and the sample solutions were filtered through 0.45 μm membrane before injection into the HPGPC system (injection volume of sample: 20 μl; carrier liquid flow rate: 0.6 ml/min and column temperature: 50°C). Dextran MW standards ranging from 1.0 to 670 kDa (Sigma, St Louis, MO) were used for the MW calibration, and the peak molar mass (M_p) was computed from the calibration equation with Breeze V3.3 software (Waters).

4.5 Electronic microscopy of mushroom powders

Scanning electronic microscopy (SEM) was employed to observe the solid microstructures and morphological characteristics of fungal particles. The sample powder of mushrooms and mycelia was coated with a gold layer and the SEM images were taken before and after UAE on a JEOL JSM-6490F instrument.

Chapter 5 Comparison of ultrasound-assisted extraction with hot water extraction of medicinal fungi

5.1 Introduction

Due to the solubility of many bioactive PS and PSP complexes, hot-water extraction (HWE) is a common technique to isolate those from mushroom fruiting bodies or fungal mycelium (Wasser, 2002; Zhang et al., 2007). HWE is also employed in the preparation of herbal decoctions in Chinese and other traditional medicines to isolate water-soluble bioactive compounds from natural materials. However, thermal destruction of temperature-sensitive components is a critical concern with the HWE application in separation of natural products, for example, the protein constituents of PSPs from mushrooms. Another drawback of HWE is its poor efficiency, and slow extraction rate. Several groups recently studied UAE of PS from medicinal plants and fungi or mushrooms, and demonstrated the feasibility and potential advantages of UAE, which include simple and convenient equipment setup and low-temperature operation with a high efficiency (Ebringerova & Hromadkova, 2010; Chen et al. 2010). However, an evaluation and understanding of the effects of ultrasonic treatment on the molecular properties of PS, as well as on the extraction process is needed. This part of our study was to examine the effects of

UAE on the yield, chemical composition, molecular properties and antioxidant activities of PS isolated from three mushrooms, *Grifola frondosa*, *Coriolus versicolor* and *Lentinus edodes*.

5.2 Materials and methods

5.2.1 Medicinal mushrooms

G. frondosa (Maitake), *C. versicolor* (Yunzhi) and *L. edodes* (Shiitake) were selected for the study. Dry fruiting bodies of the mushrooms were supplied by Zhejiang Fangge Pharmaceutical Co., Ltd. (Qingyuan County, Zhejiang, China).

5.2.2 Conditions of UAE and HWE

Mushroom powders were suspended in distilled water at the ratio of 1:30 (3 g mushroom sample in 90 ml water) in a 250 ml plastic centrifuge bottle. UAE was then performed by the Sonics VCX-130 with 12 mm-diameter horn tip being inserted into the sample solution. A fixed power amplitude 70% (corresponding to an intensity of 21.7 W/cm^2 tip surface) was applied with a total irradiation period of 60 min to complete the UAE process. The centrifuge bottle was immersed in an ice-bath during the whole process maintain the maximum extraction temperature not exceeding 50 ^{o}C. A UAE experiment was also performed without

the ice bath (UAE, no-cooling) to evaluate the temperature effect on the PS yield and composition, during which the maximum temperature was about 80 ^{o}C. Hot-water extraction (HWE) was performed on the mushroom samples in boiling water (3 g in 90 ml) with reflux for 120 min.

5.2.3 Separation and analysis of water-soluble PS

PS was obtained by ethanol precipitation (80%, v/v ethanol) of the liquid extract and weighed after lyophilization. Composition content of PS was analyzed by the Anthrone test and Lowery method for the total carbohydrate and protein contents respectively. The protein constituents and the relative MW of the PS samples were detected by SDS-PAGE gel electrophoresis (Laemmli, 1970) with 10-170 kDa protein markers as references. The molecular weight (MW) profiles of the PS samples were characterized by HPGPC. IR was performed in the 4000–400 cm^{-1} region on an Avatar 360 FTIR spectrophotometer (Thermo Nicolet, Cambridge, UK) in order to study the chemical bonding of the PS.

5.2.4 Antioxidant activities of PS

The antioxidant activities of PS obtained by UAE and HWE were determined with three assay methods, TEAC (Trolox equivalent antioxidant capacity), FRAP (ferric reducing ability of plasma) and ferrous ion chelating activity assay. The TEAC and FRAP assays were

performed with the procedures and conditions as reported as Leung et al. (2009), and the activities expressed in μmol Trolox/g PS and μmol $FeSO_4$/g PS, respectively. The ferrous ion chelating activity assay was performed according to Decker and Welch (1990), using EDTA as a reference, and expressed in μmol Fe^{2+}/g PS.

5.3 Results

5.3.1 PS yield and extraction rate

The UAE- and HWE-derived PS from each mushroom species were similar in color and morphology, but the PS from different mushroom species were very different. The PS extracted from *G. frondosa* was dark brown in color and sponge-like in morphology, while those from *C. versicolor* and *L. edodes* were light brown and in the form of fine particles. The PS yields and extraction rates of UAE were higher than those of HWE for *G. frondosa* and *L. edodes* but not for *C. versicolor* (Table 5-1).

Table 5-1. Yield and extraction rate of PS from three mushrooms by UAE and HWE (all in %, w/w of crude water extract).

Mushrooms	Extraction yield (wt%)		Extraction rate (mg PS/min)	
	UAE	HWE	UAE	HWE
G. frondosa	6.30± 0.07	5.71± 0.07	2.89± 0.08	1.43± 0.05
C. versicolor	1.61± 0.07	6.58± 0.04	0.82± 0.04	3.28± 0.03
L. edodes	12.4± 0.70	6.57± 0.05	6.20± 0.35	3.33± 0.06

Note: all data values are represented by mean±SD (n = 3).

5.3.2 Chemical composition of PS

The PS obtained by UAE from all three mushroom species had significantly lower total carbohydrate but higher protein contents than when obtained by HWE (Table 5-2). At the meantime, the protein constituents of the PS detected by SDS-PAGE also showed significant differences between the two extraction methods (Fig. 5-1). Distinct protein bands with MW of 10-130 kDa were found in the PS extracted by UAE from all three mushrooms but there was no clear protein band with any of the PS extracted by HWE. Therefore, the results from both chemical composition analysis and protein electrophoresis of the PS suggest significant differences in the quantitative content and the qualitative nature of carbohydrates and proteins between UAE-and HWE-extracted PS. In other words, UAE favored the extraction of protein but not carbohydrate fractions from mushrooms. However, PS from UAE at a higher

temperature (up to 80^{o}C) without ice-cooling (Table 5-2, UAE no cooling), were exhibiting a higher carbohydrate content and a lower protein content for all three mushrooms compared with those obtained by UAE with cooling, which suggests that the ratio of composition contents of PS could be highly depended on the extraction temperature.

Table 5-2. Total carbohydrate, protein and reducing sugar contents of PS from mushrooms by UAE and HWE (all in % w/w of the crude extract).

Mushroom	Carbohydrate			Protein		
	UAE	HWE	UAE, no cooling	UAE	HWE	UAE, no cooling
G. frondosa	28±0.4	60±4.8	48±0.3	33±2.9	21±0.3	30 ±1.9
C. versicolor	21±0.5	66±3.0	77±3.6	25±0.3	15±0.7	1.5±0.1
L. edodes	36±1.4	46±1.9	66±3.2	34±0.3	29±0.1	20 ±2.7

Note: all data values are represented by mean±SD (n = 3).

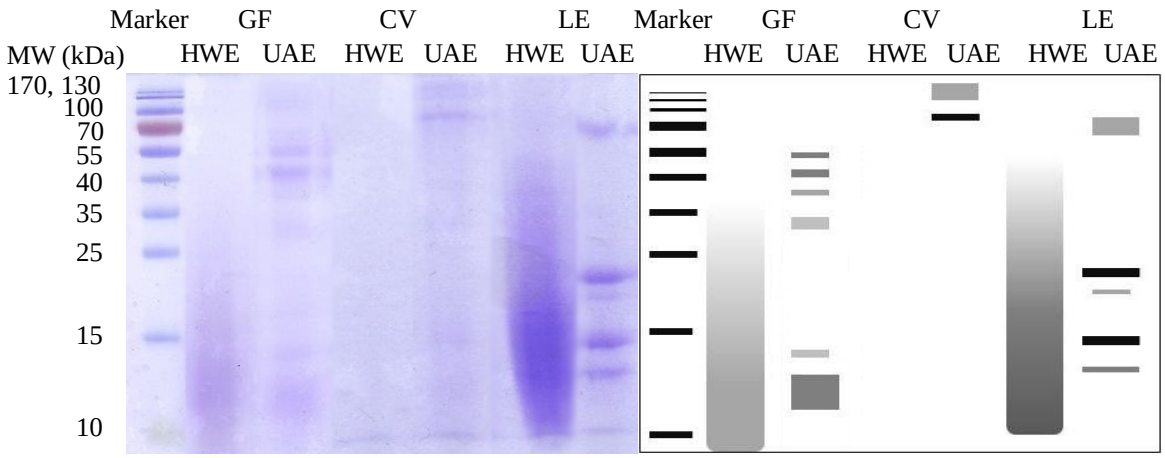

Fig. 5-1. Protein profiles of PS extracted by UAE and HWE on SDS-PAGE (left: real image; right: self-sketch; GF: *G. frondosa*; CV: *C. versicolor*; LE: *L. edodes*).

5.3.3 Molecular weight distribution and structural properties of PS

The PS extracted by UAE from all three mushrooms exhibited a large peak of low-MW fraction (<1.0 kDa) with a long retention time (35.8 min) in the GPC profiles (Fig. 5-2), which was not present in the profiles of HWE-extracted PS. On the other hand the high-MW peaks in the shorter retention time range existed in smaller amount of fraction in the UAE-extracted PS than those by HWE. The GPC profiles of PS by UAE showed an overall increase of lower-MW peaks and a decrease of higher-MW peaks in peak area and number, or the shift of MW distribution from high to low MW range compared with those by HWE.

The IR spectra of PS extracted from the three mushrooms by UAE and HWE are shown in Fig. 5-3. The spectra of PS from each mushroom species by the two different extraction methods were nearly identical in the major peaks, including the characteristic absorption

bands of glycan between 2800-3400 cm^{-1} (peak 1 & 2) and 1200-1400 cm^{-1} (peak 5 & 6), and the protein bands around 1650 cm^{-1} and 1550 cm^{-1} (peak 3 & 4) (Wang et al., 2010). However, both protein bands were notably enhanced for the PS extracted by UAE in comparison with those by HWE for all three mushrooms. This is consistent with the higher protein contents of PS obtained by UAE than those by HWE as shown in the above composition analysis.

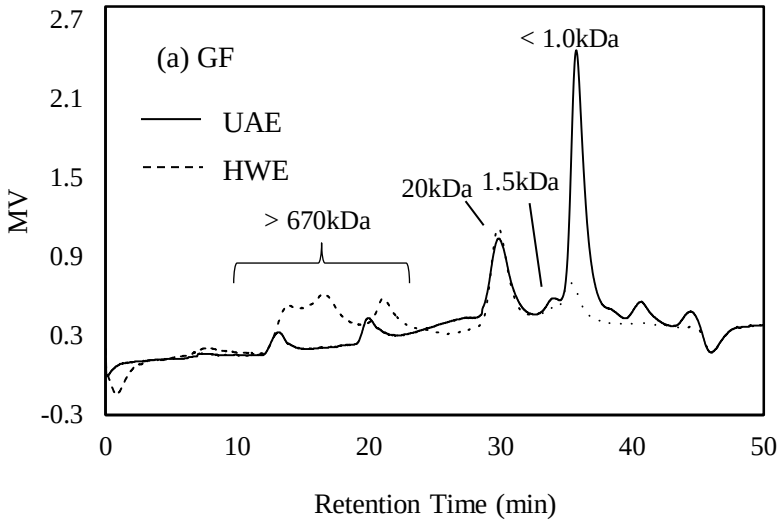

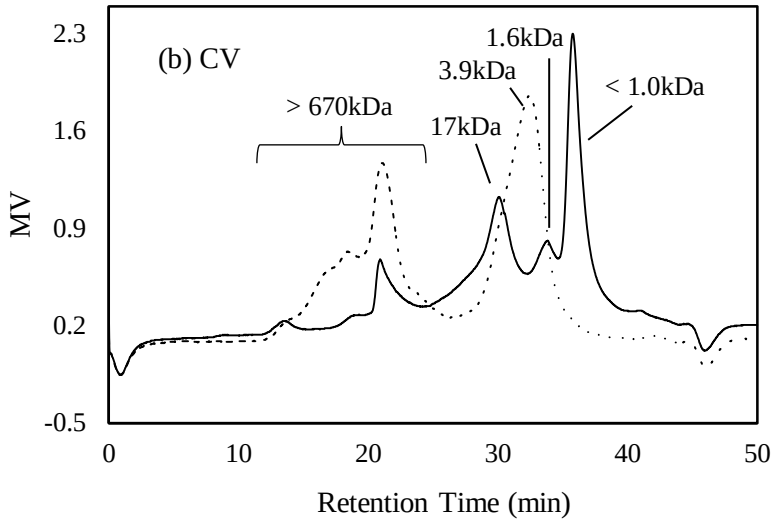

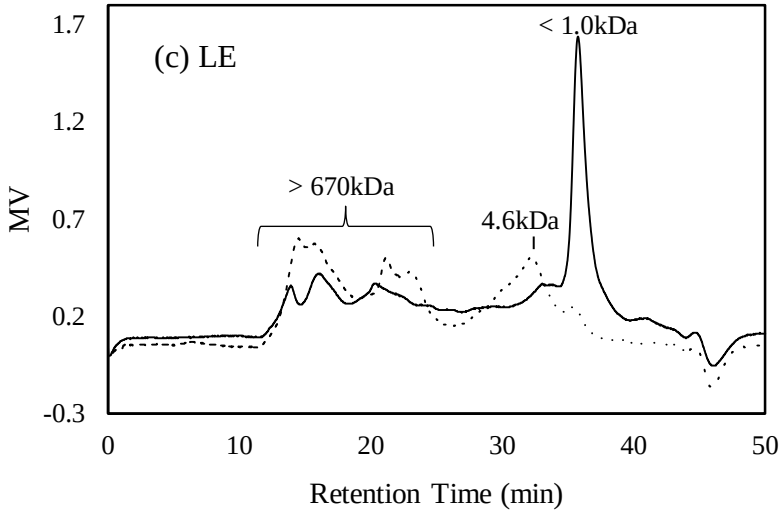

Fig. 5-2. GPC profiles of PS fractions isolated from the mushrooms extracted by UAE and HWE, (a) *G. frondosa*, GF (b) *C. versicolor*, CV (c) *L. edodes*, LE. (MW values determined by calibration with dextran MW standards in the range of 1-670 kDa).

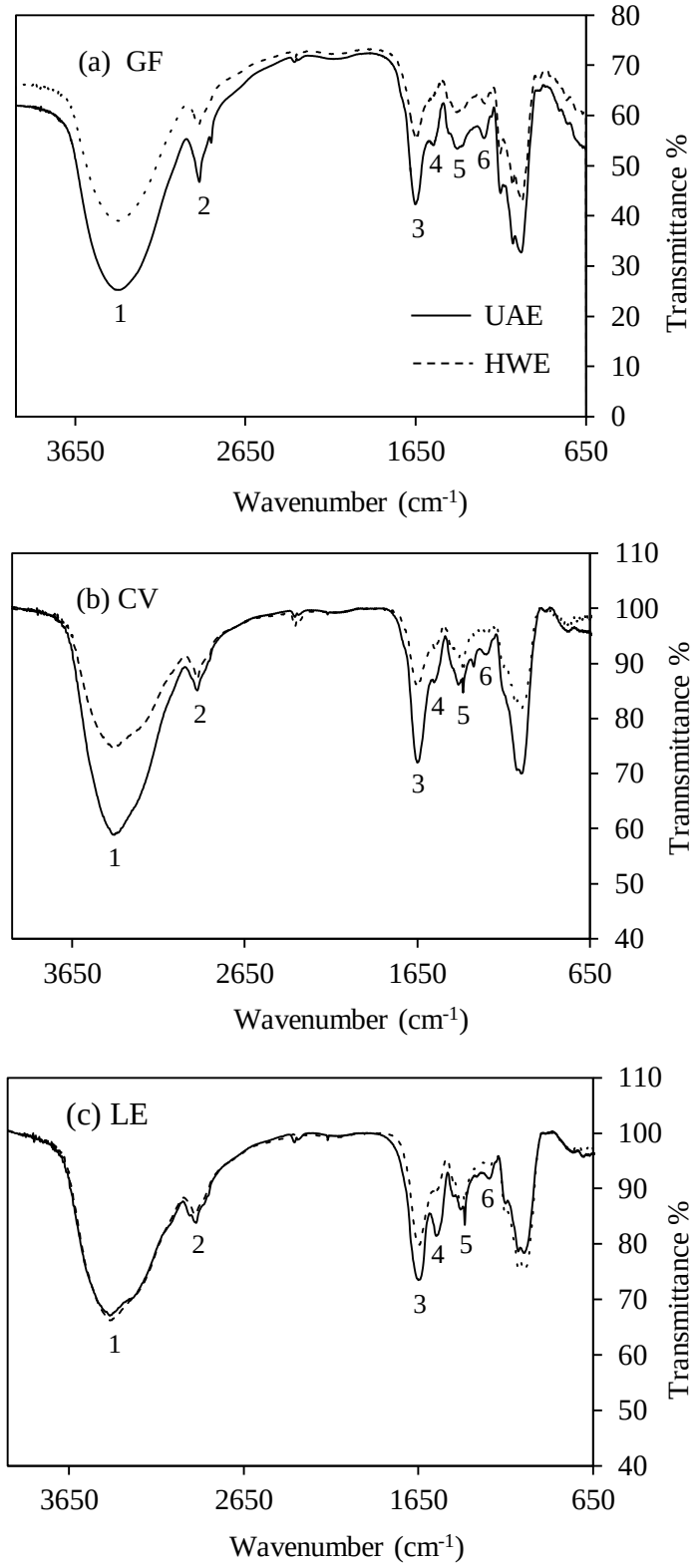

Fig. 5-3. FT-IR spectra of PS extracted by UAE and HWE from (a) *G. frondosa*, GF (b) *C. versicolor*, CV (c) *L. edodes*, LE.

5.3.4 Antioxidant activities of PS

When reviewing these three tests, the antioxidant activities of PS extracted by UAE were mostly higher than those extracted by HWE for the three mushrooms (Fig. 5-4). The different antioxidant activities of PS from the two extraction methods can be directly related to the differences in chemical composition and molecular properties as shown above. The higher protein contents (Table 5-2) and lower average MW (Fig. 5-2) of PS obtained by UAE may be the responsible factors for their higher antioxidant activities than the PS obtained by HWE.

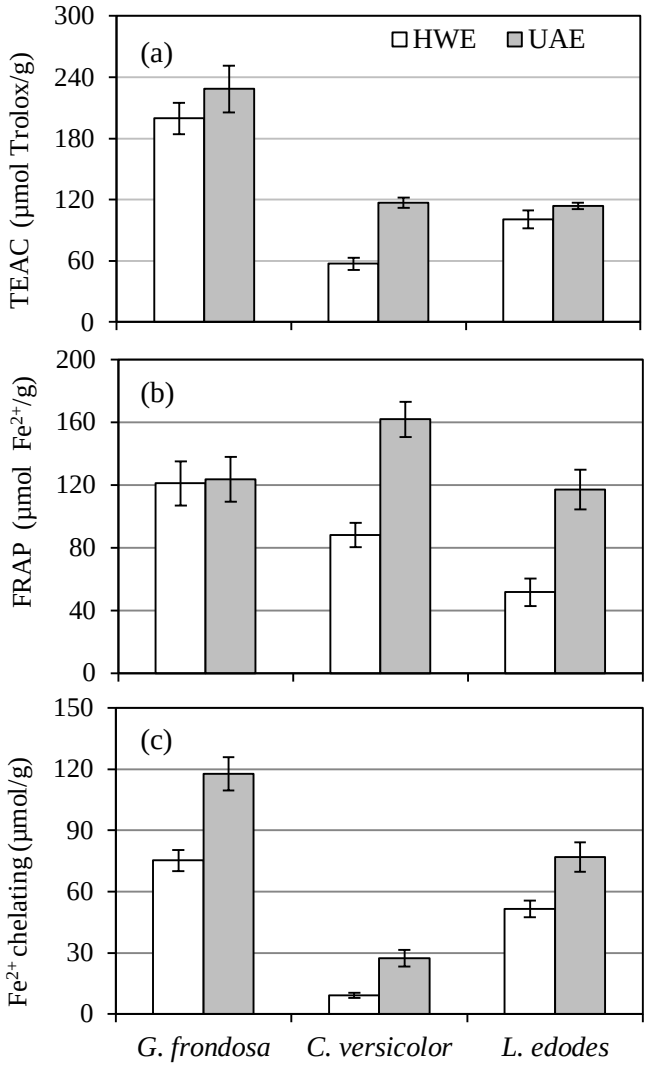

Fig. 5-4. Antioxidant activities of PS extracted by UAE and HWE measured with (a) TEAC assay, (b) FRAP assay and (c) Ferrous ion chelating activity.

5.4 Discussion

The different effects of UAE on the efficiency of PS extraction may be attributed to the physical properties of different mushroom species (Zhang et al., 2007). The powders of *G. frondosa* and *L. edodes* mushrooms being used in UAE were as dispersed particles in water but those of *C. versicolor* formed large aggregates (Fig. 5-5). As shown by Sun et al. (2011), the enhancement of extraction from a solid material by ultrasound is effective only for particles smaller than a certain size.

The differences in the MW ranges and protein constituents of PS obtained by the two extraction methods may be partly attributed to the different extraction temperatures, 40-50^{o}C for UAE and about 100^{o}C for HWE. The low extraction temperature of UAE avoided the denaturation of proteins and retained more protein constituents of PS, which could be denatured during HWE. On the other hand, the low extraction temperature during UAE was less effective for the extraction and dissolution of higher-MW polysaccharides (Villetti et al., 2002), and also to partial degradation of PS or the cleavage of the polysaccharide chains under the ultrasound power, leading to an overall shift to lower MW and a lower total carbohydrate content of PS (Ramesh & Tharanathan, 1999) as opposed to that by HWE. The proposed effects by temperature are further supported by the results of PS obtained by UAE at a higher temperature without ice-cooling (Table 5-2).

Leung et al. (2009) found a significant correlation between the TEAC and protein content of exopolysaccharide fractions produced by a *Cordyceps sinensis* fungus in mycelial culture, which stated that the protein content of samples plays an important role for the relative antioxidant activities. In previous studies, such as chitosans and derivatives (Xing et al., 2005) and sulfated PS isolated from a green alga (Qi et al., 2005), the results showed that there was a general trend of increasing antioxidant activity with decreasing molecular weight of various natural PS. The reason for that is, at an equal mass concentration, lower-MW PS molecules in a solution can have a larger number of hydroxyl groups to take part in the antioxidant action (Leung et al., 2009).

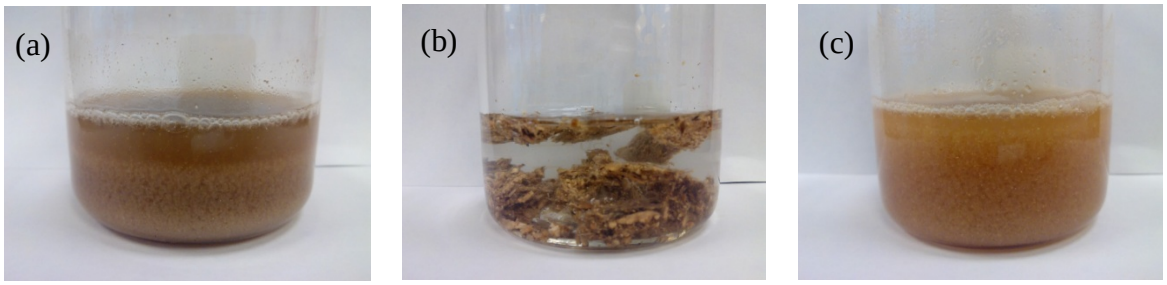

Fig. 5-5. Raw material powders dispersed in water of (a) *G. frondosa* (b) *C. versicolor* (c) *L. edodes*.

5.5 Summary

The PS attained by UAE from *Grifola frondosa*, *Coriolus versicolor* and *Lentinus edodes* mushrooms showed significant differences from those by HWE in the chemical composition and molecular weight range, and in the antioxidant activities as a consequence. These differences are most probably attributable to the different mechanisms (mechanical versus thermal) and conditions (low versus high temperature) of the two extraction methods. Another notable phenomenon observed in this study was a strong dependence of UAE efficiency on the morphology and aggregation of the mushroom particles. These findings provide useful considerations in the application of UAE for isolation of polysaccharides and PS complexes from mushrooms as components of health food and medicinal products.

Chapter 6 Kinetic models for ultrasound-assisted extraction of water-soluble components and polysaccharides from medicinal fungi

6.1 Introduction

Different empirical kinetic models have been developed based on the hypothesized and simplified extraction mechanism for solid–liquid extraction. Those models applied satisfactorily in the extraction of food and medicinal products in water and organic solvents (Kitanović et al. 2008; Meziane and Kadi 2008). For design and optimization of the extraction processes, these empirical model equations are very useful. Also they are essential for analysis and understanding of the major factors and their effects. The models applicable or the kinetic characteristics for a given solid–liquid extraction case are strongly dependent on the solid material being extracted. However, there are no previous studies documented on kinetic models for UAE of edible and medicinal fungi for isolation and recovery of polysaccharides. The aim of this part was to evaluate the suitable kinetic models for UAE of water-soluble constituents and polysaccharides from several important edible and medicinal mushroom fruit bodies and fungal mycelia and to gain better understanding of the ultrasound effects on the extraction rate and the connection with the fungal species and the solid particles

in the extracting solvent.

6.2 Materials and methods

6.2.1 Medicinal mushrooms

Five common and important species of edible/medicinal fungi were chosen for the study: *Grifola frondosa* (maitake) and *Lentinus edodes* (shiitake) in fruit body form; *Cordyceps sinensis* (Dong chong xia cao) Cs-4 and Cs-HK1, and *Ganoderma lucidum* (Linzhi) in mycelium form. Mushrooms of *G. frondosa*, and *L. edodes* were attained from Zhejiang Fangge Pharmaceutical Co., Ltd. (Qingyuan County, Zhejiang, China), and Cs-4 and *G. lucidum* mycelia (solid biomass) were provided by Shenzhen Huikang Bio-Technology Co., Ltd. (Shenzhen, Guangdong, China). Cs-HK1 mycelial biomass was produced by liquid fermentation in our lab as reported by Leung et al. (2006).

6.2.2 UAE of medicinal fungi to attain total extract and PS

UAE was performed with Sonics VCX-130 ultrasonic processor with 12 mm-diameter horn tip probe at fix power amplitude of 70% (corresponding to an intensity of 21.7 W/cm^2 tip surface) for all experiments. Sample powders (3 g) were mixed with distilled water (90 ml) in the solid-to-liquid ratio of 1:30 in the 250-ml centrifuge bottle. The bottle was immersed in

cold water or ice during the UAE to maintain an average temperature 45-50^{o}C. The total time for the sample powder being suspended in water before UAE was maintained equal (about 30 min) for all samples. The extraction was performed for a selected period of 1 to 60 min and then the sample bottle was centrifuged to separate the liquid extract from the solid residue. The solid residue was freeze-dried and weighed for calculation of the extract yield by subtraction from the mass of raw mushroom powder. The total extract yield was represented by the mass fraction of water extract over the mass of raw fungal material. Crude PS was isolated from the water extract by ethanol precipitation. The PS yield was represented by the mass fraction of crude PS over the mass of raw fungal material. Water extraction was carried out of the fungal materials at 45 ^{o}C±3 ^{o}C in a water bath for 1 to 60 minutes for comparison with UAE.

6.2.3 Kinetic models for solid-liquid extraction for UAE

Six empirical kinetic models for solid-liquid extraction were applied to fit the experimental data from the UAE of mushrooms in water: unsteady diffusion, parabolic diffusion, power law, Peleg hyperbolic model, Weibull's exponential equation, Elovich's logarithmic equation as shown in Table 6-1. These models have been previously applied to extraction of natural products from various sources such as food and medicinal plants (Veličković et al., 2006; Kitanović et al., 2008). These models are based on the following

general assumptions, (1) all solid particles are spherical with a uniform size; (2) the extractable component is evenly distributed in the solid; (3) the diffusion coefficient of extractable component is constant; (4) solid particles are evenly dispersed in the extracting solvent. Additional assumptions are also applied for different models. Both the unsteady diffusion model and the parabolic diffusion model assume a two-step extraction mechanism, the initial and rapid washing step for the compounds on the particle surface followed by diffusion through the particle. The power-law model describes the extraction mechanism by the diffusion of compounds through a non-swelling device. The Elovich's equation, which is widely applied to chemisorptions (Mclintock, 1967), signifies that the extraction rate of a substance from solid declines exponentially with the extraction yield ($dy/dt = \beta\ exp^{-\alpha y}$). Kitanović et al. (2008) found that the extraction data of resinoids from aerial parts of St. John's wort with boiling ethanol-water could be fitted well to five kinetic models and the best to Elovich equation. Kim et al. (2002) and Bucić-Kojić et al. (2007) successfully applied the hyperbolic model for the extraction of nuclides from paraffin waste, and total polyphenols from grape seeds, respectively.

All experiments were performed in triplicate and the results were represented by their means and standard deviation (SD). The experimental data, total extract yield or PS yield from the water extract versus time of UAE for each fungal species were fitted to the kinetic models by linear regression analysis to derive the model parameters. The goodness of model

fit to the experimental data was evaluated by the correlation coefficient (R^2), F-value and the relative P-value (Peck & Devore, 2012).

Table 6-1. Kinetic model equations and constants (*y* is the total extract or PS yield in w/w; *t* is the extraction period in minute):

Model	**Equation**	**Linearity**	**Constants**
Parabolic diffusion	$y = y_o + y_1 t^{½}$	$y \sim t^{1/2}$	y_o: initial yield; y_1: diffusion coefficient.
Power law	$y = B t^n$	$ln\ y \sim ln\ t$	B: rate constant; n : diffusional exponent (kinetic order)
Weibull's exponential	$y = 1 - e^{(-\frac{t^m}{D})}$	$ln[-ln(1-y)] \sim ln\ t$	D: scale parameter for reciprocal rate constant; m: shape factor
Elovich's logarithmic	$y = E_o + E_1 ln\ t$	$y \sim ln\ t$	$E_1 e^{Eo/E1}$: initial extraction rate; E_o: initial yield
Unsteady diffusion	$y = (1 - b)\ e^{-kt}$	$ln\ y \sim t$	b: washing coef.; k: rate constant
Peleg hyperbolic	$y = C_1 t / (1 + C_2 t)$	$1/y \sim 1/t$	C_1 : initial rate; C_1/C_2: capacity constant

6.3 Results

6.3.1 Kinetic models for total extract yield from UAE

Fig.6-1 shows the time courses of total extract yields by UAE of the five fungal species in water. The extract yield increased rapidly in the early period (0-20 min) and slowly in the later period of UAE in most species. Among the five fungal species, *G. frondosa* and *L. edodes* mushrooms and Cs-HK1, mycelium had significantly higher average extract yields than the other two species. Thus the former three species had a higher extractability by water than the latter two.

Table 6-2 represents the correlation coefficients, F-values and the relative P-values from regression fit of the experimental data (yield versus time) in different kinetic models for all fungal species and the corresponding model parameters. In the F-distribution table, the critical F-value with 1 degree of freedom in the numerator and 6 degrees of freedom in the denominator at 99% confidence level ($\alpha = 0.01$) is equal to 13.745 (Peck & Devore, 2012). The regression results (F-values) of most models for the five fungal species were with range from 15.17 to 1189, which is greater than the critical F-value and P-values (3.98×10^{-8}-5.91×10^{-3}) is lower than 0.01 (α value). This indicates that the time courses of total extract yields by UAE could be statistical-significantly represented by the kinetic models at the 99% confidence level. Also the better fitting of the kinetic models would obtain the higher F-value

from the critical one and the lower P-value from α value, together with the higher R^2 value. For the two mushrooms *G. frondosa* and *L. edodes* (in fruit body form), the power law, Weibull's and Elovich's models had a close fit to the experimental data with fairly large R^2 values (0.984-0.964) and low P-values (1.29×10^{-6}-1.56×10^{-5}). For the mycelia of all three fungal species, the parabolic diffusion model got relatively large R^2 values (0.955-0.995) and small P-values (3.98×10^{-8}-1.33×10^{-5}). Fig. 6-2a shows the plots of extraction time courses with the linearized power-law model for the two mushrooms; Fig. 6-2b plots the extraction time courses with the linearized parabolic model for the three fungal mycelia. The hyperbolic model attained the smallest R^2 values (< 0.8) and largest P values (>0.01) for most mushroom species and can be considered unsuitable for UAE kinetics with these mushroom materials among the six models.

Comparing of the model constants among three fungal species (mycelia), results in *G. lucidum* and Cs-4 were similar, and much lower than those in Cs-HK1. Both *G. lucidum* and Cs-4 mycelia were produced on solid substrate (solid fermentation) but Cs-HK1 mycelium was produced by liquid fermentation. The results of two mushroom species, *G. frondosa* and *L. edodes* showed they have similar kinetic constants. The *G. frondosa*, and *L. edodes* mushrooms and the Cs-HK1 mycelium retained a much higher yield throughout the extraction period (Fig. 6-1) and higher initial yield (y_0 in the parabolic model, 0.45-0.52), indicates a higher water extractability, than the other two species. The initial yield for most

species was about 50% or more of the maximum yield attained at the end of extraction period.

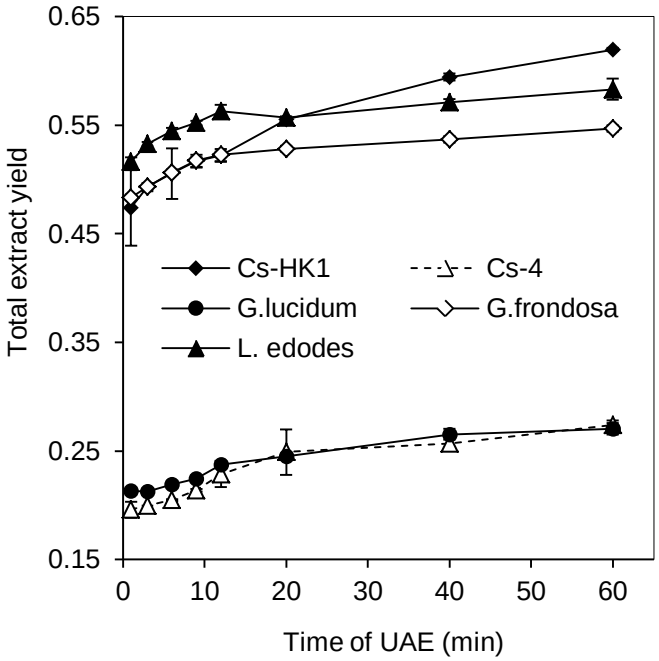

Fig. 6-1. The time courses of total extract yields (w/w) attained by UAE from two mushrooms and three fungal mycelia (error bars for SD at $n = 3$).

Table 6-2. Correlation coefficients (R^2), F-values and relative P-values, and model constants for various kinetic models fitted by linear regression to the UAE experimental data (total extract yield *y* vs. time *t*) of five fungal species. [$F_{(0.01, 1, 6)} = 13.745$ from F-distribution table]

Model [a]		*G. frondosa*	*L. edodes*	Cs-HK1	Cs-4	*G.lucidum*
Parabolic diffusion	R^2	0.907	0.871	0.995	0.955	0.965
	F-value	58.23	40.67	1189	125.8	166.7
	P-value	2.64×10^{-4}	6.99×10^{-4}	3.96×10^{-8}	3×10^{-5}	1.33×10^{-5}
	y_o	0.483	0.520	0.452	0.181	0.200
	y_1	0.009	0.009	0.022	0.012	0.010
Power law	R^2	0.984	0.964	0.926	0.900	0.879
	F-value	368.73	160.1	75.29	53.89	43.41
	P-value	1.29×10^{-6}	1.49×10^{-5}	1.29×10^{-4}	3.27×10^{-4}	5.87×10^{-4}
	B	0.481	0.517	0.457	0.184	0.202
	n	0.031	0.028	0.067	0.089	0.066
Weibull's exponential	R^2	0.984	0.964	0.913	0.898	0.877
	F-value	365.86	158.7	63.07	52.69	42.78
	P-value	1.32×10^{-6}	1.53×10^{-5}	2.12×10^{-4}	3.48×10^{-4}	6.11×10^{-4}
	D	1.526	1.374	1.649	4.918	4.434
	m	0.045	0.043	0.101	0.101	0.076
Elovich's logarithmic	R^2	0.984	0.963	0.906	0.885	0.868
	F-value	359.94	157.6	57.57	46.35	39.55
	P-value	1.39×10^{-6}	1.56×10^{-5}	2.73×10^{-4}	4.92×10^{-4}	7.53×10^{-4}
	E_o	0.480	0.517	0.453	0.181	0.200
	E_1	0.016	0.016	0.036	0.020	0.016
Unsteady diffusion	R^2	0.743	0.717	0.927	0.859	0.890
	F-value	17.35	15.17	76.60	36.43	48.60
	P-value	5.91×10^{-3}	8.03×10^{-3}	1.23×10^{-4}	9.35×10^{-4}	4.33×10^{-4}
Peleg hyperbolic	R^2	0.710	0.767	0.534	0.483	0.422
	F-value	14.72	19.77	6.868	5.596	4.048
	P-value	8.59×10^{-3}	4.35×10^{-3}	3.95×10^{-2}	5.59×10^{-2}	9.09×10^{-2}

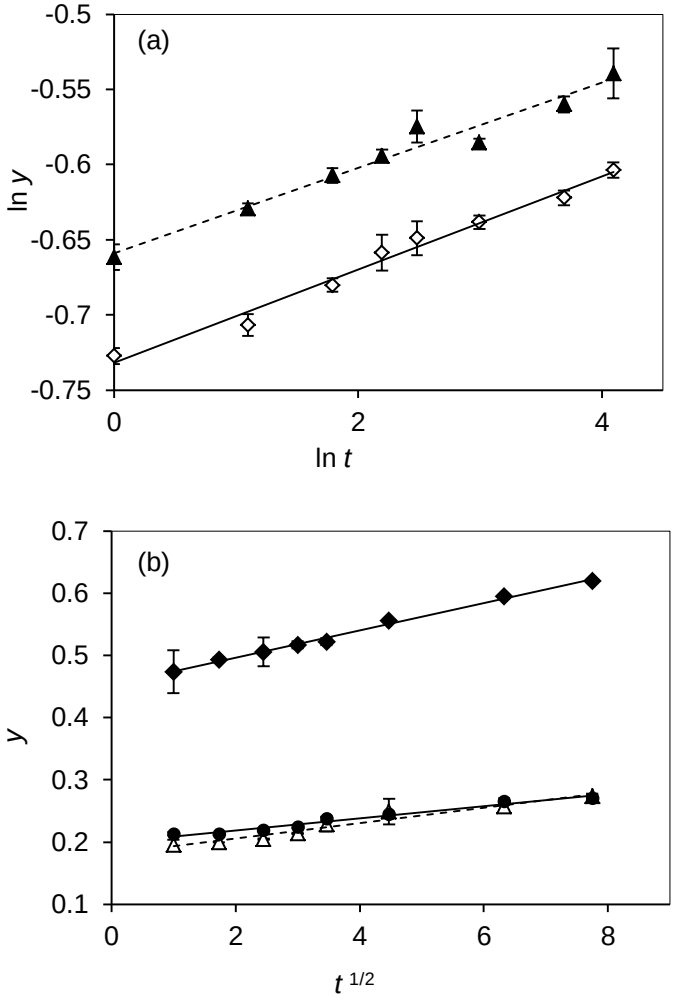

Fig. 6-2. Plots of extract yields with UAE experimental data (markers) and the best-fit linearized kinetic model (lines): (a) Power law for two mushrooms; (b) Parabolic diffusion model for three fungal mycelia (*y*: total extract yield; *t*: time of UAE; Marker-line style designated for each specie same as in Fig. 6-1; error bars for SD at $n = 3$).

6.3.2 Kinetic models for PS yield from UAE

Fig. 6-3 shows the time courses of PS yields isolated from the water extracts of the five fungal species by UAE, and the trend varied significantly among the different species. Table

6-3 shows the correlation coefficients and relative P-values from linear regression fit of the PS data to the kinetic models for all the fungal species. With the two mushrooms, the PS data did not statistical significantly fitting to any of the kinetics models with relatively small R^2 values < 0.83 and large P-values > 0.03. With the three fungal mycelia, all the PS data had the best fit to the parabolic model with large R^2 values of 0.97-0.98 and P-values of 1.51×10^{-6}-0.001, statistical-significantly linear-regressed to different models, and the poorest fit to the hyperbolic model with R^2 < 0.63 and P-value > 0.01.

Table 6-3. Correlation coefficients (R^2) and relative P-values for linear regression fit of the PS yields isolated from the water extracts by UAE of five fungal species to various kinetic models.

Model		***G. frondosa***	***L. edodes***	**Cs-HK1**	**Cs-4**	***G. lucidum***
Unsteady	R^2	0.071	0.308	0.929	0.918	0.824
diffusion	*P-value*	0.5230	0.1536	1.14×10^{-4}	1.77×10^{-4}	0.0018
Parabolic	R^2	0.192	0.414	0.983	0.980	0.967
diffusion	*P-value*	0.2779	0.0853	1.51×10^{-6}	2.37×10^{-6}	1.11×10^{-5}
Power law	R^2	0.440	0.555	0.924	0.926	0.947
	P-value	0.0728	0.0339	1.39×10^{-4}	1.33×10^{-4}	4.84×10^{-5}
Peleg	R^2	0.728	0.783	0.593	0.613	0.630
hyperbolic	*P-value*	0.0071	0.0035	0.0253	0.0216	0.0187
Weibull's	R^2	0.440	0.556	0.921	0.924	0.946
exponential	*P-value*	0.0730	0.0338	1.61×10^{-4}	1.40×10^{-4}	4.97×10^{-5}
Elovich's	R^2	0.424	0.559	0.854	0.865	0.913
logarithmic	*P-value*	0.0801	0.0331	0.0010	8.08×10^{-4}	2.15×10^{-4}

[$F_{(0.01,\ 1,\ 6)}$ = 13.745; F-values of all models, except hyperbolic, for (i) *G. frondosa* & *L. edodes*: 1.4229 – 7.5905 (ii) Cs-HK1, Cs-4 & *G. lucidum*: 35.13-349.4]

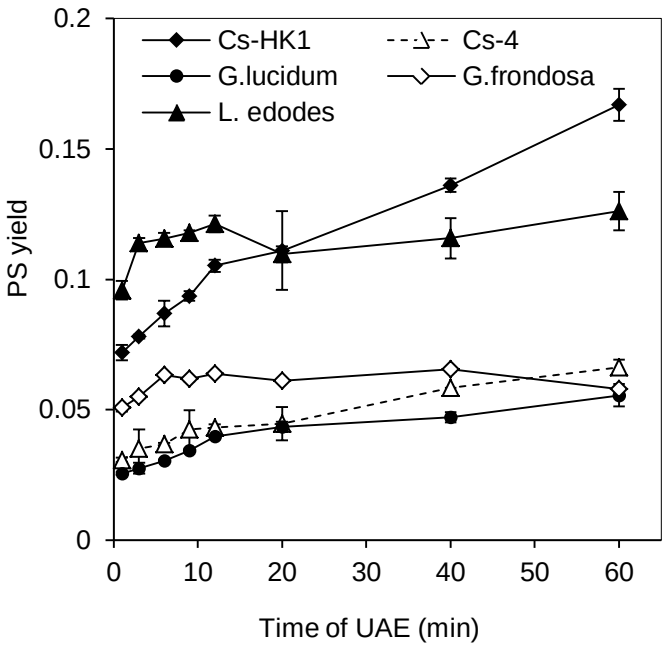

Fig. 6-3. The time courses of PS yields isolated from water extracts attained by UAE from five fungal species (error bars for SD at n = 3).

6.3.3 Microstructures and morphological characteristics of fungal particles

The microstructures and morphological characteristics of the powdered fungal particles before and after UAE were observed by scanning electronic microscopy (SEM). As seen from the SEM images (Fig. 6-4), the mushroom and mycelial particles of most species were composed of compact, particulate aggregates before UAE and turned to more porous, flatten fragments after UAE.

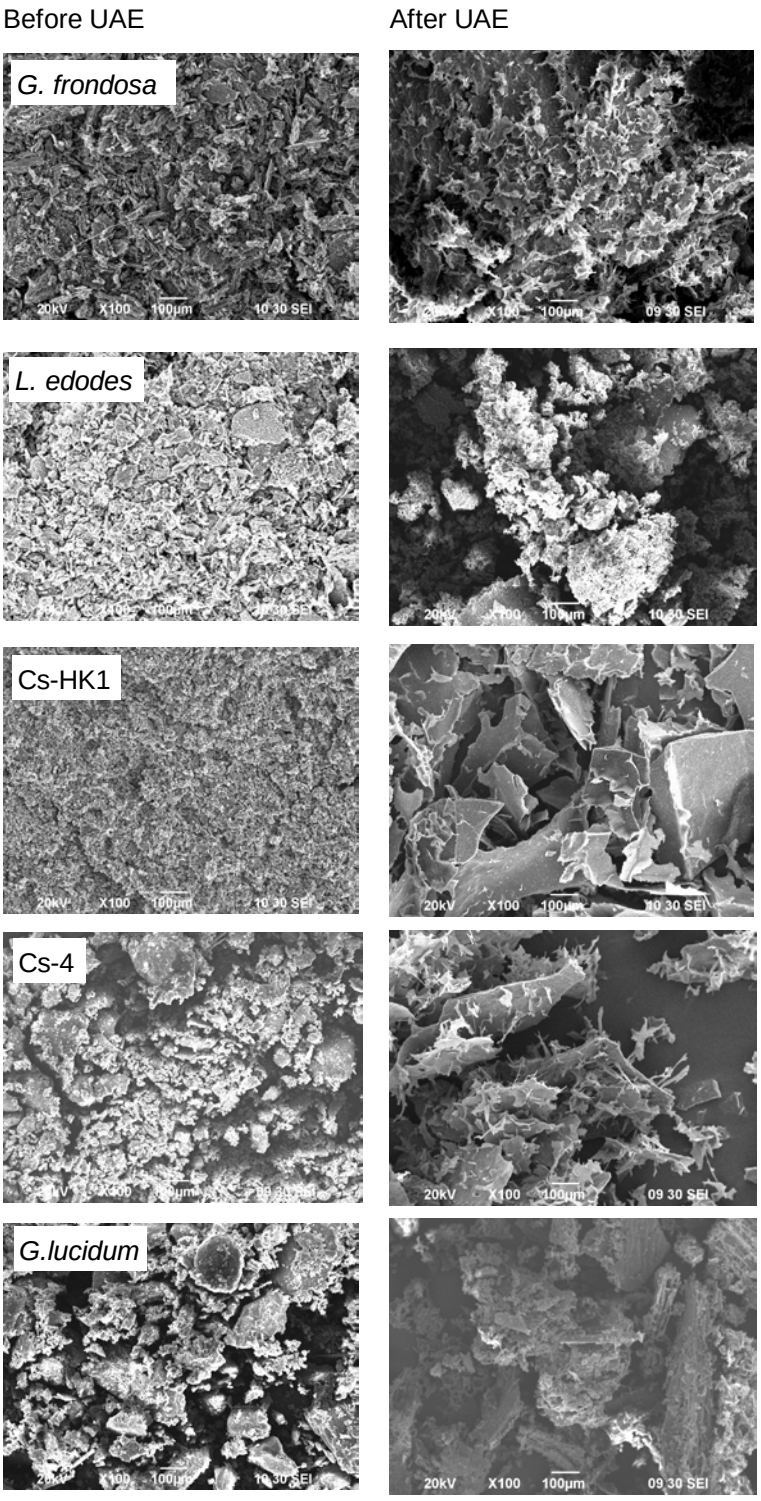

Fig. 6-4. Scanning electron micrographs of mushroom and mycelial particles before and after UAE for 60 min. SEM was performed on a JEOL JSM-6490F instrument. (The dry sample powder of mushrooms and mycelia was coated with gold.)

6.3.4 Effects of ultrasound on water extract and PS yields

Table 6-4 shows the PS yields attained over 60-min period of UAE were significantly higher than those from water extraction at the same temperature for all five species. Compared with the total extract yield, the PS yield was increased more significantly (52%-169% net increase) for most species, suggesting that UAE was generally more effective for the extraction of high-MW constituents. On the other hand, the results from GPC analysis of the PS fractions (Table 6-5) showed no notable change in the number and retention time of major PS peaks over the period of UAE. The results suggest that the MW distribution of PS was not significantly affected by the ultrasound treatment or no significant polymer degradation occurred during UAE.

Table 6-4. Total water extract and PS yields from UAE compared with water extraction at 45^{o}C of five fungal species (60 min extraction period; yield in g/100 g raw fungal material).

	Total extract		PS	
Fungal species	UAE	Water	UAE	Water
G. frondosa	0.547 ±0.0028	0.487 ±0.0004	0.058 ±0.0009	0.027 ±0.0012
L. edodes	0.583 ±0.0097	0.541 ±0.0024	0.126 ±0.0073	0.077 ±0.0013
Cs-HK1	0.650 ±0.0046	0.522 ±0.0032	0.180 ±0.0048	0.067 ±0.0009
Cs-4	0.274 ±0.0044	0.178 ±0.0034	0.066 ±0.0028	0.039 ±0.0027
G. lucidum	0.270 ±0.0053	0.228 ±0.0041	0.056 ±0.0043	0.037 ±0.0004

Table 6-5. Retention time of the major molecular weight peaks on GPC of the PS fractions isolated from the water extracts of five fungal species in various periods of UAE.

UAE Time	Mw (kDa) (RT, min)			
(min)	Peak 1	Peak 2	Peak 3	Peak 4
G. frondosa				
1	27.8 (25.43)	0.6 (32.31)	-	-
20	26.8 (25.50)	0.5 (32.45)	-	-
60	33.8 (25.08)	0.6 (32.23)	-	-
L. edodes				
1	380 k (14.17)	4.5 k (21.20)	0.5 (35.77)	-
20	520 k (13.67)	4.3 k (21.27)	0.5 (35.76)	-
60	445 k (13.93)	6.3 k (20.47)	0.5 (35.78)	-
CS-HK1				
1	2.4 (29.78)	0.6 (32.17)	-	-
20	2.2 (29.97)	0.5 (32.52)	-	-
60	3.2 (29.32)	0.7 (31.95)	-	-
Cs-4				
1	250 k (14.83)	5.4 k (20.93)	2.1 (33.40)	0.5 (35.75)
20	243 k (14.88)	4.5 k (21.22)	2.4 (33.15)	0.5 (35.78)
60	237 k (14.92)	5.3 k (20.95)	2.8 (32.92)	0.5 (35.78)
G. lucidum				
1	3.4 k (21.66)	1.3 (34.15)	0.5 (35.68)	-
20	3.1 k (21.82)	1.2 (34.23)	0.5 (35.69)	-
60	3.8 k (21.47)	1.5 (33.97)	0.5 (35.54)	-

6.4 Discussion

The power law model is most applicable in the extraction of a substance from a non-swelling device (Sinclair & Peppas, 1984) with a diffusion exponent $n < 1$ for extraction of plant materials (Kitanović et al., 2008). As experiments observations, the powder of mushrooms *G. frondosa* and *L. edodes* appeared being well dispersed in the extracting solvent (water), which suggesting a higher degree of rigidity and similarity to a non-swelling device. The parabolic diffusion model represents a two-stage extraction process, an initial washing stage (to an initial yield y_0) then a slow stage (with the yield increasing linearly with $t^{1/2}$). The mycelial powder suspended in water aggregated and became soft and loose flocs, which were more accessible to the solvent. The hyperbolic model indicates an extraction kinetics that is 1^{st} order, yield increasing linearly with time in the initial stage and becomes zero order at the very late stage, when yield reaches a maximum or plateau. However, the extraction time courses (Fig. 6-1) of most species showed there are a non-linear increase in the early period and a constant increase (no plateau) in the late period.

In comparison with the regression results for the total extract yields (Table 6-2), the PS yields from the three fungal mycelia were fitted closely to the same kinetic model as the total water extract but those from the two mushrooms were not fitted closely to any model. The difference in the kinetic trends between PS and water extract of the two mushrooms was

associated with the variation of PS content in the water extract during UAE.

The observation of powdered fungi by SEM (Fig. 6-4) suggests that the ultrasonic treatment caused the disruption of particle microstructures and fungal cell walls, facilitating the release and transport of intracellular and/or intra-particle constituents into the extracting liquid. In other words, the enhanced extraction rate by ultrasound can be attributed to the changes in the microstructures and morphology of fungal particles.

6.5 Summary

The modelling studies on the UAE kinetics of different fungal species and materials have shown that the kinetics of UAE was strongly dependent on the fungal materials, particularly the microstructure and morphology of the fungal cells and solid particles. Ultrasound was effective to enhance the extraction of water-soluble polysaccharides at a relatively low temperature from medicinal fungi. Further studies are needed to characterize the microstructures of mushroom particles and to determine the correlation of kinetic parameters to the ultrasound power.

Chapter 7 Kinetic models and process parameters for ultrasound-assisted extraction of Cs-HK1 fungal mycelia

7.1 Introduction

Many studies have shown that UAE improved the extraction efficiency (shorter time) and also attained higher bioactivity of the extracted products than HWE (Patist & Bates, 2008; Ebringerova & Hromádková, 2010). In the previous study we has shown that the UAE was more effective and favorable for extraction of polysaccharides at a lower temperature than HWE from two edible mushrooms, retaining higher protein content and higher antioxidant activities. However, most previous studies on UAE have been focused on the optimization of the experimental conditions or process factors and qualitative description of their effects, and very few on the quantitative relationships between the extraction kinetics and the process factors, particularly ultrasound power and energy. Present study was to establish the relationship between the UAE kinetics and the process factors for extraction of water-soluble components and PS from the mycelial biomass of *C. sinensis* fungus Cs-HK1 and to identify the ultrasonic power and energy parameters for predicting the extraction rate and yield. Modelling the extraction kinetics is useful not only for predicting the rate and yield but also for understanding the major process factors and their effects on the extraction process.

7.2 Materials and methods

7.2.1 Fungal material

Cordyceps sinensis species Cs-HK1 was chosen as the representative medicinal fungus for the kinetic study. The Cs-HK1 fungus was previously isolated in our lab from the fruiting body of a wild *C. sinensis* organism (China General Microbiological Culture Collection Center Registration No. 6004). The Cs-HK1 mycelial fermentation was performed in the liquid medium and conditions as reported by Leung et al. (2006). After 6-7 days of liquid fermentation, the mycelium biomass was separated from the liquid medium by filtration and then dried at 50^{o}C in an oven. The dry mycelium biomass was stored in sealed plastic bags at room temperature (23±2^{o}C) before use.

7.2.2 UAE conditions of fungal mycelium

The Cs-HK1 mycelium was ground into powder with an electric mill and then screened through mesh sieves into different mean particle sizes (156.5 – 750 µm). The sample powder was suspended in distilled water in a 250-ml plastic centrifuge bottle during the ultrasonic extraction. The mass of sample was fixed at 3 g for all experiments and the volume of water varied from 90-210 mL for the desired solid-liquid ratio (1/30-1/70 g solid/ml liquid). The

sample powder was suspended in water for 30 min at room temperature (23 ± 2^{o}C) (without stirring) before ultrasonic treatment in all experiments to ensure an equal starting point. UAE was performed for a selected period of 10 to 80 min with the ultrasonic probe, which was dipped into the liquid about 2 cm deep. The sample bottle was immersed in a water bath to maintain a constant extraction temperature during UAE. The liquid extract was separated from the solid residue by centrifugation after the extraction. The solid residue was dried at 50^{o}C for 2 days and its weight was measured, and deducted from the initial solid mass to attain the mass of water-soluble extract. Crude PS was isolated from the water extract by ethanol precipitation (80% final concentration) at 4^{o}C for overnight. The precipitated PS was recovered by centrifugation and freeze-dried. The total extract/PS yield attained from UAE was given by,

$$y = \frac{m - m_o}{M} \qquad \text{(Eq. 7-1)}$$

where m_o and m are the mass of total water extract/PS at the beginning of UAE (after 30-min suspension in water) and at a given time of UAE, respectively, and M is the initial mass of mycelium sample (3 g).

Water extraction (WE) (maceration) was performed at 40^{o}C with solid-liquid ratio of 1/30 (g/ml) and mean particle size of 156.5 μm for comparison with the UAE of the Cs-HK1 mycelia at the same conditions. The solid sample (3 g) was suspended in 90 mL water in a 250-mL centrifugal bottle and placed in a water bath for 10-80 min.

7.2.3 Kinetic models of solid-liquid extraction for UAE

As shown in the our previous study on UAE of water soluble components and PS from different medicinal fungi, the kinetic characteristics and the suitable models are dependent on the fungal species and the morphological form (mycelium or fruit body). The total water extract and PS yields of UAE from fungal mycelia of *C. sinensis* Cs-HK1 and two other medicinal fungi were fitted most closely to the parabolic diffusion model ($R^2 > 0.98$) and less well to the power-law model ($R^2 > 0.92$),

Parabolic diffusion: $y = y_o + y_1 t^{1/2}$ (Eq. 7-2)

Power law: $y = \beta t^n$ (Eq. 7-3)

where y is the total extract or PS yield and t the time of extraction; in Eq. 7-2, y_o is the initial washing-out yield at $t = 0$ and y_1 is the diffusion coefficient for the diffusion of solute molecules from the interior of particles to the solvent; in Eq. 7-3, β is a constant related to extraction rate and the power-law exponent (<1). These two models were applied in this study to fit the experimental data of UAE.

7.2.4 Experimental variables (process factors) of UAE

With a given solid material and an extracting solvent (Cs-HK1 fungal mycelium extraction with water in this study), particle size, solid-liquid ratio and temperature are three

of the most significant factors affecting solid-liquid extraction processes (Kitanović et al., 2008). These are also identified as the major factors on UAE of bioactive natural products (Li et al., 2004; Alessandro et al., 2012) and polysaccharides from mushrooms (Sun et al., 2010) and fungal mycelia (Chen et al., 2012). In addition to these factors for solid-liquid extraction, ultrasound power (*P*) applied to the system will have a significant influence on the UAE process and kinetics. Therefore the UAE experiments in this part of study were performed with four variables (factors), ultrasound power intensity (3 levels: 2.44, 21.7, 44.1 W/cm^2, corresponding to 30.7, 272.7, 856.6 kW/m^3 power density in 90 mL liquid), temperature of the extraction liquid (3 levels: 40, 55, 70 ^oC), solid-to-liquid ratio (3 levels: 1/30, 1/50, 1/70 g/ml) and mean particle size of sample powder (2 levels: 156.5, 750 μm). All experiments were conducted by with one factor variable and the other three fixed (one-factor-at-a-time test) in a set of experiments.

All experiments were performed in triplicate and the results were represented by means and standard deviation (SD). The experimental data, total water extract yield or PS yield from the water extract versus time of UAE for each fungal species, were fitted to the kinetic models by linear regression (using Microsoft Excel), and to derive the model constants and the correlation coefficients (R^2).

7.3 Results

7.3.1 Enhancement of PS extraction by ultrasound

Table 7-1 shows the total extract and PS yields attained by UAE and water extraction (40ºC) for various extraction periods. At all the time points, the total extract and PS yields by UAE were notably higher than those by water extraction. With 80-min UAE, for instance, the total extract yield was increased by 35% (net increase 0.17 g/g) and the PS yield was increased by double compared with those of water extraction.

Table 7-1. Comparison of the total extract and PS yields by UAE and water extraction (WE) at 40^{o}C (solid-liquid ratio: 1/30 g/mL; mean particle size: 156.5 μm).

Time (min)	Total extract yield (g/g)		PS yield (g/g)	
	UAE	WE	UAE	WE
10	0.540 ± 0.026	0.443 ± 0.020	0.122 ± 0.011	0.081 ± 0.005
20	0.588 ± 0.051	0.450 ± 0.076	0.145 ± 0.016	0.081 ± 0.006
40	0.615 ± 0.033	0.462 ± 0.052	0.154 ± 0.026	0.083 ± 0.010
80	0.658 ± 0.035	0.488 ± 0.031	0.180 ± 0.028	0.085 ± 0.004

Note: Yield in this table is *m/M*, inclusive of m_o attained before UAE

7.3.2 Effects of process factors on UAE yields

Fig. 7-1 shows the UAE time courses of total extract and polysaccharide yields with respect to the four process variables in an overall period of 80 min. In most of these figures, the yields increased with time more rapidly in the early period (10-20 min) and slower in later period (after 20 min). The increase in ultrasound intensity from 2.44 to 44.1 W/cm^2 (or power density from 30.7 to 856.6 kW/m^3) resulted in increases in both total extract and PS yields (Fig. 7-1a), proving the enhancing effect of ultrasound on the extraction. Both yields also increased with the increase in temperature from 40 to 70 ºC (Fig. 7-1b) and the decrease in particle size from 156.5 to 750 μm (Fig. 7-1c). Increasing temperature promotes diffusion mass transfer, and reducing particle size increases the mass transfer area, contributing to the enhanced extraction. However, temperature increase from 55 to 70 ºC led to a notable increase in the PS yield but not in the total extract yield. This was due probably to that the dissolution of PS from the mycelia with water was more dependent on a higher temperature than the dissolution of low molecular weight components. Increasing the solid-liquid ratio or reducing the liquid volume resulted in a higher PS yield but no significant change in the total extract yield (Fig. 7-1d).

.

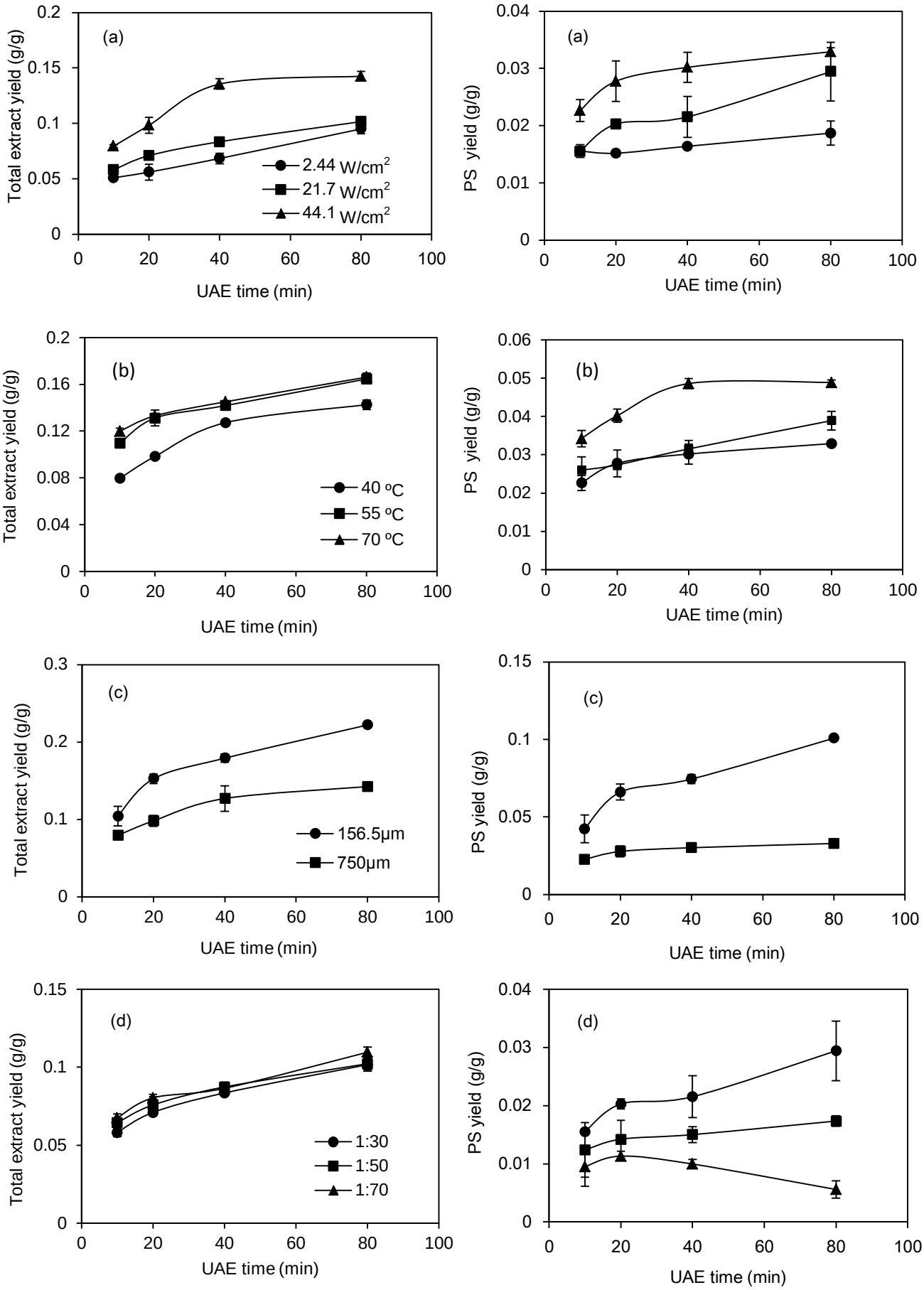

Fig. 7-1. Time courses of total extract yield (left) and PS yield (right) during UAE of fungal mycelia performed with four process variables: (a) Ultrasound intensity (W/cm^2); (b) Temperature (^{o}C); (c) Mean solid particle size (μm); (d) Solid-liquid ratio (g/mL). (The other three variables were fixed at the levels as noted under Table 7-2).

7.3.3 Kinetic models for UAE

Table 7-2 shows the model constants and correlation coefficients (R^2) obtained from linear regression fit of the experimental data to the two kinetic models. The total extract yields in all conditions were fitted closely to the two models as indicated by the high R^2 values in the range of 0.937-0.999. The PS yields also fitted closely to the models with R^2 values in the range of 0.935-0.977 in most conditions. Fig. 7-2 shows the plots of experimental data with the linearized parabolic model (y *versus* $t^{½}$) against four experimental variables, including ultrasound intensity (Fig. 7-2a), temperature (Fig. 7-2b), mean particle size (Fig. 7-2c) and solid-liquid ratio (Fig. 7-2d), which demonstrate a close fit of experiment data to the kinetic model in most cases. However, the regression results do not show a significant trend of the model constants y_o, y_1, β and n with the process variables. The power-law constant β and exponent n varied from 0.0241-0.0836 and 0.154-0.354 respectively for the total extract yields, and from 0.0081-0.0195 and 0.172-0.399 respectively for most of the PS yields (except for the two PS yields with poor fit $R^2 < 0.8$) (Table 7-2).

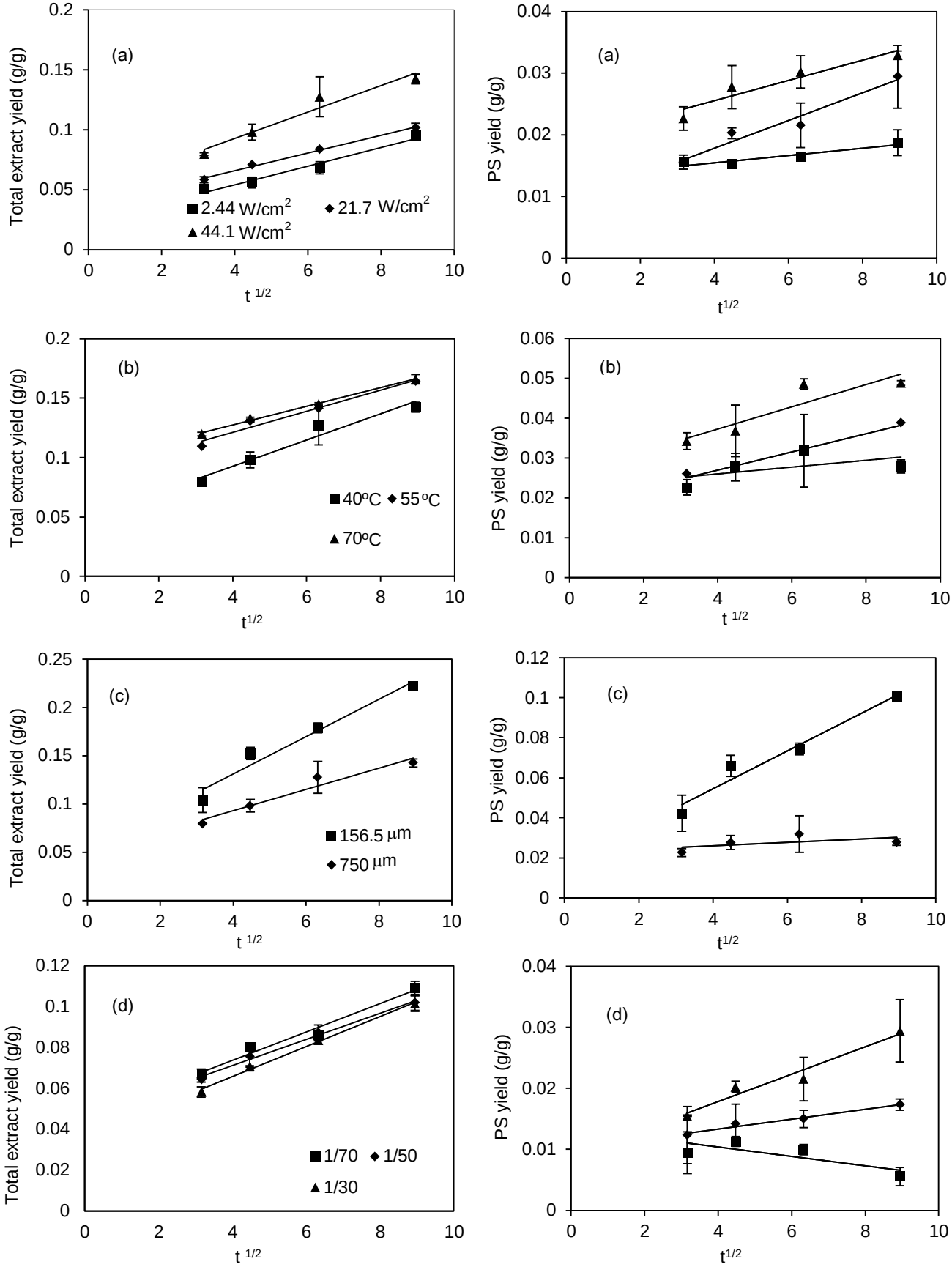

Fig. 7-2. Fitting of UAE experimental data (left: total extract yields; right: PS yields) (markers) to linerized parabolic diffusion model (lines) with four process variables: (a) Ultrasound intensity (W/cm2); (b) Temperature (^{o}C); (c) Mean solid particle size (µm); (d) Solid-liquid ratio (g/mL). (Error bars for SD at n =3; Experimental data same as shown in Fig. 7-1.)

Table 7-2. Kinetic model constants and correlation coefficients for the total extract and PS yields of UAE derived from linear regression of experimental data.

UAE conditions		Parabolic diffusion (Eq. 7-2)			Power-law (Eq. 7-3)			
		y_0, g/g	y_1, $min^{-1/2}$	R^2	β	n	$k = \beta n$	R^2
Total extract yield								
Power intensity [a] (W/cm^2)	2.44	0.0231	0.0078	0.969	0.0241	0.300	0.0072	0.937
	21.7	0.0363	0.0074	0.995	0.0317	0.265	0.0084	0.999
	44.1	0.0487	0.0110	0.950	0.0414	0.289	0.0122	0.980
Mean particle size [b](μm)	156.5	0.0535	0.0193	0.960	0.0484	0.354	0.0171	0.964
	750	0.0487	0.0110	0.950	0.0414	0.289	0.0120	0.980
Temperature [c] (±3 °C)	40	0.0487	0.0110	0.950	0.0414	0.289	0.0120	0.980
	55	0.0855	0.0089	0.969	0.0725	0.1860	0.0135	0.980
	70	0.0962	0.0078	0.995	0.0836	0.154	0.0129	0.992
Solid to liquid ratio [d] (g/mL)	1/70	0.0460	0.0069	0.974	0.0403	0.222	0.0089	0.964
	1/50	0.0455	0.0064	0.992	0.0387	0.221	0.0085	0.999
	1/30	0.0363	0.0074	0.995	0.0317	0.265	0.0084	0.999
PS yield								
Power intensity [a] (W/cm^2)	2.44	0.0131	0.0006	0.869	0.0121	0.0897	0.0011	0.763
	21.7	0.0088	0.0022	0.954	0.0082	0.282	0.0023	0.943
	44.1	0.0189	0.0017	0.902	0.0156	0.175	0.0023	0.950
Mean particle size [b](μm)	156.5	0.0168	0.0094	0.959	0.0178	0.399	0.0071	0.952
	750	0.0189	0.0017	0.902	0.0156	0.175	0.0023	0.950
Temperature [c] (±3 °C)	40	0.0189	0.0017	0.902	0.0156	0.175	0.0023	0.950
	55	0.0179	0.0023	0.976	0.0160	0.1943	0.0031	0.934
	70	0.0257	0.0025	0.979	0.0216	0.195	0.0042	0.939
Solid to liquid ratio [d] (g/mL)	1/70	0.0135	-0.0008	0.619	0.0195	-0.243	-0.0047	0.463
	1/50	0.0101	0.0008	0.971	0.0081	0.172	0.0014	0.977
	1/30	0.0088	0.0022	0.954	0.0082	0.282	0.0023	0.943

[a] Temperature = 40 ºC; Mean particle size = 750 μm; Solid-to-liquid ratio = 1/30 (corresponding power densities: 30.7, 272.7, 856.6 kW/m^3).

[b] Temperature = 40 ºC; Power intensity = 44.1 W/cm^2; Solid-to-liquid ratio = 1/30.

[c] Mean particle size = 750 μm; Power intensity = 44.1 W/cm^2; Solid-to-liquid ratio = 1/30.

[d] Temperature = 40 ºC; Mean particle size = 750 μm; Power intensity = 21.7 W/cm^2.

(Mass of extract in water before UAE (m_o in Eq. 7-1): 0.327±0.0161 total extract and 0.0235± 0.0059 PS, except for the cases with mean particle size of 156.5 μm, m_o = 0.436±0.0029 total extract and 0.0792±0.0055 PS).

7.4 Discussion

The results in Table 7-1 proved the enhancement of extraction by the application of power ultrasound. The more significant increase in the PS yield suggests that the UAE was more effective or favourable for the extraction of high molecular weight constituents than low molecular constituents, which were contained in the total extract. As most polysaccharides exist as the structural components of cell walls, high-intensity ultrasound may cause the breakup of cell walls through cavitation to release the wall constituents into the extracting solvent. Water at a relatively low temperature (~40 ºC) does not cause significant disruption of the cell walls and is not effective to extract the cell wall polymers.

Increasing temperature promotes diffusion mass transfer, and reducing particle size increases the mass transfer area, contributing to the enhanced extraction. However, temperature increase from 55 to 70 ºC led to a notable increase in the PS yield but not in the total extract yield. This was due probably to that the dissolution of PS from the mycelia with water was more dependent on a higher temperature than the dissolution of low molecular weight components. As the liquid volume increases at a fixed ultrasound power (*P*), the power per volume (*P/V*) decreases, leading to lower PS yield. This resulted in the higher PS yield but no significant change in the total extract yield by increasing the solid-liquid ratio or

reducing the liquid volume (Fig. 7-1d). For the total extract, the yield is probably more dependent on the concentration-difference driving force which increases with the liquid volume (dilution effect). The decrease of PS yield shown in Fig. 7-1d with time from 40 to 80 min at 1/70 solid-liquid ratio may be attributable to the degradation of the PS extracted into the liquid by the high mechanical force of cavitation, which tends to be more intense in a liquid with low solid content and low PS concentration (Mason & Lorimer, 2002).

The lack of correlation for the model constants y_o, y_1, β and n with the process variables was probably attributed to the empirical nature of the models and the complex effect of various factors on the extraction process, plus experimental errors (in the control of experimental conditions and the measurement of extract yields). Table 11 also shows the rate constant, $k = \beta n$, which is from the derivative of power law Eq. 7-3,

$$\frac{dy}{dt} = kt^{n-1} \qquad \text{(Eq. 7-4)}$$

In most cases, k value for the total extract yield increased with the increase in ultrasound intensity and the decrease in particle size, and k value for the PS yield increased with ultrasound power and extraction temperature, and the decrease in particle size. Solid-liquid ratio had a significant effect on the PS extraction rate but only slight effect on total extraction rate. Ultrasound power and temperature also had more significant effect on the PS extraction rate than the total extraction rate. Most of the factor effects on the rate followed the same trends as on the yields of extraction (Fig. 7-1).

The result of ultrasonic treatment (e.g., improved extraction yield and/or rate) is a function of the power (P) and exposure period (*t*). These two variables can be combined into a total ultrasonic energy, the product of power and exposure period, $E = P \times t$. Here, we introduce two scalable ultrasonic process parameters independent of the volume of liquid, i.e. the power and energy per volume (V) of liquid, *P/V* (power density) or and *E/V* (energy density). The extraction rate for total extract represented by Eq. 7-4 at various conditions showed a significant and linear correlation to *P/V* (Fig. 7-3) with $R^2 > 0.80$ and the slope of line, representing the enhancing effect of ultrasound power on the extraction rate, decreased with time. Based on regression analysis, the experimental data of total extract yield showed a significant correlation to *E/V* (Fig. 7-4a) with an $R^2 > 0.80$; while the PS yield had a relative poor correlation to *E/V*, with a $R^2 > 0.75$ (Fig. 7-4b).

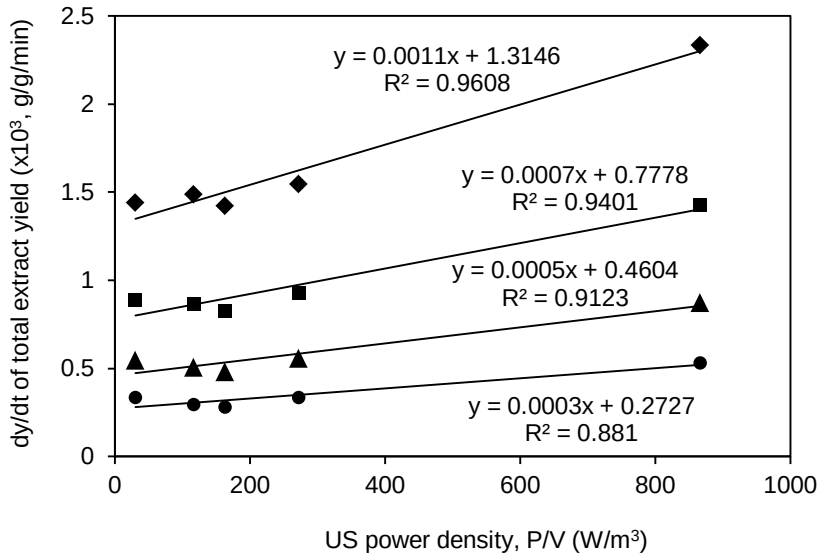

Fig. 7-3. Correlation of extraction rate (*dy/dt*, *y* = total extract yield) with ultrasound power per unit volume of liquid over various extraction periods (◆10 min ■ 20 min ▲ 40 min ● 80 min) (constant temperature 40 ºC and mean particle size 750 µm).

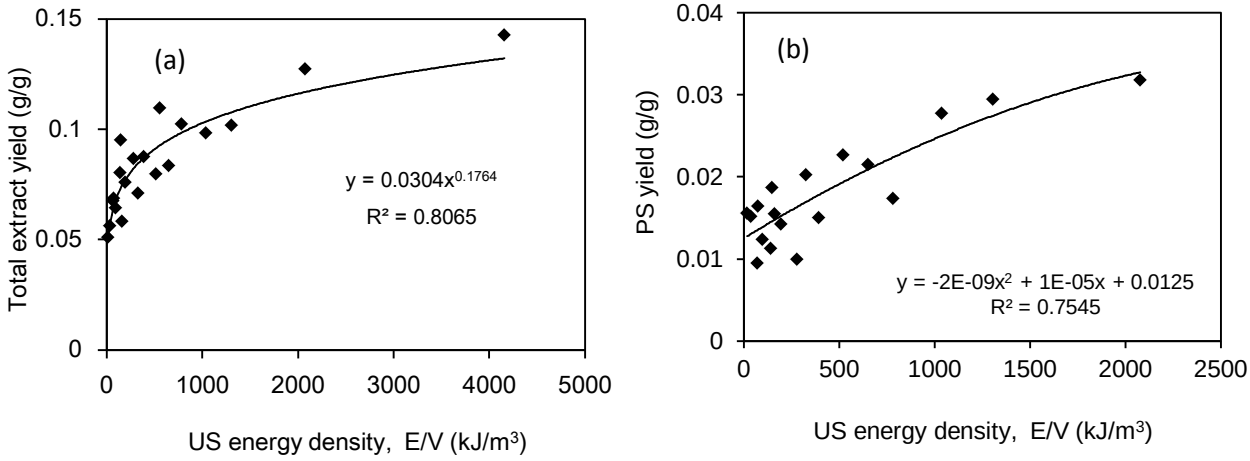

Fig. 7-4. Correlations of total extract yield (a) and PS yield (b) with ultrasound energy *E* per unit volume of liquid (temperature 40 ºC and mean particle size 750 µm).

7.5 Summary

The UAE kinetics of water soluble components and polysaccharides from a medicinal fungus at various operating conditions and particle sizes can be adequately represented by two empirical models, parabolic diffusion and power-law. According to the modelling analysis, power ultrasound mainly enhanced the slow diffusion step of extraction and only affected slightly the initial washing-out step. The models provide the quantitative relationship between the extract yield and extraction time, and the ultrasound power. The rate of extraction can be correlated to the ultrasound power per volume of liquid and the yield correlated to the ultrasound energy per volume of liquid. These scalable parameters may be useful for design, operation and scaling–up of UAE processes.

Part III

Ultrasonic degradation and modification of high molecular weight polysaccharides

Chapter 8 General materials and methods for ultrasonic modification

8.1 Ultrasonic treatment conditions

Ultrasonic treatment was performed with a Model VCX-130 ultrasonic processor with a probe horn of 20 kHz frequency and 130W power (Soncis & Materials Inc., Newton, USA). Polysaccharide solution was prepared in a 50-ml plastic centrifuge tube by dissolving 0.05 g lyophilized polysaccharide in 25 mL DI water (at the concentration of 2 g/L). The ultrasound probe (6 mm diameter) was submerged into the solution at a fixed depth of 2 cm. The centrifuge tube was placed in an ice bath throughout the sonication process for maintaining the treatment temperature at 40±5 ^{o}C. The power output of the processor is proportional to the amplitude setting. The ultrasound power intensity for the treatment was calibrated by calorimetric method as done in the part of UAE. Fig. 8-1 and Table 8-1 show the experimental results for the calibration of power intensity for US treatment.

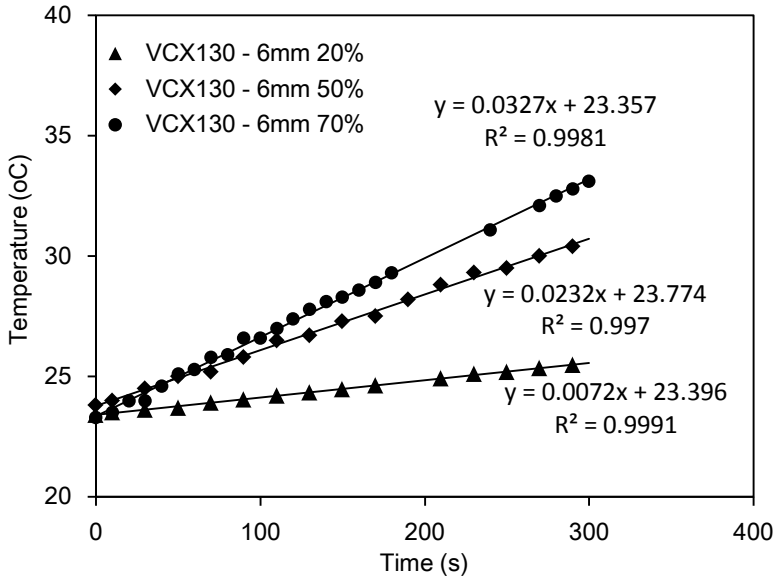

Fig. 8-1 Temperature (T) increase due to absorption of ultrasound energy from the 6-mm probe horn of ultrasonic processor VCX-130 during the initial 5 min period of sonication.

Table 8-1 Actual ultrasound power and intensity transferred into the polysaccharide solution corresponding to the amplitude reading in ultrasonic processor VCX-130 (by Eq. 4-1 and Eq. 4-2).

Processor	Amplitude	Probe tip D (mm)	*dT/dt* ($^oC/s$)	Power, P (W)	Intensity, I (W/cm^2)	Power density, P/V (kW/m^3) [a]
VCX130	70%	6	0.0327	13.7	48.4	564.7
	20%		0.0232	9.70	34.3	387.9
	20%		0.0072	3.01	10.6	120.4

[a] $I = P/\pi r^2 = P/\pi (0.6)^2$; $P/V = P/25 \times 10^3$ kW/m^3 (r = tip diameter/2 = 6 mm/2 = 0.3 cm; liquid volume of US treatment V = 25 mL).

8.2 Molecular weight properties of polysaccharides

As in the previous study of UAE, the molecular weight (MW) profiles of PS were analysed by high-pressure gel permeation chromatography (HPGPC) with the instruments and conditions reported previously in Chapter 4. Intrinsic viscosity [η] of 10 g/L of the polysaccharide solution was determined by the dilution method (Yan et al., 2009). An Ubbelohde viscometer of 0.5-0.6 mm capillary diameter was used for the measurement at 30 ± 0.1 ^{o}C. The value of [η] of each sample was found out by the linear regression method (Wang et al., 2010).

8.3 Particle size distribution of polysaccharide solution

Particles in solutions are in random movement due to the bombardment with the surrounding solvent molecules. Particle diffusion due to Brownian motion, which relates to the particle size, could be measured by scattering light through the polymer solution with a laser beam. Particle size should be related to the translational diffusion coefficient (D) by using the Stokes-Einstein equation (Dahneke, 1983),

$$\mathrm{D} = \frac{kT}{6\pi\eta d_h} \qquad \text{(Eq. 8-1)}$$

where d_h is the hydro-diameter, D is the translational diffusion coefficient , k is the

Boltzmann's constant, T is the absolute temperature and η is the viscosity. Particle size distribution (0.1 – 1000 μm) was first figured out based on the intensity of light scattering. Under the assumption that all particles are spherical and homogenous, the intensity distribution obtained could be transformed to base of the volume distribution (Dahneke, 1983). The relative dependency of intensity and volume distribution on the particle size should be d^6 (from Rayleigh's approximation) and d^3 (based on sphere volume $4/3\pi r^3$) respectively. The average hydro-diameter ($Z_{average}$ in nm) is mean size of the particles under measurement. It only gives a single value for particle size comparisons, but not the information on the entire size distribution (Camino et al. 2009; Gordon and Pilosof, 2010). In this study DLS was done by using a Malven Zetasizer (3000 HSA). Each measurement was an average of 5 sub measurements at a scattering angle of 90° at 25^{o}C with 1-2 g/L sample concentration, using distilled water as solvent. The intensity and volume distribution were analysed out by the Zetasizer 3000HSA-Advanced Software.

Chapter 9 Ultrasonic degradation and modification of a high-molecular-weight polysaccharide of Cs-HK1

9.1 Introduction

High-intensity ultrasound (16-100 kHz, 10-1000 W/cm^2) is regarded as a safe and convenient food processing method, widely applied in the food industry for the last 10 years. *Cordyceps sinensis,* which is commonly called Dong chong xia cao, has demonstrated health-prompting effects on humans (Li & Tsim, 2004). Due to its rarity and increasing marketing demand, laboratory cultivation by fermentation has been developed. Mycelia cultivation of *C. sinensis* Cs-HK1 has been well established from the wild *Cordyceps* by our group for a few years (Leung et al., 2009). A fraction of exopolysaccharides (EPS) with significant high-molecular weight (>500 kDa) was separated from the liquid culture medium, and has been proved to show strong immunomodulation properties on a mammalian cell line. Besides EPS, intracellular polysaccharides (IPS) extracted from the Cs-HK1 mycelia were also found to enhance the immunomodulation activities in humans (Yan et al., 2011). Because of the differences in growth environment, the molecular structures and the relative physicochemical properties of the EPS was totally different from that of the IPS. In this part of study, we investigate how the molecular structures and physicochemical properties of IPS

are affected under various sonication conditions of time duration and power intensity. The obtained results could be used to be compared with the sonication effect on EPS done our previous study (Wang et al., 2010). This helps to predict the relationship between the sonication effect and the original molecular structure of the polymer being treated.

9.2 Materials and methods

9.2.1 Medicinal mushroom

Cs-HK1 fungus was previously isolated from the fruit body of a wild *Cordyceps sinensis* by our group (Leung *et al*., 2006). Cs-HK1 mycelial liquid fermentation was performed in a culture medium which contains 40 g/L glucose, 10 g/L yeast extract, 5 g/L peptone, 1 g/L KH_2PO_4 and 0.5 g/L $MgSO_4 \cdot 7H_2O$, on a shaking incubator at 150 rev/min at 25^{o}C for 7 days . After fermentation, the mycelia broth was separated from the liquid medium (supernatant) and the mycelia (precipitate) by high speed centrifugation. The mycelia were dried by spray-drying method. The dried mycelia were grounded into powder with an electric mill, screened through a 250-μm mesh sieve and stored at 25^{o}C before use.

9.2.2 Extraction and purification of PS

Extraction was carried out by mixing powders of Cs-HK1 mycelium with de-ionized (DI) water in a solid to solvent ratio of 1:30 to reflux for 2 hours. Extract solution was separated from mushroom residue by centrifugation of 6000 rpm for 10 minutes. Deproteination of the solution was done by the method of Sevag (Staub, 1956) for 8 times. The polysaccharide solution was mixed with 5-fold of ethanol (final concentration of ~80%) for overnight precipitation at 4 ^{o}C. The precipitates were redissolved in 200 ml DI water to dialysis (6000-8000 Da) for at least 2 days. The polysaccharide solution after dialysis was reduced in volume by rotatory evaporator for freeze-drying. The lyophilized polysaccharides (IPS) were stored in desiccator at room temperature before use.

9.2.3 Ultrasonic treatment of IPS

Ultrasonic treatment was done at fixed power of 20% and 70% amplitude (corresponding to a power intensity of 10.6 and 48.4 W/cm^2 tip surface respectively). Polysaccharide solution was sonicated under selected periods of time (2 to 60 minutes). After treatment the solution was re-lyophilized and the sonicated polysaccharide sample was stored in desiccator at room temperature before use.

9.2.4 Morphological study by transmitted electron microscopy (TEM)

The morphology of the polysaccharides before and after US treatment was compared directly by imaging through a JEOL 100 CXII TEM. Polysaccharide solution of 20 uL in 0.05 g/L was sprayed on a copper grid. The copper grid was then stained by 2% (w/v) ammonia molybdate tetrahydrate solution for 1-2 minutes after the polysaccharide solutions were dried. The image of the polysaccharide sample was captured at 100 kV accelerating voltage under different magnification.

9.3 Results

9.3.1 Ultrasonic effect on polysaccharide morphology

The morphological change of PS from *C. sinensis* by ultrasonic treatment was observed through TEM. As shown on Fig. 9-1a, the polysaccharides were originally in round-shape and clouded as a cluster with a diameter of about 200 nm. Through sonication by a lower power (20% amplitude), the cluster of polysaccharides was destroyed and the aggregation was reduced, forming a main network with thin cross-linked branches in the initial sonication period (2 min) (Fig. 9-1 (b1)). After longer treatment time, the network was disbanded and more seriously distorted (Fig. 9-1 (b2)). However, the morphology was greatly changed by the application of high power (70% amplitude). Fig. 9-1 (c1) and (c2) show that by a short

period of sonication treatment, the polysaccharides were modified from circular shape to longitudinal shapes in cluster form, and the size of cluster was increased with treatment period (from 2 to 10 minutes). After a prolonged period of high power sonication (60 minutes in 70% amplitude), the polysaccharides were totally broken down into small fragments of length less than 50 nm (Fig. 9-1 (c3)).

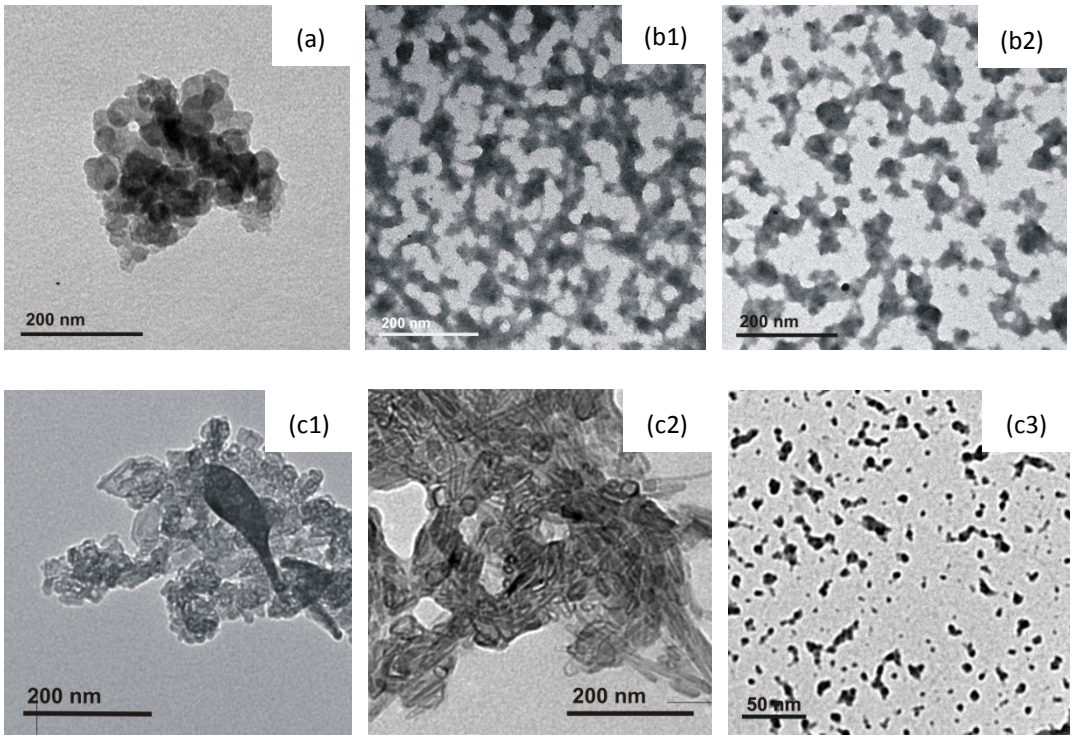

Fig. 9-1. TEM images of Cs-HK1 polysaccharides solution (0.05 g/L) before and after various conditions of US treatment: (a) before US (b1) 2 minutes in 20% amplitude (b2) 60 minutes in 20% amplitude (c1) 2 minutes in 70% amplitude (c2) 10 minutes in 70% amplitude (c3) 60 minutes in 70% amplitude.

9.3.2 Ultrasonic effect on particle size distribution

Fig. 9-2 shows the particle size distribution on the dependency of the scattering intensity and volume population of the polysaccharide solution upon sonication treatment of 20% and 70% amplitude. The original polysaccharide solution without any sonication treatment showed a monomodal particle size distribution in % intensity (Fig. 9-2 (a1 and b1)) with a mean size of 81.9 nm (Table 9-1). By increasing the sonication time for both 20% and 70% amplitudes, it was observed that such size population was gradually decreased in % intensity and shifted to a smaller mean size of about 40 – 50 nm, and two new size populations of mean size at about 250 nm and 1500 nm eventually appeared with increasing % intensity. On the other hand by the treatment of 70% amplitude, the intensity distribution shifted to larger size within 10 minute sonication time, and eventually shifted back to smaller ones after prolonged period.

By referring to the particle size distribution in % volume (Fig. 9-2 (a2 and b2)), it was observed that the newly formed particle fractions with mean size of about 250 nm and 1500 nm were both significantly low in % volume. This means that such newly formed particle fractions only accounted for a very small proportion of the whole polysaccharide solution. The major particle population of the polysaccharide solution was still with a mean size of about 40 nm. Therefore the intrinsic viscosity of the polysaccharide solution was still

decreased with treatment time, and not being affected by the newly formed large particle fractions.

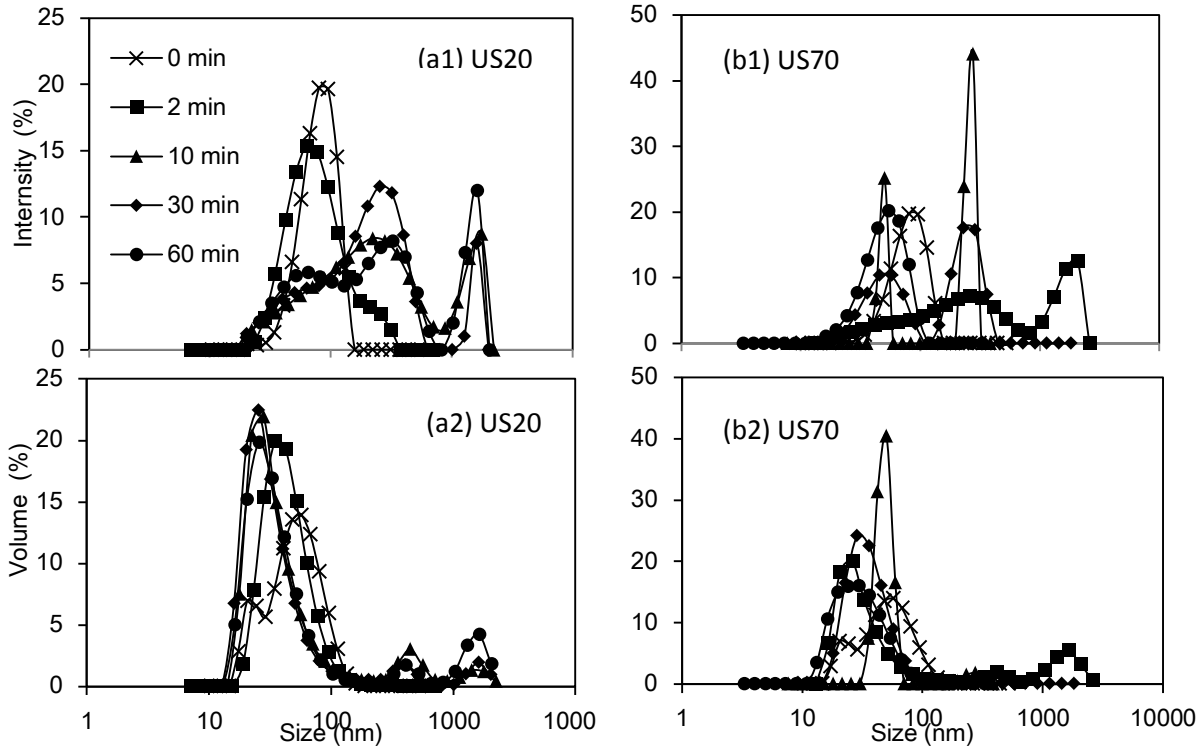

Fig. 9-2. The variation of particle size of Cs-HK1 polysaccharide solution based on (1) intensity of light scattering and (2) volume distribution upon ultrasonic treatment at 2 g/L sample concentration under amplitude of 20% (US20) 70% (US70).

Table 9-1. Variation of mean particle size of Cs-HK1 polysaccharide solution upon ultrasonic treatment at 2 g/L sample concentration under the amplitude of 20% (US20) and 70% (US70).

US Amplitude	US Time (min)	Mean size by Intensity (nm) (Area %)			Mean size by Volume (nm) (Area %)		
		Peak 1	Peak 2	Peak 3	Peak 1	Peak 2	Peak 3
-	0	81.9 (99.3)	-	-	23.4 (20.6)	59.3 (79.4)	-
20%	2	89.3 (100)	-	-	45.9 (100)	-	-
	10	223 (79.5)	1469 (20.5)	-	37.6 (87.5)	467 (8.4)	1487 (4.1)
	30	200 (91)	1563 (9)	-	34.6 (91.2)	373 (4.8)	1601 (3.9)
	60	69.1 (36.4)	297 (43.2)	1455 (20.4)	35.8 (84.6)	399 (4.4)	1491 (11)
70%	2	232 (64.8)	1632 (35.2)	-	34 (78.2)	407 (5.1)	1538 (16.7)
	10	48.4 (32)	259 (68)	-	48 (95.6)	262 (4.4)	-
	30	51.4 (44.5)	251 (55.5)	-	36.8 (97.8)	268.8 (2.2)	-
	60	52.5 (100)	-	-	32.2 (100)	-	-

9.3.3 Ultrasonic effect on viscosity

Fig. 9-3 shows the intrinsic viscosity of the polysaccharide solution as a function of the sonication time for 20% (US20) and 70% (US70) amplitude. The intrinsic viscosity was decreased significantly (about 25% and 40% for US20 and US70 respectively) upon a 10-minute sonication time. For 20% amplitude the viscosity was further decreased by increasing the period of ultrasonic treatment. The viscosity was overall decreased by about 50% for 60-minute sonication. However, for 70% amplitude the viscosity of the polysaccharide solution by 60-minute sonication was higher than that by 30-minute treatment, which resulted in an overall decrease of about 30% only.

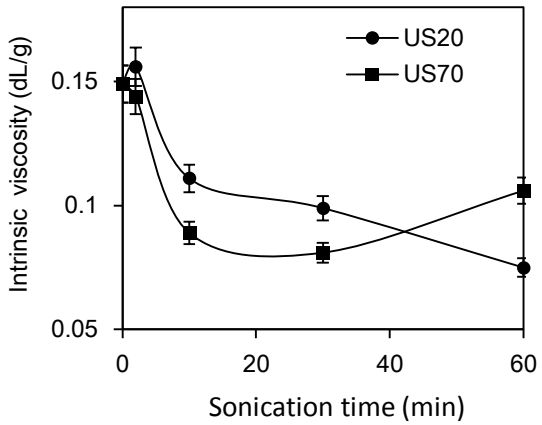

Fig. 9-3. Variation of intrinsic viscosity (dL/g) of polysaccharide solution extracted from *C. sinensis* Cs-HK1 upon ultrasonic treatment at 2 g/L sample concentration under amplitudes of 20% (US20) and 70% (US70).

9.3.4 Ultrasonic effect on MW distribution

The GPC chromatogram of the original polysaccharide solution (without any sonication treatment) shows two major peaks (peak 1 at 12.50 min and peak 2 at 34.73 min) were present (Fig. 9-4). This means that the polysaccharide solution was a composite of molecular fractions of different MW. By referring to the retention times of dextran standards of different known MW, the retention time of peak 1 was shorter than that of the dextran standard sample with the highest MW (670 kDa), which indicates that that the polymer solution consisted the MW fraction larger than 670 kDa. The relative MW of peak 2 should be around 1.4 kDa according to the calibration curve. From the GPC profiles of the ultrasound-treated polymer solution, it was observed that the sonication treatment caused no significant effect on the retention time of two major peaks, but instead on the relative peak areas. Table 9-2 lists the changes of the retention time and % peak area of peak 1 and peak 2 upon the increasing sonication period. At 20% amplitude ultrasound treatment, the peak area of peak 1 was significantly decreased for about 80% while the peak area of peak 2 was doubled. On the other hand, at the initial period (2 – 30 minutes) of the 70% amplitude treatment the peak area of peak 1 was even smaller than that at 20% amplitude treatment while area of peak 2 was nearly double the original one, similar to that treated at 20% amplitude. However, there was an increase (about 50%) of peak 1 area and without significant change of peak 2 area when

the polymer solution was treated under such high power (70% amplitude) for the period of 60 minutes.

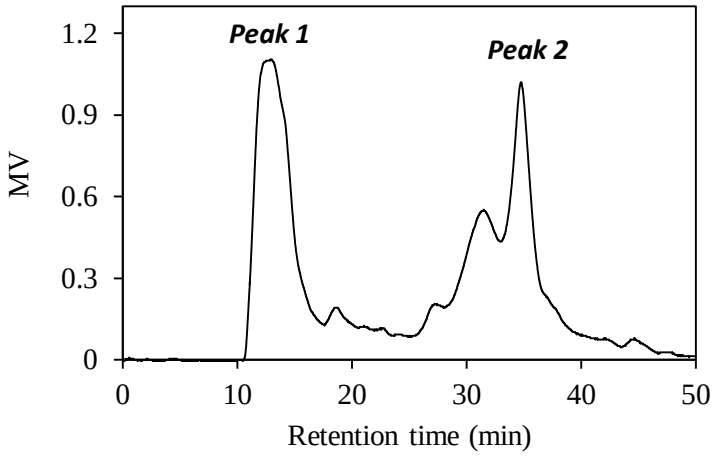

Fig. 9-4 Molecular weight distribution of polysaccharides extracted from *C. sinensis* CS-HK1 without US treatment.

Table 9-2. Retention time (RT in minute) and the relative % Area of selective main peaks of the MW profiles (referring to Fig. 9-4) of polysaccharide solution extracted from *C. sinensis* CS-HK1 upon various conditions of US treatment.

US Amplitude	US Time (min)	Peak 1		Peak 2	
		RT (min)	Area (%)	RT (min)	Area (%)
-	0	12.50	49.18	34.73	27.07
20%	2	13.62	86.40	35.68	2.71
	10	14.00	11.82	33.97	63.77
	30	13.70	5.21	34.67	72.06
	60	13.93	10.00	33.98	60.92
70%	2	14.44	7.66	34.36	76.11
	10	13.70	9.35	34.98	66.74
	30	14.08	8.99	35.14	63.95
	60	13.93	72.37	35.08	22.48

9.4 Discussion

The TEM observation of the Cs-HK1 PS (Fig. 9-1) proved that sonication power and time caused different effects on the morphology of the polymer being treated. At low power intensity, even upon a long treatment period the shear force induced by cavitation was only enough for de-aggregation, causing a superficial conformation change. However, upon high power intensity, even for a short period of time the energy was high enough for breaking the

chemical bonding and resulted in an actual conformation change of the polymer molecules. Since the light scattering energy is proportional to the molecular weight, the intensity shifts towards large particle size (Dahneke, 1983).

The detection of the two new size populations of mean size at about 250 nm and 1500 nm with increasing % intensity (Fig. 9-2) confirmed that large particles were formed in the polysaccharide solution upon sonication treatment. Such large particles may be due to the self-aggregation of the degraded polysaccharide molecules. As observed by the TEM images (Fig. 9-1 (b1-2)), the polysaccharide particles were degraded into the smaller ones in a thin cross-linked branch network by lower power (20% amplitude) upon sonication time. Such network may exist in the form of pseudo-large particles in solution, which induced the detection of the new larger size populations. By the treatment of 70% amplitude, the intensity distribution tended to shift to larger size within 10-minute sonication time, and eventually shifted back to smaller ones after prolonged period (Fig. 9-2). This result is in good agreement with the TEM images (Fig. 9-1 (c1-3)). Camino et al. (2009) reported that large particles were produced by ultrasonic treatment of hydroxypropyl methyl cellulose (HPMC), which was due to the rapid self-association caused by the hydrophobic patches in the HPMC after sonication. This confirmed that sonication treatment may induce aggregation.

The intrinsic viscosity was reduced with increasing period of ultrasonic treatment by 20% amplitude, but attained the optimum effect at around 20 minutes of sonication time for

70% amplitude. This may be related to the energy released during the ultrasonic treatment. The energy released by 60-minute sonication of 20% amplitude was about 0.52 kJ/cm^3, and the one released by 30-minute and 60-minute sonication of 70% amplitude was about 0.88 kJ/cm^3 and 2.0 kJ/cm^3. The ultrasonic treatment may become not effective on reducing the viscosity of the PS solution when the energy is above a certain level (~0.8 kJ/cm^3). The other possible reason for these results may be due to the different sonication effect at different ultrasound power (Soria & Villamiel, 2010). At lower sonication power (20% amplitude), aggregates of polymer molecules may be broken up by the shear force generated by the cavitation. As time increases, cavitation energy increases which enhances the break-up effect. This lowers the viscosity of the polymer solution when increasing the sonication period. At higher power effect (70% amplitude), much higher energy was released by the cavitation. The induced shear forces may be strong enough to cause bond-breaking instead of de-aggregation. This created polymers with shorter molecular size, and resulted in decreased viscosity when increasing the period of time (Wang et al., 2010). At the mean time bond-breaking may also have changed the conformation of the polymer. At a certain point of re-arrangement, the molecules with smaller molecular sizes may combine again to form new aggregation, although such aggregation will still have a smaller size than the original structure (Farzi et al. 2011). The TEM image in Fig. 9-1 (c3) showed the evidence for that suggested reason. This explained the higher viscosity of the polysaccharide solution after 60-minute treatment than

that after 30-minute treatment at 70% sonication amplitude. The GPC results supported the explanation of the intrinsic viscosity results. The destruction of the aggregation by the lower power intensity resulted in the MW distribution shift from higher MW to lower ones upon sonication period. For prolonged treatment period (up to 60 minutes), it induced the increase in the portion of higher MW fractions, therefore resulting in the higher viscosity at 60-minute treatment than at 30 minutes.

Yan et al. (2010) have reported that the EPS from Cs-HK1 consisted of a structure with a backbone of (1→6)-α-D-glucose residues and (1→6)- α-D -mannose residues , and branch chains composed of an (1→6)- α-D-mannose residue and five (1→6)- α-D-glucose residues and β-D-galactose residues (Fig. 9-5a). On the other hand, Yan et al. (2011) have also reported that the water-soluble IPS extracted from the mycelia of Cs-HK1 was characterized by a backbone of (1 → 4)-linked-α-D-glucose residues with short branch of (1 → 6)-linked-α-D-glucose residues (Fig. 9-5b). The molecular structures showed that EPS has higher MW, with much larger particle size than IPS. This resulted in much higher initial intrinsic viscosity of EPS (about 14 dL/g) (Wang et al., 2010) than that of IPS (about 0.15 dL/g). As reported by Wang et al. (2010), the intrinsic viscosity of EPS was not significantly decreased by 20% amplitude sonication, but 85% decrease was obtained by 70% amplitude. Compared to the results in this current study, under the same sonication conditions, the

intrinsic viscosity of IPS was decreased only 40% by 70% amplitude but the sonication effect of 20% amplitude was more significant than that on EPS. Molecules with large MW should be more susceptible to the attack by the cavitation energy. This is because smaller molecules have shorter relaxation times, and therefore can resist more easily to the sonication stress. In the meantime, the attractive forces among macromolecules increased with the viscosity. This induced a higher threshold intensity of sonication for the onset cavitation (Zhou et al., 1998; Liu et al, 2006; Iida et al., 2008). Gordon and Pilosof (2010) reported that the mean particle size of whey protein isolate was found to be increased with concentration by dynamic light scattering measurement. By confocal microscopy, it was observed that sonication effect on 15 wt% was more severe than that on 7.5 wt% sample solution under the same ultrasound conditions. This also proved the relationship between molecular size and the sonication effect.

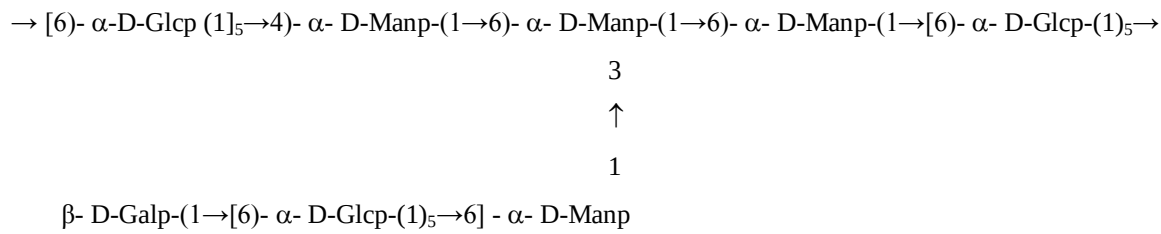

Fig. 9-5a. Repeating units of EPS of Cs-HK1 (Yan et al., 2010).

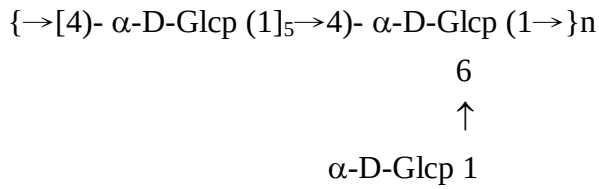

Fig. 9-5b. Repeating units of water-soluble IPS of Cs-HK1 (Yan et al., 2011).

9.5 Summary

The intrinsic viscosity, molecular weight and particle size distribution of the Cs-HK1 polysaccharide solution, and the morphology of the relative molecules, were greatly affected to different extents by ultrasound of different power intensities and treatment periods. Comparing the results between IPS and EPS, it was demonstrated that the sonication effect depends not only on the sonication environmental factors, but also on the molecules being treated. The TEM results suggest that the ultrasound effect should not be kinetically considered by treatment time only, but together with the power intensity that is applied.

Chapter 10 Study of ultrasonic degradation mechanism with a known microbial polysaccharide (Curdlan)

10.1 Introduction

Curdlan, as our selected polysaccharide for these studies, is a microbial polysaccharide extracted from the proteobacteria, *Alcaligenes faecalis*. It is a water-insoluble linear polysaccharide consisted of β-(1,3)-linked glucose residues. According to the literature, curdlan has a high MW with the estimated average degree of polymerization of 450, and possesses a maximum of 12,000 units (Futatsuyama et al., 1999). Curdlan is soluble in alkaline conditions. As experimentally demonstrated, it there is a conformational transition from helical structure to random coil by dissolving curdlan in sodium hydroxide solution, with increasing concentration from 0.19M to 0.24M (Nakata et al., 1998). Therefore by dissolving curdlan in different concentrations of sodium hydroxide solution, known-structured polysaccharide with defined conformation could be obtained.

In the previous study of US treatment of IPS from *C. sinensis* Cs-HK1, it was demonstrated that US could be applied to modify the conformation of PS molecules and improve the solution properties. Comparing the results with the US degradation of EPS from Cs-HK1 (Wang et al., 2010), it was concluded that the polysaccharides with different initial

molecular structure/ conformation are susceptible to different US effect. The exact molecular structure, molecular weight and conformation in solution should be well defined for a clear understanding of US degradation kinetics. However, such information of the IPS or EPS is still under investigation. This study was conducted to characterize the US degradation mechanism of high-order structured PS based on the different conformations of a known-structured polysaccharide, curdlan, under different pH values of alkaline solution.

10.2 Materials and methods

10.2.1 Polysaccharide sample

Curdlan powder from *Alcaligenes faecalis* (Sigma, USA) was used in the study, and the sample was stored at 4^{o}C before use. Curdlan solution was made by dissolving the sample powder in 0.1M (~pH 11.8) and 0.3M sodium hydroxide (NaOH) (~pH 13.8) solution for 2 hours at room temperature with stirring.

10.2.2 Ultrasonic treatment conditions of curdlan

Ultrasonic treatment was done at power of 20%, 50% and 70% amplitude (corresponding to a power intensity of 10.6, 34.3 & 48.4 W/cm^2 tip surface respectively). Selected periods of time between 2 to 60 minutes were selected to study the time effect of the sonication

treatment. The US-treated curdlan solution was subjected to solution properties measurements immediately after the sonication treatment.

10.2.3 Molecular weight determination by viscosity measurement

Intrinsic viscosity [η] of 2 g/L of the curdlan solution in NaOH was determined by the dilution method (Yan et al., 2009) using the Ubbelohde viscometer at 25 ± 0.1 ^{o}C. The viscosity-average molecular weight (M_v) of curdlan was determined by the Mark-Houwink equation as mentioned in Chapter 3,

$$[\eta] = KM_v{}^{a} \qquad \text{(Eq. 3-2)}$$

where K = 0.0079 and a = 0.78 for curdlan dissolved in 0.3M NaOH at 25 ^{o}C (Nakata et al., 1998); or K = 0.0032 and a = 0.85 for curdlan dissolved in 0.1M NaOH at 25 ^{o}C (Futatsuyama et al., 1999); [η] is the relative intrinsic viscosity in 0.1M and 0.3M NaOH.

10.2.4 Ultrasonic degradation kinetics model

Degradation of MW of curdlan in NaOH solution by sonication was substituted to the kinetic model suggested by Malhotra (1986),

$$\frac{1}{M_t} - \frac{1}{M_0} = kt \qquad \text{(Eq. 10-1)}$$

where k is the rate constant (mol/g·min) of the ultrasound degradation process; t is the sonication time (min); M_t and M_0 are the viscosity-average molecular weight (mol/g) at time t

and time 0 respectively. The values of *k* at different US power intensity (W/cm^2) were determined by the relative plot of ($1/M_t - 1/M_0$) against t.

10.2.5 Particle size distribution in alkaline solution

Particle size distribution of curdlan solution was determined by the dynamic light scattering method. The original curdlan solution with sonication was under measurement immediately and 24 hours after the dissolution in NaOH. The US-treated curdlan solution was also being measured immediately and 24 hours after the sonication treatment.

10.2.6 Gel formation by acidification

Due to the triple-helix conformation of curdlan molecules in solution, curdlan powders are weakly soluble in neutral conditions. A weak gel is formed by curdlan in alkaline solution when neutralized with acid. In order to test the US effect on the solubility of curdlan molecules in neutral solution, relative volume of 36% hydrochloric acid (HCl), which contained the same number of moles as NaOH, was added to each US-treated curdlan solution immediately after the sonication process, in order to neutralize the 25 mL NaOH solution. The mixture solution was mixed well by vortex. The gel formed after acidification was separated from the supernatant by centrifugation at 6000 rpm for 15 minutes. The gel was weighed after drying under 70^oC for 2 days.

10.2.7 Congo red – curdlan complex test

Congo red test was performed on the curdlan solution before and after sonication at different NaOH concentrations. The results helped to evaluate the sonication effect on the high-ordered conformation of the curdlan molecules in alkaline solution (Saitô et al., 1977; Ogawa and Hatano, 1978). Congo red was mixed with curdlan sample of 0.2% in 25 mL NaOH solution from 0.05 to 0.5 M (final concentration of 182 μL) before and after various sonication periods at the power intensity of 48.6 W/cm^2. The mixed solutions were then left standing at room temperature for 1 hour, and the wavelength of maximum absorbance (λ_{max}) of relative solution was recorded from 400 – 700 nm on a UV-vis spectrometer.

10.3 Results

10.3.1 Effect of ultrasonic power on intrinsic viscosity of curdlan

Fig. 10-1 shows the sharp decrease of intrinsic viscosity of curdlan solution after sonication treatment in both 0.1M and 0.3M NaOH. The initial intrinsic viscosity of curdlan solution on 0.1M NaOH (~4.25 dL/g) was higher than that in 0.3M NaOH (~2.5 dL/g). which should be due to the helical conformation of curdlan molecules in 0.1M NaOH while random coil was present in 0.3NaOH. Helix strucutre of molecules is rigid and tends to make

molecules to aggregate when dissolved in solution, which resulted in higher solution viscosity. In both conformations, the viscosity of the solution was decreased significantly by about 70% in the first 10-minute sonication, and eventually to a limited value with a total 90% decrease through the sonication at US 70% amplitude power. Results showed that the sonicaiton effect was increased with the sonication power applied. The same decreasing trend of viscosity through increasing sonication period after 24 hours of sonication confirmed the long-time effect of US. At 20% amplitude of 10.6 W/cm^2 power intensity, the energy may not be strong enough for a long-time US degradation effect on the curdlan molecules. Therefore it was observed that the viscosity induced by 20% amplitude power slightly increased up after 24 hours for both conformation.

The transition of conformation for the curdlan molecules by increasing concentration of NaOH was demonstrated by the variation of intrinsic viscosity from 0.1M to 0.5M NaOH (Fig. 10-2). The sharp depression of the viscosity at around 0.22M illustrates the conformation. Nakata et al. (1998) also identified the conformation change of curdlan molecules through this observation. Our experimental results showed that such specify change of viscosity at 0.22M did not exist for the curdlan solutions after 30-minute US treatment at 48.4 W/cm^2 power intensity. Instead, the intrinsic viscosity of solution was similar throughout the incresasing alkaline concentration. The results strongly confirmed that alteration of curdlan molecular conformation by US in alkaline conditions.

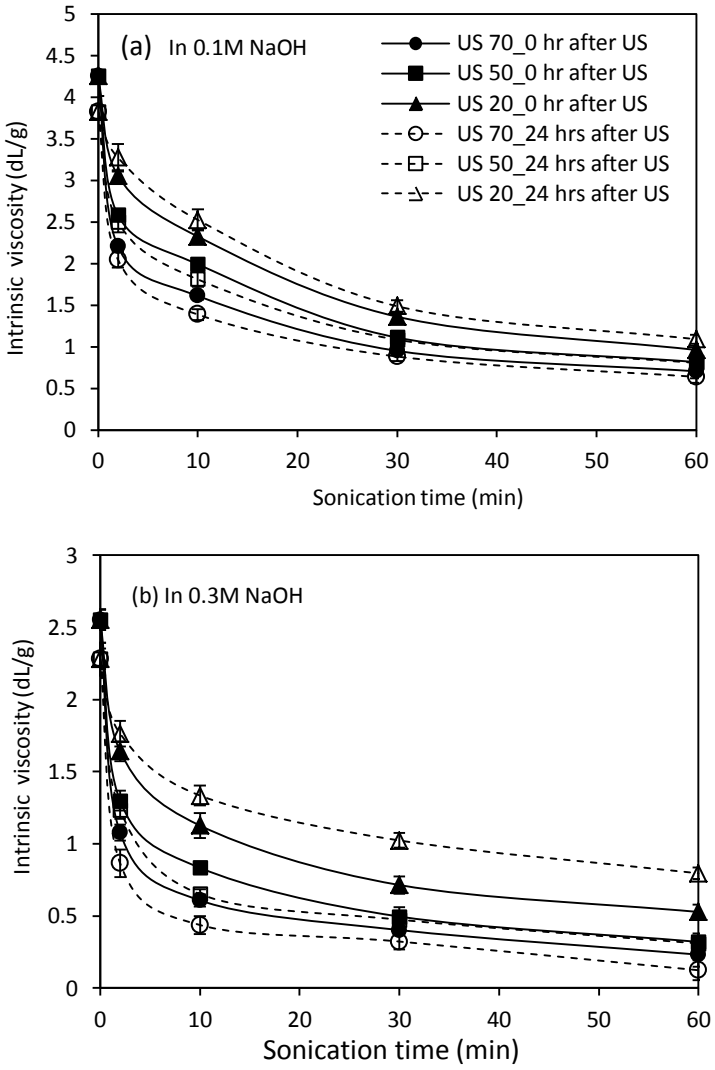

Fig. 10-1. Variation of intrinsic viscosity (dL/g) of 2 g/L curdlan solution in (a) 0.1 M and (b) 0.3M NaOH under ultrasound treatment at power intensity of 48.4 W/cm^2 (US 70), 34.3 W/cm^2 (US 50) and 10.6 W/cm^2 (US 20).

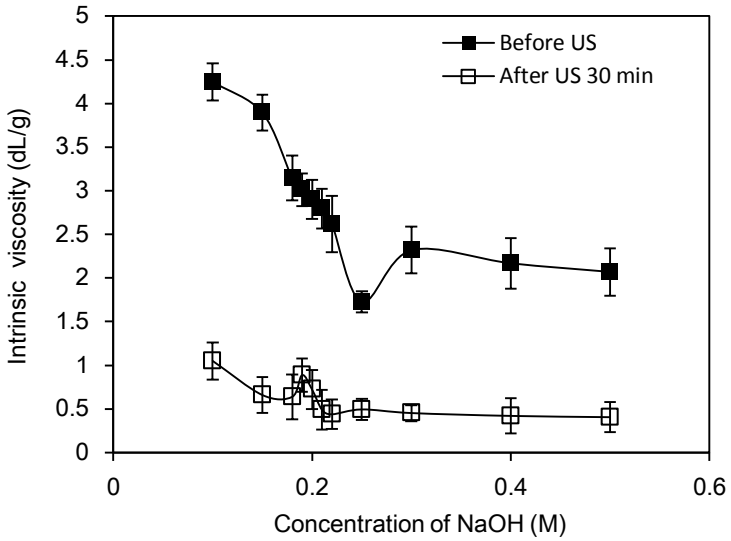

Fig. 10-2. Intrinsic viscosity (dL/g) of curdlan solution in various concentration of NaOH upon 30-minute ultrasonic treatment at 2 g/L sample concentration under power intensity of 48.4 W/cm^2 (measurement immediately after US treatment).

10.3.2 US degradation kinetics of curdlan

The relative viscosity-average molecular weight (MW) of curdlan before and immediately after sonication under various conditions was found by the measure intrinsic viscosity using the Mark-Houwink equation (Table 10-1). Degradation rate constant *k* was determined out as the slope of the kinetic model: $\frac{1}{M_t} - \frac{1}{M_0} = kt$ (Fig. 10-3). The value of *k* for degradation in 0.3M NaOH was found to be higher than that in 0.1M NaOH (Table 10-2), which suggested that the random coil conformation of curdlan molecules in 0.3M NaOH should be more favored for the degradation mechanism, rather than the rigid rod conformation in 0.1M NaOH. Besides, the degradation rate constant *k* was correlated to the power intensity being

applied (Fig. 10-4). It was found that for in both 0.1M and 0.3M NaOH, the value of *k* increased with the increasing power intensity that was applied. However, the increment of *k* against power intensity in 0.3M NaOH was much higher than that in 0.1M NaOH. This proved that degradation of random coil conformation could be more susceptible to the variation of power intensity applied than the rigid rod conformation.

Table 10-1. Viscosity-average molecular weight of curdlan before and immediately after sonication under various conditions.

US Power Intensity (W/cm^2)	US Time (min)	Curdlan in 0.1M NaOH Average viscosity MW, Mv	Curdlan in 0.3M NaOH Average viscosity MW, Mv
(Original)	0	165453	86196
48.4 (US 70)	2	71278	28515
	10	47697	13692
	30	24248	8066
	60	16500	3984
34.3 (US 50)	2	87309	36220
	10	62617	20523
	30	29590	10547
	60	19912	6022
10.6 (US 20)	2	108314	48908
	10	76345	30186
	30	38422	16836
	60	24596	11415

Table 10-2. Degradation rate constant *k* (mol/g·min) and correlation coefficient (R^2) of curdlan under ultrasound treatment at different power intensity (W/cm^2).

	Degradation rate constant, *k* (mol/g·min)		Correlation coefficient (R^2)	
Power intensity (W/cm^2)	0.3M NaOH	0.1M NaOH	0.3M NaOH	0.1M NaOH
48.4	0.0040	0.0010	0.932	0.982
34.3	0.0026	0.0008	0.977	0.952
10.6	0.0014	0.0006	0.971	0.914

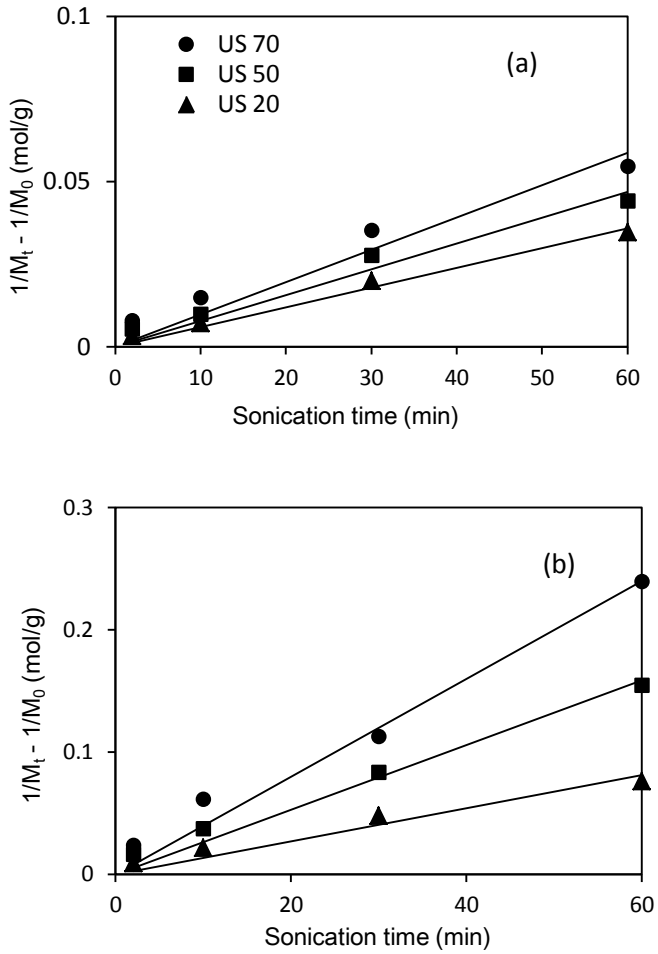

Fig. 10-3. Degradation kinetic curves of curdlan in (a) 0.1M and (b) 0.3M NaOH under ultrasound treatment at power intensity of 48.4 W/cm^2 (● US 70), 34.3 W/cm^2 (■ US 50) and 10.6 W/cm^2 (▲US 20).

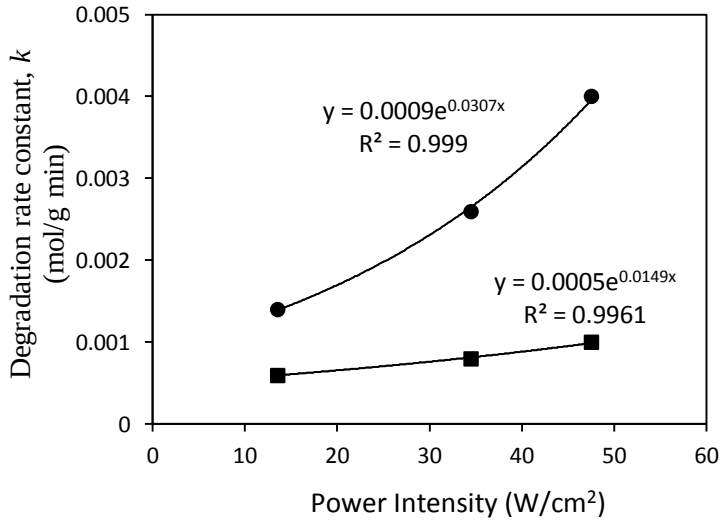

Fig. 10-4. Variation of degradation rate constant *k* (mol/g·min) against ultrasound power intensity (W/cm^2) for curdlan in 0.3M (●) and 0.1M (■) NaOH solution.

10.3.3 Effect of ultrasonic power on particle size distribution of curdlan

Fig. 10-5, shows that the particle size distribution of curdlan solution was affected after ultrasound treatment in both 0.1M and 0.3M NaOH. Sonication induced the detection of curdlan molecules with larger particle size in both alkaline concentrations. When comparing the particle size distribution of original curdlan solutions without sonication in Fig 10-5 a & b, we found that the distribution trend after 24 hours of dissolution was retained in 0.1M NaOH, but shifted to a smaller size range in 0.3M NaOH. This confirmed the alkaline degradation of curdlan molecules in higher alkaline concentrations. However, it was found that the particle size distribution of sonicated curdlan solution was retained in similar trend in both 0.1M and

0.3M alkaline concentrations after 24 hours from the US treatment. These results suggest that distorted solution conformation of curdlan molecules induced by sonication could restrict the alkaline degradation to some extent.

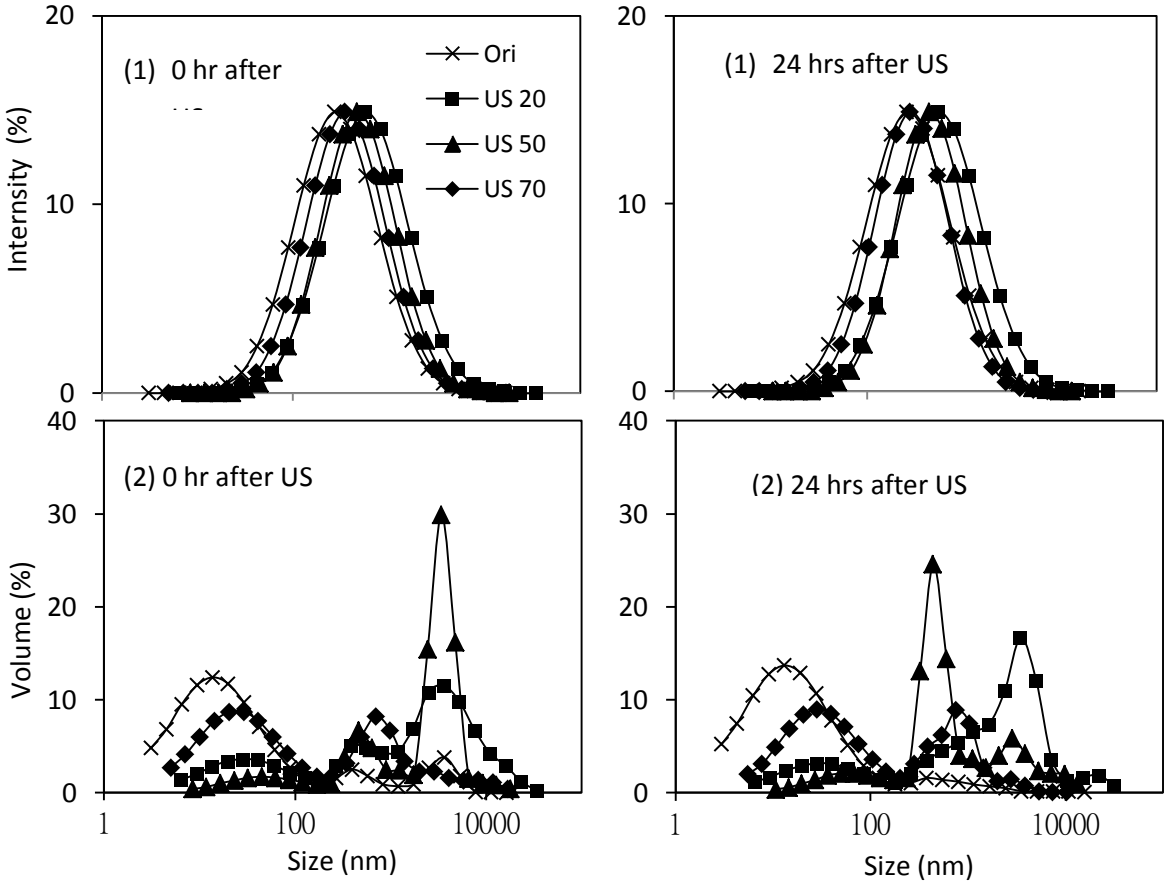

Fig. 10-5a. The particle size distribution of curdlan solution in 0.1M NaOH based on (1) intensity of light scattering and (2) volume distribution upon ultrasonic treatment at 2g/L sample concentration under power intensity of 48.4 W/cm^2 (US 70), 34.3 W/cm^2 (US 50) and 10.6 W/cm^2 (US 20) for 30 minutes, comparing to the original curdlan solution (Ori).

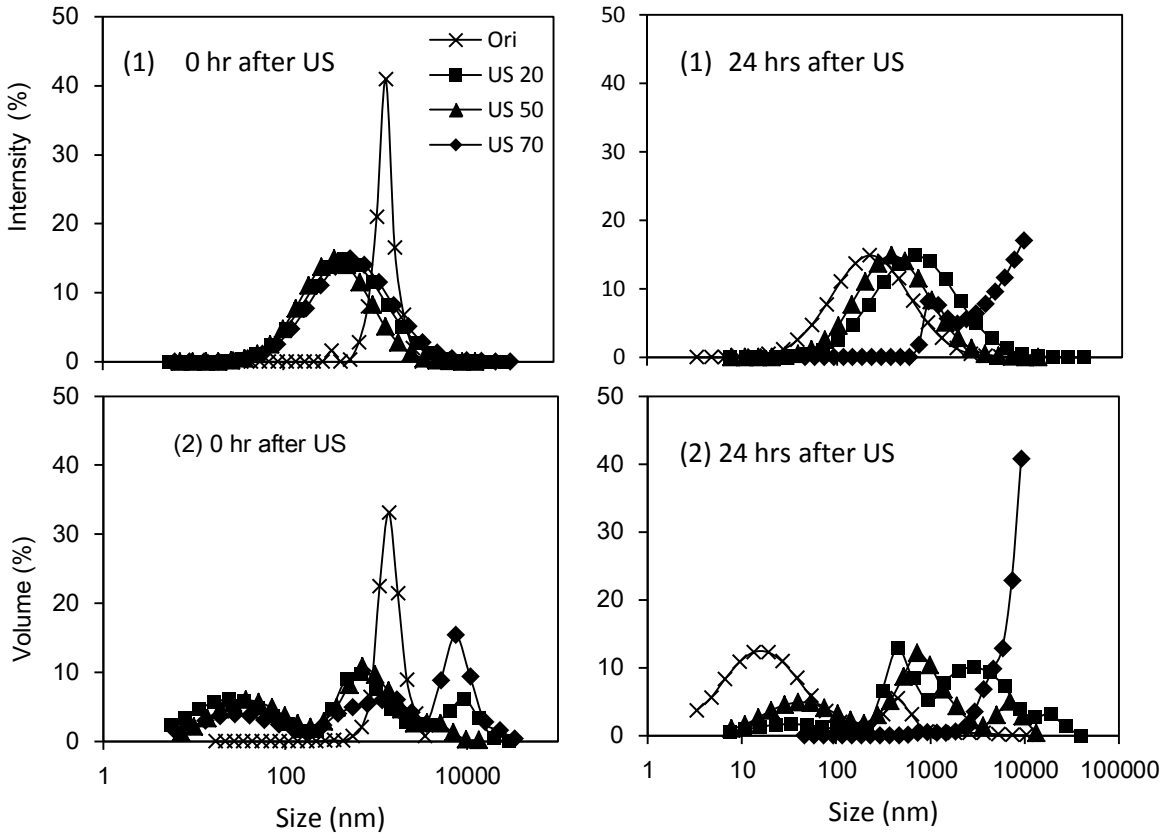

Fig. 10-5b. The particle size distribution of curdlan solution in 0.3M NaOH based on (1) intensity of light scattering and (2) volume distribution upon ultrasonic treatment at 2g/L sample concentration under power intensity of 48.4 W/cm^2 (US 70), 34.3 W/cm^2 (US 50) and 10.6 W/cm^2 (US 20) for 30 minutes, comparing to the original curdlan solution (Ori).

10.3.4 Solubility of curdlan in neutral conditions

After sonication, the amount of gel formed by acidification on alkaline curdlan solution was decreased (Fig. 10-6). In other words, solubility of curdlan molecules in neutral solutions was increased by US treatment. The decrease in the weight of gel formed in 0.3M NaOH was in a higher extent than that in 0.1M NaOH (Fig. 10-6), which suggested that the sonication

effect in random coil should be more significant than on triple helix structure.

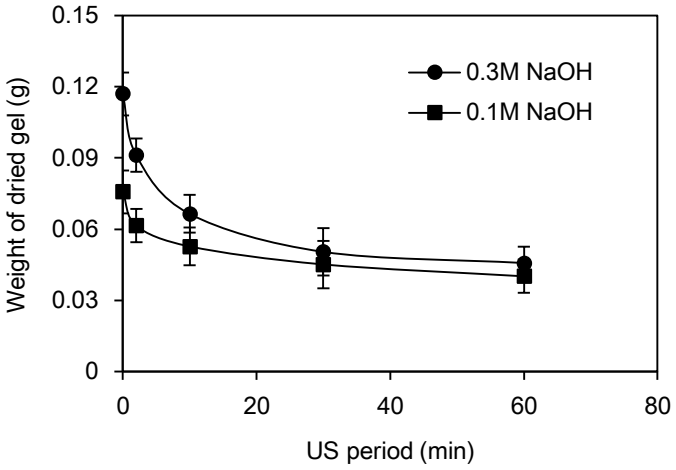

Fig. 10-6. Variation of the amount of gel formed by acidification for the curdlan solution upon ultrasonic treatment at 2 g/L sample concentration under the power intensity of 48.4 W/cm^2.

10.3.5 Sonication effect on curdlan molecular conformation

The λ_{max} value of Congo red-curdlan solution (485-506 nm) was measured to be higher than that of Congo red alone (480-490 nm) in the concentration of NaOH lower than 0.25M (Fig. 10-8). Previous studies experimentally proved that the absorption maximum (λ_{max}) of Congo red in the visible region was significantly shifted to a higher value of wavelength, called the red-shift, when it was mixed with (1→3)-β-D-glucan in NaOH solution of a concentration lower than 0.25M (Ogawa, 1978). Nakanishi et al. (1974) and Ogawa & Hatano (1978) suggested that the increased value of λ_{max} was attributed to the presence of a

complex formed between the single helices in ordered structure of the glucan and Congo red molecules. The complex was proposed to be composed by bounding six D-glucose residues of the D-glucan chain to one Congo red molecule. Under alkaline concentration of 0.1M, in which the curdlan molecules should be mainly in triple-helix conformation, the λ_{max} value of the Congo red-sonicated curdlan solution attained a maximum after 30 minutes of sonication (Fig.10-7). These results suggested that higher concentrations of the complex were formed by the increasing amount single helices of curdlan molecules after sonication. However, a sharp decrease of the λ_{max} was detected under sonication beyond 30 minutes. It is believed that a prolonged US treatment (60 minutes) may cause severe degradation of the polysaccharide, which made it lose the single helix conformation for the formation of complexes with Congo red. Such extreme degradation effect on polysaccharide morphology under high power intensity (48.4 W/cm^2) and long treatment period (60 minutes) was also proved by the TEM observation of the Cs-HK1 polysaccharide as described in the previous chapter (Fig. 9-1). Fig.10-8 showed that the λ_{max} value of Congo red with sonicated curdlan solution became lower than that of the Congo red with native curdlan solution in the alkaline concentration higher than 0.15M. This confirmed that the US effect on curdlan molecules became stronger to cause further degradation of the single helices, which in turn hindered the complex formation between the curdlan and Congo red molecules under such alkaline concentrations.

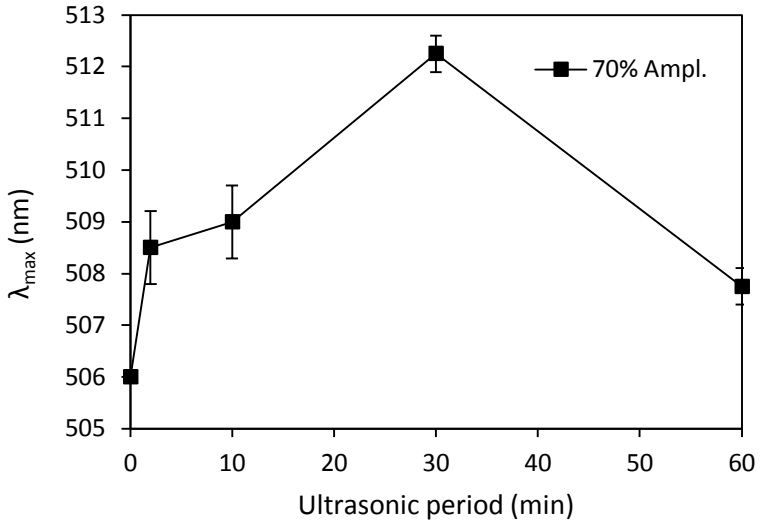

Fig. 10-7. Variation of λ_{max} of Congo red with sonicated Curdlan at 48.4 W/cm^2 in 0.1M NaOH.(Note: the average value of λ_{max} of Congo red solution alone in 0.1M NaOH was 506).

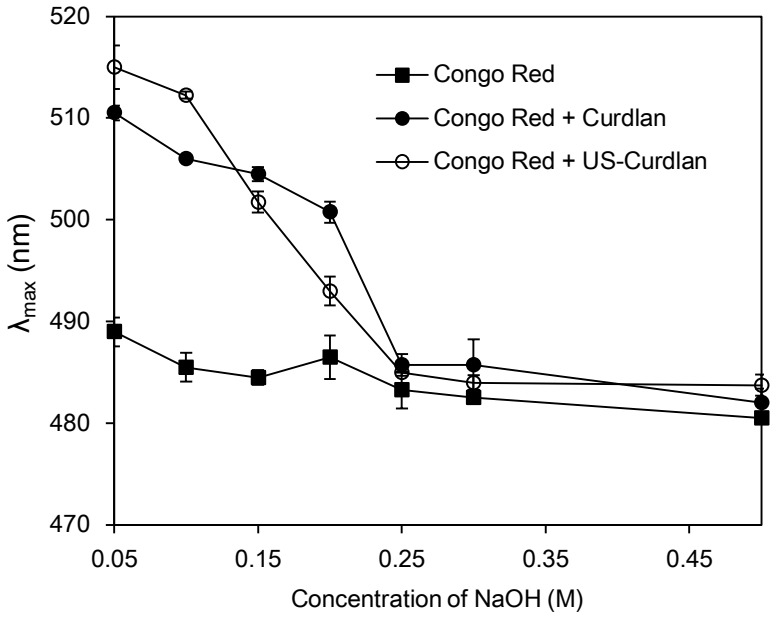

Fig. 10-8. Variation of λ_{max} of Congo red solution alone (Congo red), Congo red with native curdlan sample (Congo red + curdlan) and Congo red with sonicated curdlan at 48.4 W/cm^2 for 30 minutes (Congo red + US-Curdlan) at different concentrations of NaOH.

10.4 Discussion

Curdlan is a β-D-(1-3)-glucan shaped in the structure of straight chain without branching. Curdlan molecules are soluble in alkaline solutions but not in both neutral and acidic solutions, and form gel under acidification of alkaline solution/ thermal treatment of neutral solution. The sugar molecules are in the conformation of single/triple helix in low-concentration alkaline solutions (0.01-0.19 M NaOH). The rod-like structure destructures upon increasing concentrations of alkaline solution. There is helix-coil transition at 0.19-0.24M NaOH solution. Conformation of random coil exists in high-concentration alkaline solutions (>0.25 M NaOH) (Ogawa et al., 1972; Nakata et al., 1998). As shown in Fig. 10-9 and 10-10, when curdlan molecules are dissolved in alkaline solution at 0.1M concentration, each backbone of curdlan molecules is exited in the form of single helix by INTRA-molecular hydrogen bonds (H-bonds) between OH of C-4 and adjacent hemiacetal O atom of the residue. Molecules then eventually form the triple helix structure by INTER-molecular H-bonds between OH of C-2 every backbone. Water molecules trapped within the triple helix structures (interstitial water) form INTER-molecular H-bonds between OH of C-6 of curldan molecules; this results in the formation of micelles in the solution (Okuyama et al., 1991; Nakata et al., 1998; Grandpierre et al., 2008).

Upon ultrasound treatment (Fig. 10-11), backbones of curdlan molecules in the alkaline solution were broken by cutting the β-D-(1-3)-glucosidic linkage. This resulted in the increasing existence of single helix structures in the solution. In the meantime, due to the broken glucosidic bonds, the formation of INTRA--molecular H-bonds between OH of C-4 and adjacent hemiacetal O atom of the residue was hindered. This increased the flexibility of the backbone and therefore lowered the chance for the formation of INTER-molecular H-bonds with adjacent backbones to hold the triple helix conformation. As a result, the triple helix structure was gradually disordered to become triplex loops or even duplex loops, and finally random coil conformation. Once the triple helix structures were opened, curdlan molecules lost the chance to form INTER-molecular H-bonds with the interstitial water molecules. This aborted the formation of micelles of curdlan molecules in the solution. Consequently, increasing the sonication period decreased the amount of micelles and increased the amount of random coils. In a higher alkaline concentration of 0.3M, the INTER-molecular H-bonds between backbones were also released by the alkaline degradation. The triple helix structure could not be stabilized easily and the conformation of curdlan molecules transited to the random coils. Therefore curdlan molecules in random coil conformation should be more susceptible to the sonication effect, as the degradation was started at a further stage than that for triple-helical conformation. The higher value of US

degradation rate was constant *k* in 0.3M (Table 10-2) and its sharper increase with the US power intensity than that in 0.1M (Fig. 10-4) were evidence for this suggestion.

The significant decrease of intrinsic viscosity with the increasing sonication power and time (Fig.10-1), and the constant value of intrinsic viscosity throughout the increasing alkaline concentration after US treatment (Fig. 10-2) confirmed the disordered conformation of curdlan molecules by sonication, especially for the curdlan solution in 0.3M NaOH, from the triple helix to the random coil. The Congo red-curdlan test further proved that the US-treated curdlan solution consisted of higher amounts of single helix molecules with the higher value of λ_{max} after sonication.

Meanwhile, when the sonication time increased, the degree of cutting on the β-D-(1-3)-glucosidic bonds of backbone was increased. This induced more sites of ionization of hydroxyl groups, which increased the degree of ionization. As the MW of the backbone decreased, the charge/mass ratio of the curdlan molecules increased and therefore increased the strength of electrostatic interaction between the ionized hydroxyl groups. The amount of bound water per backbone was increased and attributed to the higher value of particle size being measured. This also favored the solubility of curdlan molecules in neutral conditions, and therefore resulted in the lower amount of gel formation after sonication. With the increased amount of bound water, curdlan molecules became more stable against alkaline

degradation after sonication. This helped the preservation of particle size distribution of US-treated curdlan solution, but not in the original one.

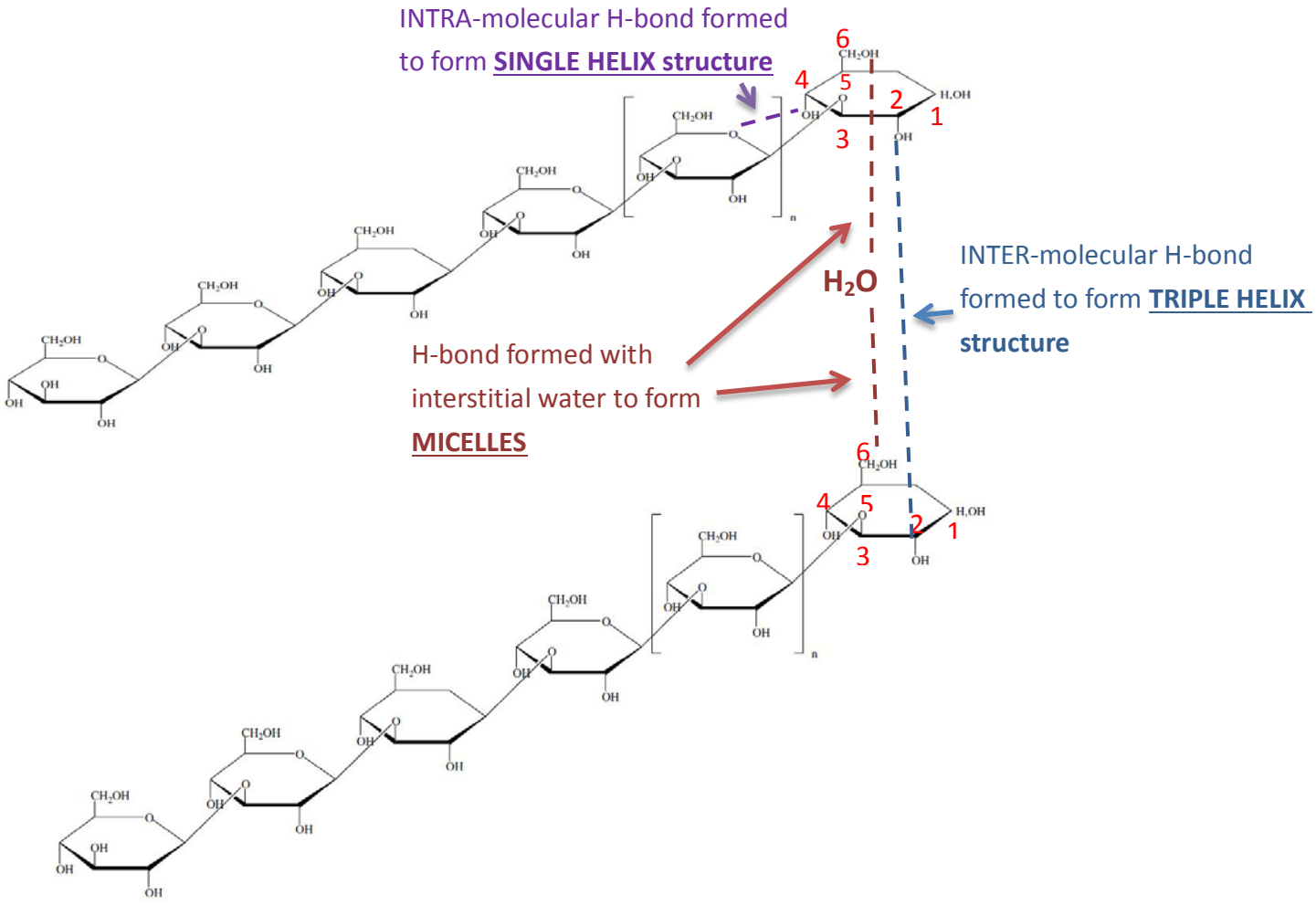

Fig. 10-9. Curdlan molecular structure in aqueous solution.

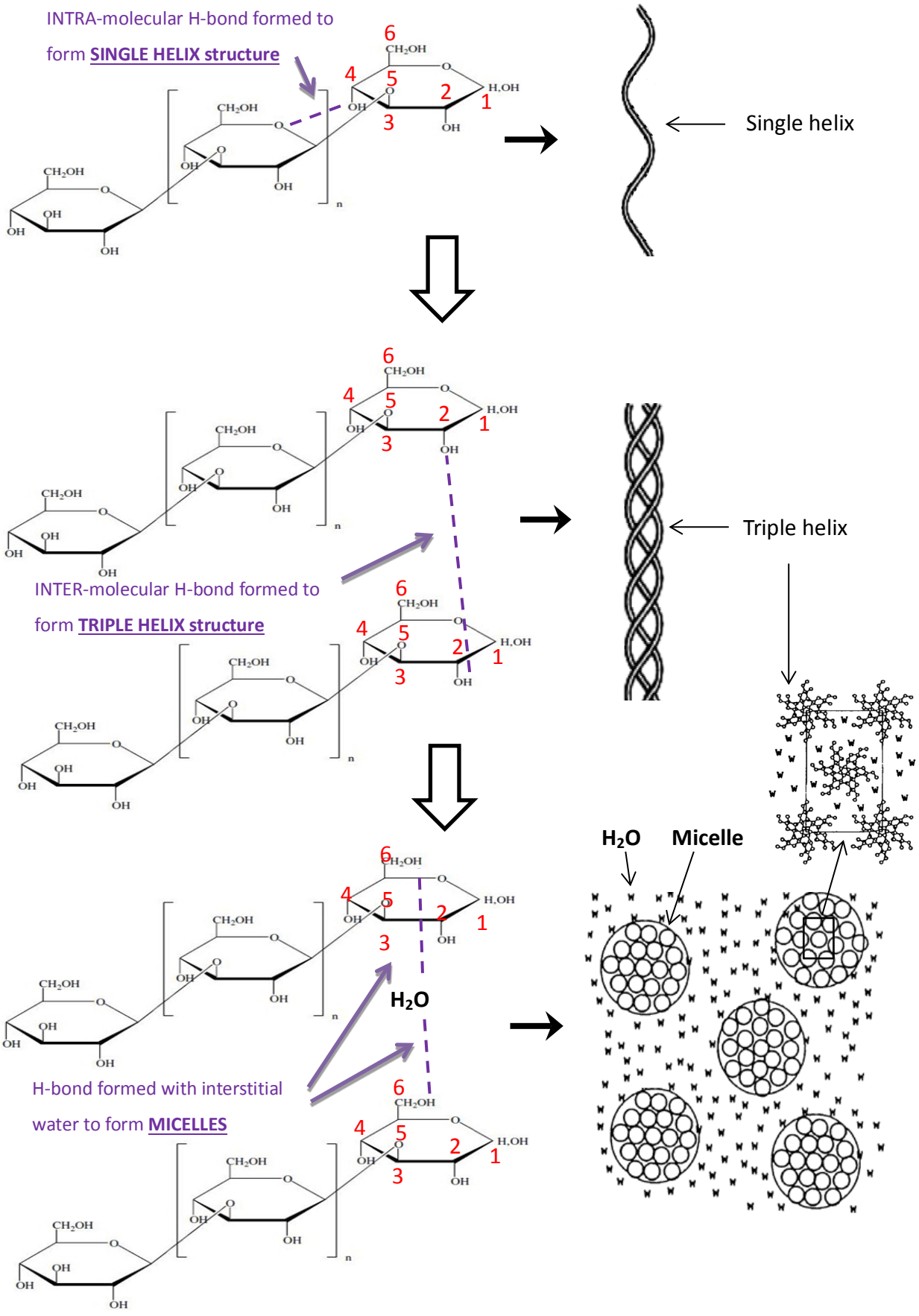

Fig. 10-10. Original conformation of curdlan molecules in 0.1 M NaOH.

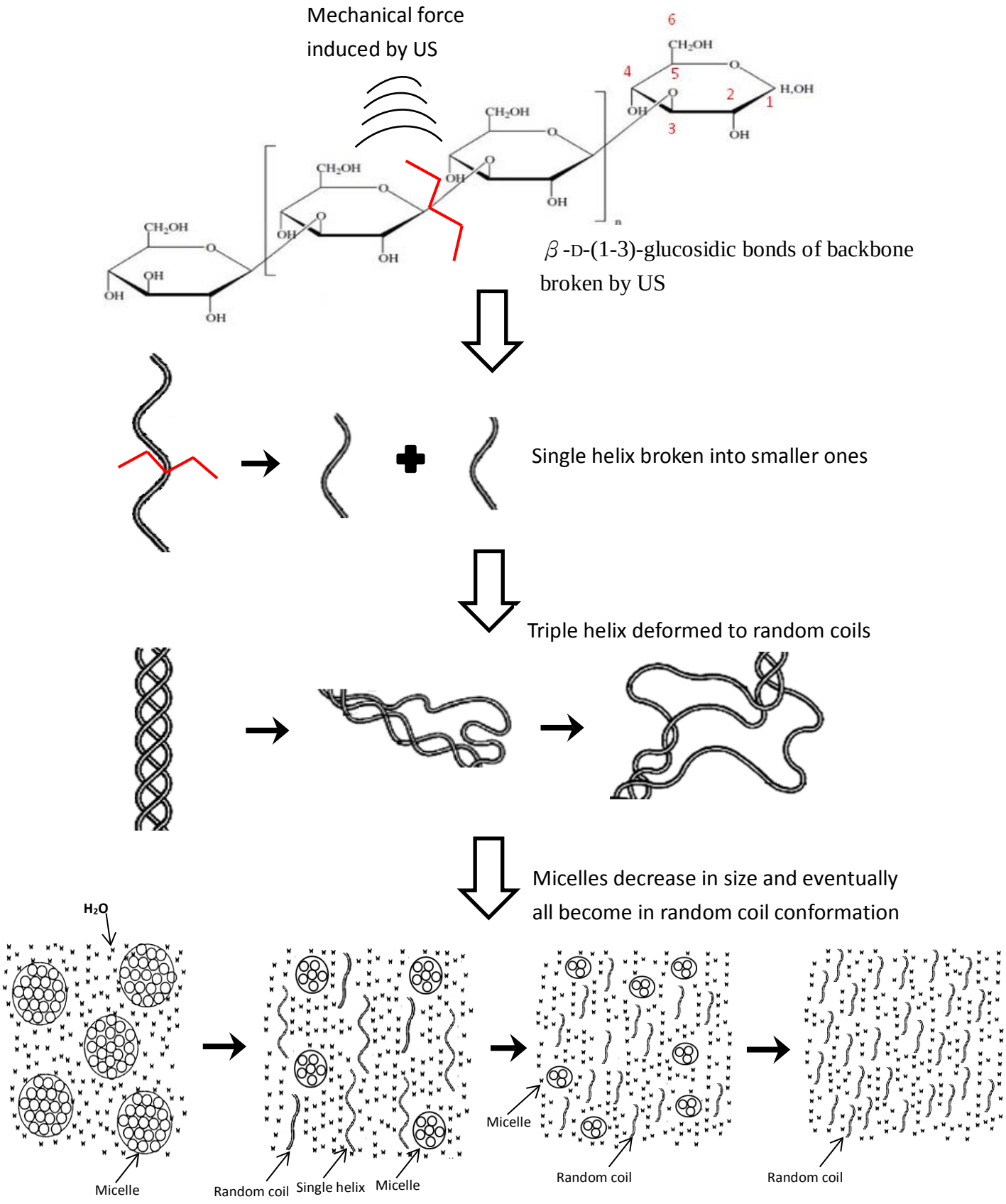

Fig. 10-11. Schematic diagram of US degradation of curdlan molecules induced modification of conformation in 0.1 M NaOH solution.

10.5 Summary

Through the US degradation of curdlan in different alkaline concentrations with different molecular conformations, the ultrasound degradation kinetics was established. The degradation rate constant *k* was correlated to the US power intensity being applied. Experimental results proved that the random coil conformation of curdlan molecules should be more susceptible to the degradation effect of US; the Congo red test further confirmed the disordered conformation induced by US cavitation attack on the glucan backbone. The schematic diagram of US degradation on triple helical conformation was therefore suggested and presented.

Part IV

Ultrasonic disruption of fungal mycelia for product recovery from Cs-HK1 fermentation broth

Chapter 11 Ultrasonic disruption of fungal mycelia for product recovery from Cs-HK1 fermentation broth

11.1 Introduction

Cordyceps (*Cordyceps sinensis*), generally known as the Chinese caterpillar fungus, is a rare and precious medicinal fungus which has been used as a favourable tonic for hundreds of years in China (Halpern, 1999; Zhou et al., 2008). Because of the very limited supply and high value of natural Cordyceps mushrooms, mycelial fermentation has become the most viable process for mass production of fungal biomass and polysaccharides. Cs-HK1 is a fungus isolated from a natural Cordyceps fruiting body in our lab and Cs-HK1 mycelial culture has been established, and evaluated for production of medicinal materials through liquid fermentation (Leung et al., 2006). In various volumes of liquid fermenters the Cs-HK1 mycelial culture could usually produce 20-25 g/L mycelial biomass and 3-5 g/L EPS over 5-7 days. Both the mycelial extracts and EPS attained from the Cs-HK1 liquid fermentation have shown notable antitumor, immumodulation and antioxidant activities (Leung et al. 2006; Leung et al. 2009).

However, the mycelial fermentation broth containing high-MW EPS of Cs-HK1 and other filamentous fungi is highly viscous and difficult to be processed by filtration or centrifugation for solid (biomass)-liquid (medium) separation. This study evaluates the use of high-intensity

US to facilitate the extraction and recovery of mycelial biomass and PS from Cs-HK1 mycelia broth containing EPS, to observe or measure the changes of mycelium morphology, broth rheology (flow behaviour and apparent viscosity) due to the US treatment, to optimize the major process factors for US enhanced PS extraction, and to establish the extraction kinetic models.

11.2 Materials and methods

11.2.1 Fungal species and mycelial fermentation

Cs-HK1 fungus was previously isolated from a natural Cordyceps fruiting body and identified as a *Tolypocladium* sp. fungus, and an anamorph of *C. sinensis* both morphologically and genetically (Leung et al. 2006). The stock culture of Cs-HK1 fungal mycelia was maintained on a solid medium in petri dishes at 20^{o}C. Liquid culture was initiated by inoculating the mycelia from the stock culture into a liquid medium composed of 40 g/L glucose, 10 g/L yeast extract, 5 g/L peptone and a few inorganic salts with an initial pH 6.8 as reported previously (Leung et al., 2006). Cs-HK1 liquid fermentation was performed in shake-flasks 250 mL Erlenmeyer flasks, each containing 50 mL of liquid medium, on a shaking incubator operated at 150 rpm and 20^{o}C. After the fermentation, the whole fermentation broth (containing fungal mycelia and EPS) from the culture flasks was

collected to be used for the ultrasound disruption and PS extraction experiments.

11.2.2 Ultrasonic treatment of mycelial broth

The mycelial fermentation broth was subjected to ultrasonic treatment with a Model VCX 750 processor (Sonics & Materials Inc., Newton, USA) of 20 kHz frequency and 750 W maximum output power. A probe horn with a 13 mm-diameter tip was used in all the experiments. The output power of US processor was controlled by adjusting the amplitude (20% to 50%, equal to about 10 W/cm^2 to 30 W/cm^2 power intensity respectively, calibrated by calorimetric method as previous). The mycelial broth (45 mL fixed volume for all experiments) was filled in a 50-mL plastic centrifuge tube; the probe tip was dipped about 2 cm into the broth. The sample tube was placed in an ice bath during the ultrasonic treatment to maintain an average temperature of 40 $\pm$ 5^{o}C over the treatment period.

11.2.3 Recovery of water-soluble product and PS from US-treated mycelial broth

After the US treatment, the mycelial broth was centrifuged at 12000 rpm for 15 min to separate the liquid extract from the mycelial biomass residue. The solid precipitate was collected, freeze-dried and weighed. The weight difference between the initial mycelial biomass and the biomass residue was taken as the total mass of intracellular released to the liquid medium due to the US treatment. Crude PS was isolated from the liquid extract by

precipitation with 5-volumes of 95% ethanol at 4^{o}C for overnight incubation. The precipitate was spun down at 14000 rpm for 15 min and freeze-dried, and collected as the crude PS. The original mycelial broth before the US treatment was also processed in the same ways to obtain the initial mycelial mass and PS concentrations in the fermentation broth. The yields of total intracellular product and PS extracted from the mycelia biomass by US treatment were all represented in wt% of the initial biomass by,

Total extract yield = (Initial mycelial mass – biomass residue after US treatment)/Initial mycelial biomass (Eq. 11-1);

PS yield = (PS attained after US treatment – PS or EPS in the original liquid medium before US treatment)/Initial mycelial biomass (Eq. 11-2).

11.2.4 Microscopic imaging and rheological measurement of mycelial broth

The mycelial broth (about 200 µl) was dropped onto a glass slide, stained by methylene blue for 3 min, and placed under an optical microscope (Leica DM 4000B microscope) which was fitted with a digital camera (Leica CH-9435, Heerbrugg, Germany). Microscopic images were obtained and analyzed by the software LAS v3.8. Rheological measurement was performed of the mycelial broth at 20 ^{o}C with a Brookfield digital viscometer (Model DV-E,

spindle No. 5) at 5 rpm rotation speed.

11.2.5 US conditions effect on total water-soluble products and PS yield

Statistical experimental design and response surface methodology (RSM) were applied to assess and optimize the major factors of ultrasonic treatment for the high extraction yields of intracellular products and PS from the fungal mycelia. Three process factors were chosen as the optimization variables, US treatment period (min, X_1), US power intensity (W/cm^2, X_2), and concentration of mycelial broth (X_3), which have also been identified as the major factors on ultrasound-assisted extraction of bioactive natural products (Li et al., 2004; Alessandro et al. 2012) from mushrooms (Sun et al. 2010) and fungal mycelia (Chen et al. 2012). The factor ranges were chosen based on our preliminary experiments, power intensity from 10-30 W/cm^2, treatment period from 5-25 min, and broth concentration from 0.25-1 (volume fraction of original broth in the diluted broth with water). A three-level three-factor Box–Behnken design (BBD) was applied and Table 11-1 shows the levels of actual and coded variables (x_1, x_2 and x_3). The total water-soluble product and PS yields were chosen as the optimization targets and the dependent variables, or the responses (Y_1 and Y_2 respectively). A total of 15 experiment runs including three replicates at the central point were conducted (Table 11-2). Regression models and statistical parameters (e.g. relative coefficient of determination R^2 and F-value or p-value) for the full quadratic equation,

$$Y = B_0 + B_1X_1 + B_2X_2 + B_3X_3 + B_{12}X_1X_2 + B_{13}X_1X_3 + B_{23}X_2X_3 + B_{11}X_1^2 + B_{22}X_2^2 + B_{33}X_3^2$$

where B_0 is the constant terms; B_i and $B_{ii\ (i=1, 2, 3)}$ are the coefficients of the relative terms in the regressions, were computed using Design Expert 7.0 software. Three-dimensional (3-D) response surface contour plots were constructed for observation of the trend and interaction of factor effects.

Table 11-1. Coded and actual values of independent variables for total water-soluble product and PS yield by BBD method.

Independent variables	Coded symbols	Levels [a]		
		-1	0	1
Sonication time (min, X_1)	x_1	5	15	25
Power intensity (W/cm^2, X_2)	x_2	10	20	30
(Power density, kW/m^3)		(295)	(590)	(885)
Concentration of mycelial broth (X_3)	x_3	0.25	0.625	1

[a] $x_i = (X_i - X_0)/\Delta X$, where X_i is the actual variable, x_i the coded variable of X_i, X_0 the central point of the actual variable X_i, and ΔX the step change of actual variable.

Table 11-2. Experimental design by BBD statistical method and the results of total water-soluble product and PS yields obtained from the experiments.

RUN	Time X_1	Power X_2	Conc. X_3	Total water-soluble product, Y_1 [a]		PS, Y_2	
	(min)	(W/cm^2)	(Fraction)	in g/L	in wt %	in g/L	in wt %
1	5	20	0.25	1.01±0.27	16.22±4.27	0.46±0.03	7.37±0.45
2	25	20	0.25	2.77±0.15	44.37±2.43	0.95±0.10	15.22±1.58
3	5	20	1	3.02±0.38	11.00±1.41	1.48±0.30	5.40±1.08
4	25	20	1	6.40±0.63	23.36±2.31	3.82±0.04	13.94±0.15
5	15	10	0.25	1.40±0.23	22.42±3.65	0.36±0.08	5.77±1.35
6	15	30	0.25	2.94±0.49	47.05±0.34	1.16±0.11	18.58±1.81
7	15	20	1	1.66±0.49	6.05±1.81	0.58±0.30	2.12±1.08
8	15	30	1	12.00±2.34	43.74±8.16	5.40±1.37	19.70±5.00
9	5	20	0.625	1.28±0.25	7.30±1.40	0.66±0.11	3.75±0.64
10	5	30	0.625	5.22±0.49	29.67±2.74	2.68±0.11	15.22±0.64
11	25	20	0.625	3.72±0.83	21.14±4.71	2.19±0.47	12.44±2.65
12	25	30	0.625	8.82±1.19	50.08±6.77	4.26±0.68	24.20±3.86
13	15	20	0.625	4.54	28.65	2.39	15.10
14	15	20	0.625	3.86	24.33	2.23	14.09
15	15	20	0.625	4.34	27.40	2.35	14.84

[a] Total water-soluble product or PSP yield: g/L = g of water-soluble product or PSP released by US treatment /liter of liquid; wt% derived from Eq. 1 or Eq. 2.

11.2.6 Kinetic modeling of ultrasound-induced release of intracellular products

The experimental data of total water-soluble product and PS yields obtained by the US disruption of mycelia at different power intensities (with one at the optimal) was fitted to the

several empirical kinetic models for solid-liquid extraction including unsteady diffusion, parabolic diffusion, power law, Peleg hyperbolic model, Weibull's exponential equation, and Elovich's logarithmic equation, which have also been applied to the extraction of natural products from food and medicinal plants (Veličković et al., 2006; Kitanović et al., 2008) and to the UAE of mushrooms and fungal mycelia in our previous study (see Part II). The kinetic models are useful not only for predicting the extract yields at a given time and ultrasound power, but also for understanding the extraction process and mechanisms.

11.2.7 Analysis of molecular properties of PS

As in the previous study, the molecular weight (MW) profiles of PS were analyzed by high-pressure gel permeation chromatography (HPGPC) with the instruments and conditions reported previously (see Chapter 4). The PS obtained at the optimal US power level (30 W/cm^2) for different US treatment periods (0-60 min) were measured to compare the effect of US on the molecular properties of PS.

11.2.8 Antioxidant activity test of PS in PC-12 cell culture

The antioxidant capacity of PS extracted with US treatment from the mycelial broth was determined by testing the cytoprotective effect against H_2O_2-induced cell injury in rat pheochromocytoma PC12 cell culture. Procedures for the cell culture and cytoprotection test

of PS samples have been described in details by Chen et al. (2013). The PS fractions extracted at the optimum US power intensity (from 0 to 60 min) were tested and were pre-dissolved in phosphate-buffered saline (PBS). In brief, the PC12 cell culture was maintained in RPMI 1640 medium supplemented with 10% fetal bovine serum (FBS) in humidified atmosphere and 5% CO_2 at 37^{o}C in an incubator. The cells were seeded into a 96 well-plate at 5×10^4 cells in 100 μl medium/well and incubated for 24 h, and then 80 μM H_2O_2 was added to the wells together with the PS sample solution (in PBS) at desired final concentrations (0.001-10 μg/mL) or with an equal volume of PBS for the negative control group, and incubated for 24 h. The cell viability after the treatment was determined with the MTT reagent according to established protocol and the optical density detected on a universal Microplate Reader (Bio-Rad model 550) at 490 nm.

11.3 Results

11.3.1 US disruption of mycelia and change in broth viscosity

Fig.11-1 shows the microscopic images of Cs-HK1 mycelia (and spores) in the broth samples before and after US treatment. As observed under the microscope, the Cs-HK1 fungus in the fermentation broth before US treatment existed in the form of long and branched hyphae surrounded by a few spores (Fig.11-1a). With the US treatment at

low-intensity or for a short period, the mycelia were slightly disrupted, and broken into shorter fragments and free spores (Fig. 11-1b) ; the disruption of mycelia was more notable at a higher US power intensity or for a longer period of exposure (Fig. 11-1c). With a very high US intensity and a relatively long period (e.g. 30 W/cm^2 for 25 min in Fig. 11-1d), the mycelia were disrupted completely and homogenized into small debris. Therefore, the microscopic observation provided direct evidence for the disruption and fragmentation of fungal mycelia by the US treatment.

During the US treatment, the apparent viscosity of mycelial broth decreased sharply in the initial period, 0-5 min, and slowly in the later period (Fig. 11-2a), implying that the US disruption of mycelia was faster with longer mycelia and larger aggregates, and stopped as the mycelia were reduced to a very small size. The ultrasonic effect on the viscosity of the mycelia broth was shown to be more significant with higher power intensity. The reduction of apparent viscosity with the rotation speed of viscometer spindle (or the shear rate) is characteristic of pseudoplastic rheology.

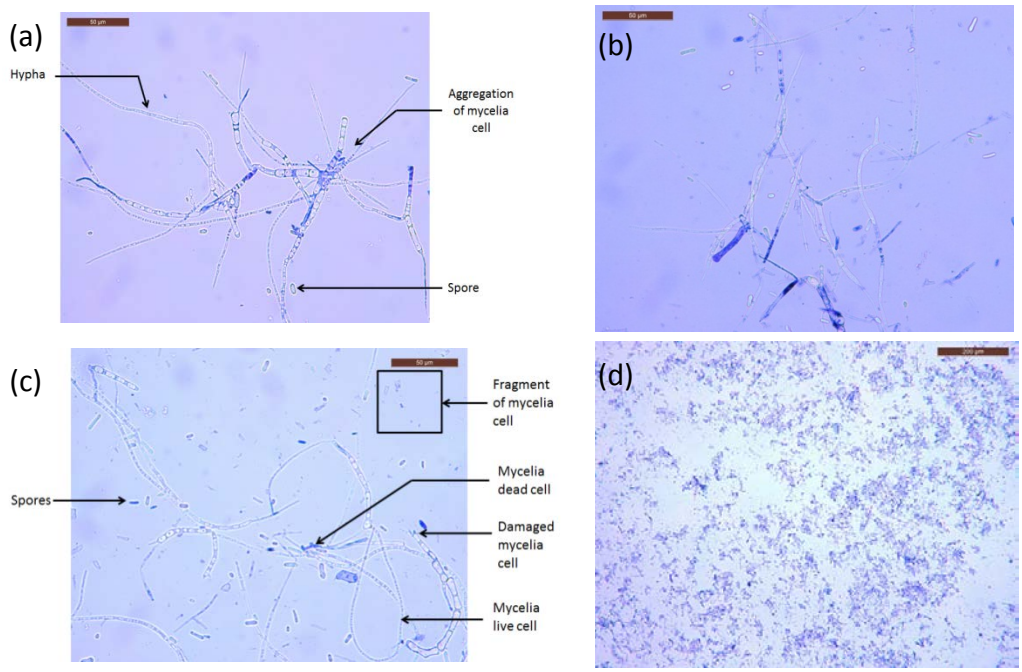

Fig. 11-1. Microscopic view of Cs-HK1 mycelial broth (a) original and after US at (b) 10 W/cm^2 power intensity for 5 minutes (c) 10 W/cm^2 power intensity for 25 minutes (d) 30 W/cm^2 power intensity for 25 minutes.

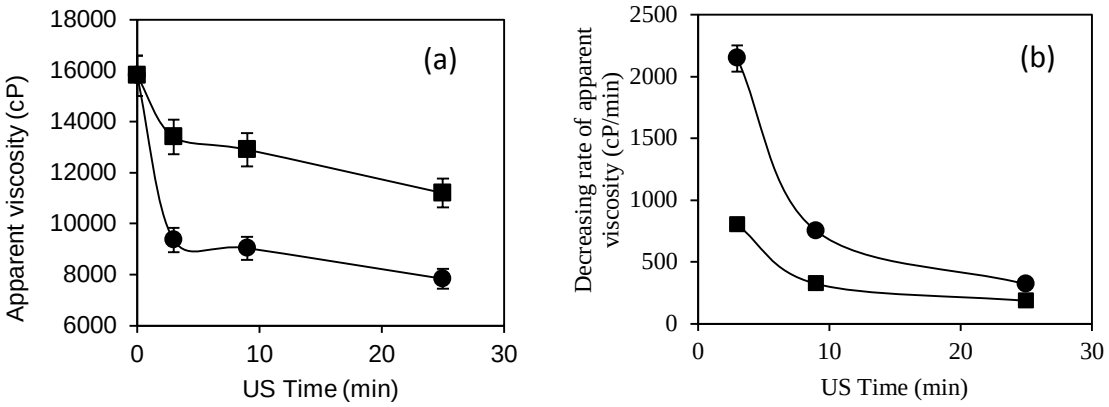

Fig. 11-2. (a) The apparent viscosity and (b) decreasing rate of apparent viscosity of Cs-HK1 culture medium upon UAE of biomass/PS at ■ 10 W/cm^2 & ● 30 W/cm^2 power intensity (both at 35% power amplitude and 0.66 concentration of mycelial broth).

11.3.2 US conditions effect on total water-soluble products and PS yield

The following correlation equations were derived for the total water-soluble product yield (Y1) and the PSP yield (Y2) versus the three major process factors by regression of the results from the BBD experiments (omitting the interactive and second order terms with negligible effects, i.e. X_1X_2 and X_1^2 from Eq. 3 and X_1X_3, X_2X_3, X_1^2, and X_2^2 from Eq. 4),

$$Y_1 = 5.58 + 2.14\ X_1 - 0.637\ X_2 - 15.6\ X_3 - 1.05\ X_1X_3 + 0.87\ X_2X_3 + 0.0317\ X_2^2 - 1.01\ X_3^2 \quad \text{(Eq. 3)}$$

$$Y_2 = -9.87 + 0.662\ X_1 + 0.401\ X_2 + 20.1\ X_3 + 0.323\ X_2X_3 - 23.3\ X_3^2 \quad \text{(Eq. 4)}$$

Both correlations had a high statistical significance with high p-values (Prob.>F) and high R^2 values (> 0.81). Based on the equations, broth concentration X_3 had the most significant effects on both Y1 and Y2 as indicted by the relatively large constant values with both the first order (X_3 and second order variables X_3^2).

Fig. 11-3 and Fig. 11-4 show the three-dimensional response surface contour plots with data predicted from above model equations for the total water-soluble product/PS yields versus the three experimental variables. With a fixed concentration of mycelial broth, both the total water-soluble product and PS yields showed a steady, linear increase with the US power intensity and also an increase with the treatment time (Fig. 11-3a & 11-4a). The total water-soluble product yield increased with the power intensity and treatment time but

decreased with mycelial broth concentration (Fig. 11-3 b & c). As for the PS yield, a maximum or peak was attained at a broth concentration of 0.66 (Fig. 11-4 b & c).

As the amounts of intracellular products and PS released from the mycelia by the US disruption were always higher with a higher US intensity and a longer time, the experiments did not reach an optimal US power or treatment time for maximum yields. Nevertheless, the experimental results indicated that the broth concentration and US power were the most significant factors affecting the efficiency of cell disruption and PS extraction from the mycelial broth. The highest total water-soluble product yield, 56.2 wt% by experiment and 58.5% by prediction from the optimization model (Eq. 11-3) was attained with 30 W/cm^2 US intensity (50% amplitude) in 25 min and 0.25 broth concentration; while the highest PS yield, 23.8 wt% by experiment and 25% by prediction from the optimization model (Eq. 11-4) was attained with 30 W/cm^2 US intensity (50% amplitude) in 25 min and 0.66 broth concentration.

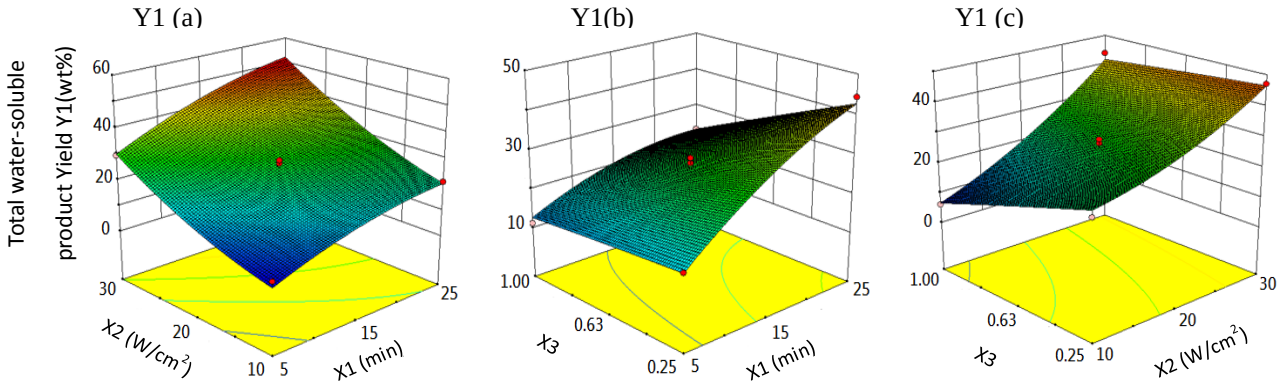

Fig 11-3. Three dimensional response surface contour plots of total water soluble product yield (Y1) versus the experimental variables: (a) Treatment time X1 and US power intensity X2 (at broth concentration X3 = 0.625); (b) Broth concentration X3 and treatmen time X1 (at X_2 = 20 W/cm^2); (c) Power intensity X2 and broth concentration X3 (at X1 = 15 min).

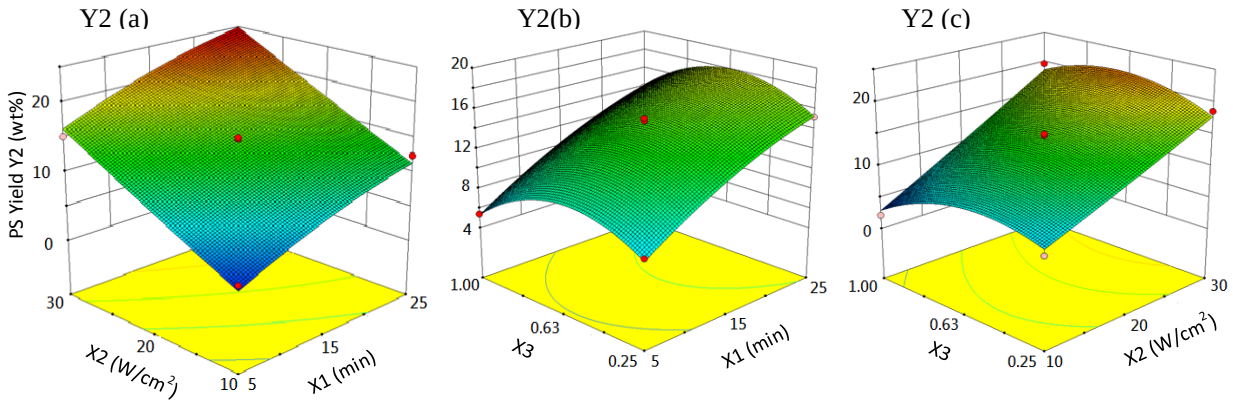

Fig 11-4. Three dimensional response surface contour plots of PS yield Y2 versus the experimental variables: (a) Treatment time X1 and US power intensity X2 (at broth concentration X3 = 0.625); (b) Broth concentration X3 and treatmen time X1 (at X_2 = 20 W/cm^2); (c) Power intensity X2 and broth concentration X3 (at X1 = 15 min).

11.3.3 Kinetic models for total water-soluble product and PS yield

Fig.11-5 shows the time courses of total water-soluble product and PS released into the liquid phase at two US power intensity levels, exhibiting a rapid and almost linear increase in concentrations in the initial period 5-10 min and a slow increase in the later period. The release rate of intracellular products (and PS) was higher at a higher US intensity. The time courses of intracellular product release from the fungal mycelia were similar to those of ultrasound-assisted extraction (UAE) of dry fungal mycelia and fruit bodies (Fig. 6-1 & 6-3). Therefore, the yield versus time data attained from experiments were fitted to the kinetic models for solid-liquid extraction by linear regression, the Elovich's logarithmic equation for the total water-soluble product yield (R^2 = 0.98-0.99) (Fig. 11-6a), and the parabolic diffusion model for the PS yield (R^2 = 0.85- 0.99) (Fig. 11-6b).

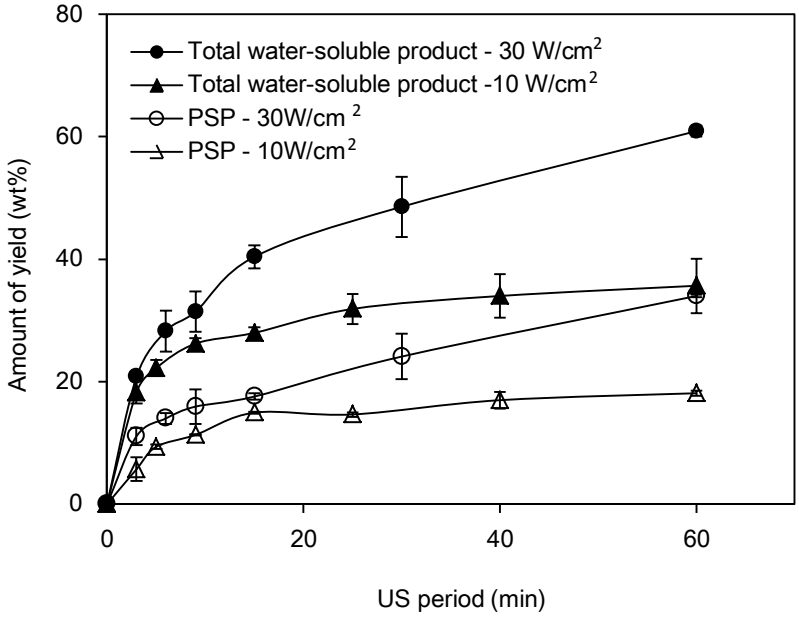

Fig. 11-5. Enhanced extraction yield (in wt% of total water-soluble product & PS by US disruption on Cs-HK1 mycelial broth at different power intensity and 0.66 concentration of mycelial broth (The original concentrations of total water-soluble product at 30 W/cm^2 and 10 W/cm^2 at time 0 are 23.2±0.26 g/L and 15.9±0.34 g/L respectively; and that of PS at 30 W/cm^2 and 10 W/cm^2 are 3.82±0.062 g/L and 3.21±0.090 g/L respectively).

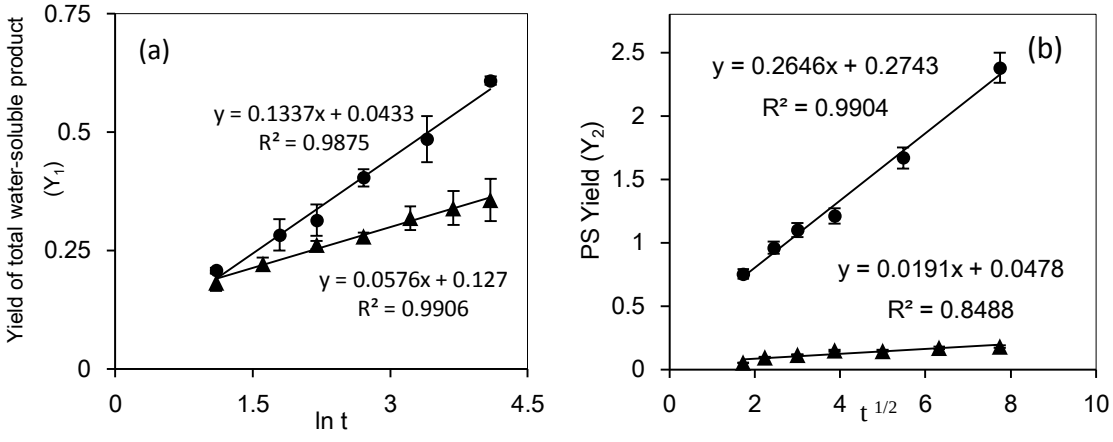

Fig. 11-6. (a) Elovich's logarithmic plot of the yield of total water-soluble product at different power intensity (▲ 10 W/cm^2 ● 30 W/cm^2) (b) Parabolic diffusion plot of the PS yield at high power intensity (▲ 10 W/cm^2 ● 30 W/cm^2).

11.3.4 Molecular properties of PS

Fig.11-7 shows the GPC MW profiles of PS isolated from the liquid broth before and after US treatment for different periods of time. The peak appearing at a shorter retention time represents a lower MW PS fraction and vice versa. The PS before the US treatment was the exopolysaccharide (EPS) produced by the fungus and released into the medium during mycelial fermentation (3-4 g/L); the PS attained after US treatment was a mixture of EPS and the PS released/extracted from the mycelia by US disruption. As seen from Fig. 11-7, the EPS or PS before US treatment exhibited a large peak (peak 1) at the shortest retention time of 12 min and a few small peaks at much longer retention times, implying that it contained mainly high MW PS. The high MW peak at 12 min was very small for the PS attained after 3 and 15 min of US treatment, and eventually disappeared after 30 min US treatment, while several lower MW peaks 2-9 appeared or increased in their peak size (area and height) in the PS attained after US treatment. The decrease or disappearance of the high MW peak 1 after US treatment may be attributed partially to polymer degradation by the ultrasonic power (Wang et al., 2010), and the lower MW peaks including 2, 3 & 5 could be PS fractions resulting from the degraded peak 1 PS fraction and/or the release of lower MW PS from the mycelia.

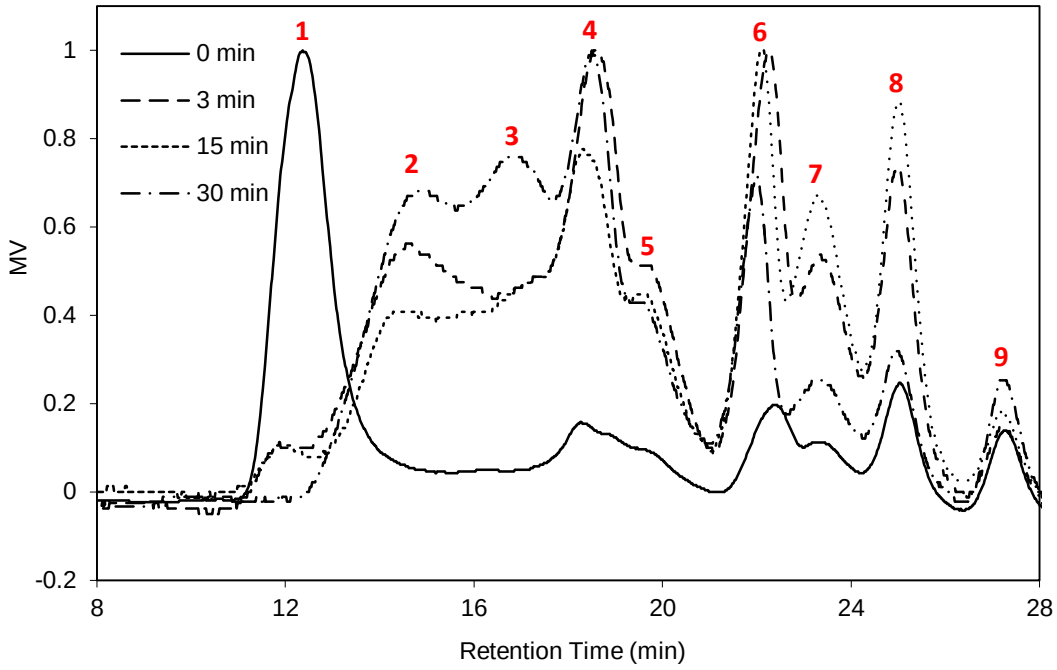

Fig. 11-7. The GPC profiles of PS extracted by US disruption of Cs-HK1 mycelial broth at optimal power intensity (30 W/cm^2) for various period of time.

11.3.5 Antioxidant activity of US-extracted PS

Fig.11-8 shows that protective effect of PS fractions obtained before and after 3-60 min US treatment at a selected power intensity against H_2O_2-induced PC12 cell death or viability loss. The PS obtained before the US treatment (0 min), which was the EPS in the mycelial broth, and the PS obtained after 3 min US treatment showed no effect, while the PS obtained after 15-60 min of US treatment showed a concentration-dependent protective effect, maintaining a higher cell viability than that with no or very low dose of PS. The cytoprotective or antioxidant activity of PS fraction extracted from the mycelia was notably

increased with the treatment period from 15 to 60 min. This activity trend can be related to changes in the chemical composition (e.g. carbohydrate and protein content) and the molecular weight profiles of the PS fraction with the US treatment time (Fig. 11-7). The PS obtained with a longer period of US treatment had higher contents of proteins and low MW molecules, which may have stronger antioxidant activities.

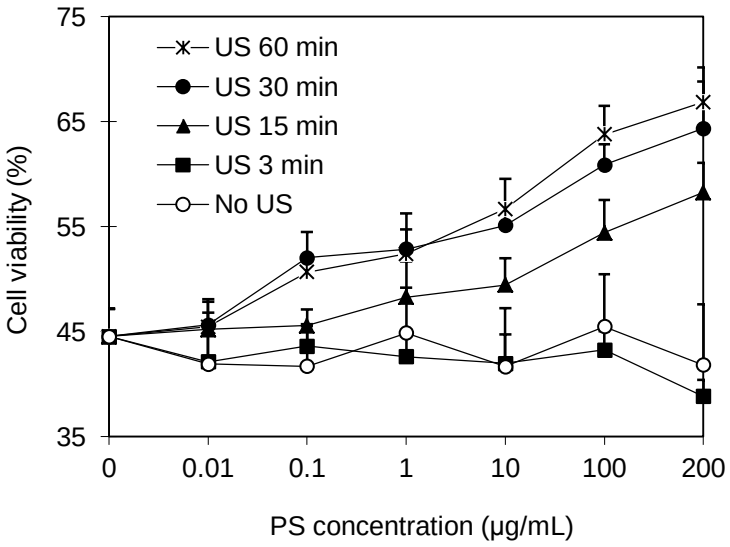

Fig. 11-8. Cell viability of PC12 cells of treated with various concentrations of PS isolated from Cs-HK1 mycelial broth before and after various periods of US treatment at 30 W/cm^2 power intensity. (Cells were treated with 80 μM H_2O_2 and the PS sample at a selected concentration for 24 h followed by MTT measurement of cell viability. Viability % was relative to the control cell culture without H_2O_2 and PS treatment.)

11.4 Discussion

The viscosity reduction of mycelial broth induced by the US treatment can be mainly attributed to the disruption and fragmentation of mycelia and mycelial aggregates. The notable reduction of mycelial broth viscosity can greatly facilitate the separation of solid-liquid by filtration. The disruption of fungal mycelia by US was intensified with the increase in US power intensity, leading to more rapid release of intracellular products such as PS. The amount of intracellular products released and the PS yield increased with the treatment period. As the cell disruption was mostly effected through cavitation, which is usually hampered by a high viscosity (Mason & Lorimer, 2002), the rate and extent of cell disruption was increased by diluting the broth to a lower viscosity. However, dilution of the mycelial broth also led to lower concentrations of total water soluble products and PS released into the broth. Therefore the concentration factor could have both positive and negative influence on the extraction yields, and an optimal concentration was found to obtain the highest PS yield.

A proportional relationship was found to correlate the yield of total water-soluble product and the process factors; while an optimal value was obtained for PS yield. Due to the efficient US effect, the amount of total water-soluble extracts should be increased with sonication time and power decreased with the mycelial concentration. PS was obtained by

ethanol precipitation, which targeted PS with certain high MW. By increasing US time/ power to some extent, the IPS released from cell disruption and the EPS that existed in the mycelial broth were degraded by cavitation to a lower MW. This was evidenced by the GPC result in Fig. 11-7. Our previous study in Chapter 9 and the study done by Wang et al. (2010) also provided such evidence. Therefore, instead of increasing amounts, an optimal was attained for PS yield throughout the variation of the three process factors.

As shown in previous studies, the antioxidant activities of the PS and PSP fractions produced by the Cs-HK1 fungus in liquid fermentation were usually higher with a higher protein content and/or a lower MW (Leung et al., 2009; Huang et al. 2013). The enhanced antioxidant activity through the US treatment was an extra benefit and interesting effect of the US disruption of the fungal mycelia in addition to the rapid release of intracellular products for recovery.

11.5 Summary

Ultrasonic disruption of filamentous fungal mycelia broth was dependent mainly on US power intensity and mycelial broth concentration, being more effective with a higher power and a lower mycelium concentration. Similar to many other applications of high intensity US in solid-liquid systems, the mycelial disruption by US was mainly attributed to the

mechanical forces arising from acoustic cavitation. The application of high-intensity US generated several beneficial effects for extraction and recovery of bioactive products especially the PS from the highly viscous fermentation of a medicinal fungus, including a dramatic reduction of broth viscosity, a rapid release of intracellular products and PS, and a notable improvement of the antioxidant activity. Although the US technique has been applied successfully and effectively to extract small volumes of broth in the laboratory, its potential application in the industrial process is subject to practical considerations including the energy consumption, scale up capability and comparison of the overall efficiency with the existing mechanical means for cell disruption such as ball milling and high pressure homogenizers. As the first study on the US extraction of PS from mycelial fermentation broth of medicinal fungi, these results are promising and attractive for further research and development.

Appendix – Statistic Results

Table 11-3. Analysis of variance (ANOVA) for Response surface equation model.

Source	Total water-soluble product yield		PS yield	
	F-Value	p-value	F-Value	p-value
Model	43.53	0.0003	42.82	0.0003
A-Time	99.00	0.0002	7.04	0.0453
B-Power intensity	228.60	< 0.0001	1.97	0.2194
C-Concentration	37.30	0.0017	8.41	0.0338
AB	1.53	0.2713	0.014	0.9104
AC	8.84	0.0311	0.082	0.7856
BC	6.04	0.0574	3.94	0.1038
A^2	4.43	0.0892	2.15	0.2027
B^2	5.24	0.0707	0.053	0.8268
C^2	0.01	0.9221	27.44	0.0034
Lack of fit	4.84	0.1830	8.05	0.1124

Table 11-4. Test of significant of regression coefficient.

Factor	Total water-soluble product yield		Enhanced PS yield	
	Coefficient estimate	Standard error	Coefficient estimate	Standard error
Intercept	5.58	1.53	-9.87	4.48
A-Time	2.14	0.92	0.66	0.25
B-Power intensity	-0.637	0.14	0.40	0.29
C-Concentration	-15.7	2.91	20.13	6.94
AB	0.0164	3.25×10^{-3}	7.105×10^{-4}	6.007×10^{-3}
AC	-1.05	0.37	0.046	0.16
BC	0.871	0.32	0.32	0.16
A^2	-0.0291	3.52×10^{-3}	-9.161×10^{-3}	6.25×10^{-3}
B^2	0.0317	2.64×10^{-3}	1.441×10^{-3}	6.25×10^{-3}
C^2	-1.01	0.40	– 23.29	4.45

Part V

General discussion and Conclusion

Chapter 12 General discussion

12.1 Kinetic characteristics of UAE

The experimental results from UAE of various mushroom materials have shown significant differences in the composition and molecular properties between the PS extracted by UAE and HWE respectively. These differences should be attributed to the different extraction mechanisms of the two methods, UAE by mechanical energy and HWE by thermal energy (heat). Heat enhances the molecular diffusion mass transfer rate through mushroom particles and cell walls and the dissolution of PS into the extracting solvent, thereby enhancing their extraction by HWE. On the other hand, ultrasound irradiation provides a source of mechanical energy to the liquid solvent, causing disruption of the particles and cells and promoting mass transfer. Evidence for the disruption of mushroom cell walls by power ultrasound during water extraction has been once observed previously by electron microscopy (Toma et al., 2001). The disruption of cell walls may increase the access of solvent to the PS molecules and their release from the cell walls, thus increasing the extract yield and/or extraction rate. Similarly, Hromadkova et al. (1999) once attributed the higher yield of polysaccharides from *Salvia officinalis L.* plant material attained through UAE to an increased accessibility of the polysaccharides by mechanical disruption of the plant cell walls.

The experimental results suggested that the product contents and its relative medicinal properties should be related to the extraction method. Therefore, when we apply the extraction technique, despite of the extraction efficiency, we need to carefully consider the composition & properties of the obtained product for useful application(s).

The detailed microstructures and morphological characteristics varied among the different fungal species. The microstructures of the *C. versicolor* fruit bodies before and after UAE was observed by SEM as shown in Fig. 12-1. The SEM images show clearly that the morphology of *C. versicolor* fruit bodies was totally different from that of *G. frondosa, L. edodes, G. lucidum, C. sinensis Cs-HK1 and Cs-4* as shown in Fig. 6-4. Instead of being shaped as glands, powders of *C. versicolor* were in long fiber-shape. The fibers are crisscrossing and not showed significant changes after UAE; while the other five fungi powders showed obvious disruption of the microstructures after UAE (Fig. 12-1 & 6-4). The significantly lower extraction yield obtained from *C. versicolor* by UAE compared with HWE suggested that the extraction efficiency of UAE could be highly related to the morphology of the extracting raw materials. And noticeably fiber-liked microstructure could not be favorable for high efficiency with UAE. Detail and qualitative characterization of the particle microstructures before and after UAE help understand their kinetic characteristics and the influence by ultrasound.

The extraction kinetics of UAE for the five representative medicinal mushrooms was

well represented by parabolic diffusion, power law, Weibull's exponential equation, and Elovich's logarithmic equation with high correlation coefficient values ($R^2 > 0.8$). However, the regression results of the best-fitting model with the extraction data suggest that the kinetic characteristics of UAE should be dependent on both the species and the biological form (fruit body or fungal mycelium) of fungal materials. Previous studies have shown a strong dependence of UAE kinetics on the plant materials as well as the extraction conditions and the applicability of different kinetic models. The UAE processes for garden (*Salvia officinalis* L.) and glutinous (*Salvia glutinosa* L.) sage were fitted closely to the unsteady diffusion and the film model (Veličković et al., 2006). The UAE of oils from tobacco seeds was fitted to the unsteady diffusion model (Stanisavljević et al., 2007); the UAE of antioxidants from pomegranate peel was fitted to a second-order kinetic model (Pan et al., 2011). The different kinetic models suitable for UAE of various plants and fungi are most probably attributable to the different physical properties of the plant and fungal materials, particularly the mechanical strength of cell walls and the microstructures of solid particles.

Among all the kinetic models used in our study, the parabolic diffusion and power law model were the best fit to the UAE of water-soluble components including PS from various mushroom materials. These two models are actually very similar (Eq. 7-2 and Eq. 7-3) except that the parabolic model has an initial yield y_o and a fixed exponent ½ and power-law model has a zero initial yield (at $t = 0$) and a variable exponent n. The parabolic model assumes that

the overall mass transfer process involved in the solid-liquid extraction is divided into two major steps, an initial washing-out step for dissolution of the solute molecules on the solid surface and a diffusion step for the transfer of solute molecules from inside of the solid particle into the liquid solvent (Coulson et al., 1991). Compared with the washing out step, the diffusion step is much slower and the rate limiting step for most solid–liquid systems, which should be mainly influenced and enhanced by the ultrasound power as shown. It is probably more meaningful and realistic to ignore or eliminate the washing-out yield from the kinetic models of UAE as in this study. In contrast, a recent report on UAE kinetics of plant components suggests that ultrasound mainly enhanced the washing-out step but not the diffusion step (Milić et al., 2013). As the yield y of total extract and PS from UAE had deducted the extract yield attained during the 30 min of sample mixing with water before UAE (Eq. 7-1) which was quite significant (up to 50% of the maximum yield y), y_o was small in the study of Chapter 7 (accounting for 10% or less of y). This may be the main reason why the power-law model was a better fit than the parabolic diffusion model to most of the experimental data in this study, but parabolic model was better in the previous study in Chapter 6, in which UAE was started immediately after the sample was added to water and the initial yields were quite high (accounting for 50% or more of y).

(a) Before UAE (b) After UAE

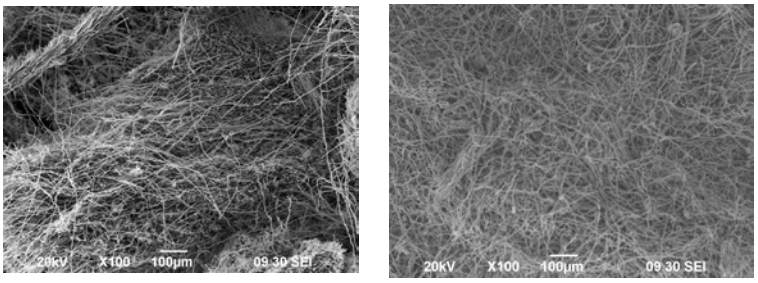

Fig. 12-1. Scanning electron micrographs of *C. versicolor* fruit bodies (a) before and (b) after UAE for 60 min. SEM was performed on a JEOL JSM-6490F instrument. (The dry sample powder of mushrooms and mycelia was coated with gold.)

12.2 Effects of US on PS structure

As shown by the experimental results (Fig. 9-3 & 10-2), the application of US to the PS solution caused a notable reduction of the intrinsic viscosity, suggesting the decrease of the average MW or the degradation of the PS. On the other hand, US treatment of the PS solution resulted in increase in the hydrodynamic diameter. Polysaccharides extracted from natural sources were composed of various monosaccharaides linked by different types of glycosidic bonding. The bioactivities of polysaccharides are related to their molecular composition, chemical structures chain conformations in solution (Tao et al., 2007; Yang & Zhang, 2009). Besides the (1→3)-β-D-glucan in linear chain such as curdlan in our study, several bioactive polysaccharides from natural sources have branch chains. For example, two

well-known antitumor mushroom polysaccharides, Lentinan from *Lentinus edodes* (Surenjav et al., 2006; Zhang et al., 2005; Halpern, 2013) and schphylizophyllan from *Schizophyllum commune* (Okamura et al., 1986; Tsuzuki et al., 1999; Halpern, 2013) were composed of (1→3)-β-D-glucan backbone chain with branch chains. Both the main chain and the side chain structures affect the conformation of polysaccharides. The conformation is also dependent on the main the position of the glycosidic linkages of the backbone (e.g. 1→3, 1→4, or 1→6) and also the anomerity (α or β) of each sugar residue. For a more comprehensive study on the effects of US on the PS structure, conformation and the physicochemical properties, various representative polysaccharide structures should be examined such as dextran from *Leuconostoc spp.* which is a α-1,6-glucan with α-1,3-branches, and Lentinan from *Lentinus edodes* which is a β-1,3-glucan with β-1,6-branches. .

12.3 US disruption of fungal mycelia for product recovery from fermentation broth

Ultrasonic disruption of living cells and microorganisms is a common procedure in the laboratory for homogenization and extraction of biological samples in small volumes but not in large-scale bioprocesses. Although many previous studies have been done on US disruption of bacteria and yeast cells and a few also on filamentous fungi, no study has been reported (to our knowledge) on the US disruption of fungal mycelia for recovery of PS and

PSP from fermentation broths of medicinal fungi. The US treatment caused changes in mycelial morphology and aggregation before complete disruption, and lead to a dramatic reduction of the broth viscosity. Changes in mycelium morphology and aggregation caused by high-intensity US treatment have also been observed in other filamentous fungi such as *Aspergillus terreus* (Herran et al. 2008). The reduction of apparent viscosity was also observed in bacterial broth of *E. coli* by mechanical disruption with high-energy acoustics and high pressure (Li et al. 2012). The morphological changes and cell disruption have been mostly attributed to the shear forces induced by acoustic cavitation. The process kinetics of US disruption for release and extraction of intracellular products and PS from the live (fresh) fungal mycelia was fitted to the similar empirical models as for UAE, due probably to the similarities between the two processes in the equipment and process scheme. The release kinetics of intracellular products such as proteins from yeast and bacteria disrupted by mechanical means such as bead mills is represented by a first order model as given by (Middelberg 1995),

$dR/dt = k(R_{max} - R)$ (Eq. 12-1a) or

$$ln\frac{R_{max}}{R_{max}-R} = ln\frac{1}{1-R/R_{max}} = kt \quad \text{(Eq. 12-1b)}$$

where R is the mass of product release per unit mass of cells (i.e. the extract yield) and R_{max} is the maximum yield achievable. However, this model had a poor fit to the total water-soluble product and PS yields ($R^2 < 0.8$) by US from the Cs-HK1 mycelia. The

difference in the kinetic characteristics may be attributed to the different morphology characteristics, filamentous fungi versus unicellular yeast and bacteria.

Chapter 13 General conclusions and future work

13.1 General conclusions

This research project has accomplished an experimental study on several applications of high power US in the processing and modification of high MW PS from different species and of edible and medicinal fungi in both mushroom fruiting body and fungal mycelium forms. The chief findings and relationships derived from this project are summarized below.

1. The UAE efficiency for the enhancement of PS extraction from mushrooms and fungal mycelia depended strongly on the fungal material, especially the morphology and aggregation of the solid particles in the extraction liquid. UAE attained PS from various mushroom species with different composition and properties than those from HWE.

2. UAE kinetics for water extract and PS yields could be adequately represented by simple empirical kinetic models for solid-liquid extraction. The most suitable kinetic models depended on the physical properties and microstructures of fungal cells and particles. The parabolic diffusion and power-law model had the best fit to the UAE kinetics of water extract and PS yield from the fungal mycelia of *Cordyceps sinensis* Cs-HK1. The rate of

extraction was correlated with the US power density, while the extraction yield was correlated to the US energy density.

3. US degradation of high MW PS led to reduction of intrinsic viscosity, molecular weight, and particle size of the PS molecules were to an extent dependent on the US power and treatment period also on the PS molecular structure being treated. The US treatment also caused

4. Changes the chain conformations of PS molecules in an aqueous solution, associated with changes in other solution properties. Polysaccharide presented in random coil conformation tended to be more susceptible to US degradation than in triple-helical structure.

5. Power US was effective to disrupt filamentous fungal mycelia, leading to a sharp reduction of apparent viscosity of the Cs-HK1 mycelial broth, and release of intracellular products. The crude PS (mixed with proteins) recovered from the broth through a longer period of US treatment exhibited a stronger antioxidant activity, due probably to the high contents of lower MWPS and PSPs.

Overall the results from this project have shown that high power US is an efficient and versatile means for extraction, processing and controlled degradation of bioactive PSPs from edible/medicinal fungi. The kinetic models and process parameters derived from the project will be useful for design and operation of the ultrasonic processes. The major findings and quantitative relationships derived from the project will make novel and useful contributions to the advancement of the US processing science and technology.

13.2 Further studies

The results from our project can also provide useful references and foundation for further research and development, and more efficient application of the US processing technology. Specifically the following areas are suggested for future work.

1. The US experimental equipment and set up (for UAE, US PS degradation and mycelial disruption) may be modified or replaced with those that can provide more uniform conditions of mixing and temperature and can be scaled up, such as a flow-through tank or column with liquid circulation.

2. The physical properties and microstructures of mushroom materials for the UAE (e.g. shape and size of mushroom tissue and aggregates in the extraction liquid) should be examined and measured more carefully for better understanding of their effects on or relationship to the UAE efficiency and kinetics.

3. Although the US effects for PS degradation have been generally attributed to the mechanical effects (forces) of cavitation, the actually contribution of cavitation to the degradation should be examined and measured through experiments, particularly, by measuring the cavitation intensity corresponding to each set of US power and treatment conditions. In addition to the mechanical effects, radical generation may rise from cavitation and its contribution to the PS degradation should also be detected.

References

Aguilera, J. M., Stanley, D. W. (1999). Microstructural Principles of Food Processing and Engineering (2nd ed.), Aspen Publishers, Inc.

Akyuz, A., Giz, H. C,, Giz, A. T. (2008). Kinetics of Ultrasonic Polymer Degradation: Comparison of Theoretical Models with On-Line Data, *Macromolecular Chemistry and Physics*, 209, 801-809.

Alessandro, L. G., Kriaa, K., Nikov I., Dimitrov, K. (2012). Ultrasound assisted extraction of polyphenols from black chokeberry. Separation and Purification Technology, 93, 42–47.

Apar, D. K., Turhan, M., Ozbek, B. (2006). Enzymatic hydrolysis of starch by using a sonifier. *Chemical Engineering Communications*, 193, 1117–26.

Ashokkumar, M., Sunartio, D., Kentish, S., Mawson, R., Simons, L., Vilkhu, K., et al. (2008). Modification of food ingredients by ultrasound to improve functionality: a preliminary study on a model system. *Innovative Food Science and Emerging Technologies*, 9, 155-160.

Benzie, I. F. F., Strain, J. J. (1996). The ferric reducing ability of plasma (FRAP) as a measure of "antioxidant power": The FRAP assay. *Analytical Biochemistry*, 239, 70-76.

Boh, B., Berovic, M. (2007). *Grifola frondosa* (Dicks.: Fr.) SF Gray (Maitake mushroom): Medicinal properties, active compounds, and biotechnological cultivation. *International Journal of Medicinal Mushrooms*, 9, 89-108.

Bucić-Kojić, A., Planinić, M., Tomas, S., Bilić, M., Velić, D. (2007). Study of solid–liquid extraction kinetics of total polyphenols from grape seeds. *Journal of Food Engineering*, 81, 236-242.

Camino, N. A., Pérez, O. E., Pilosof, A. M. R. (2009). Molecular and functional modification of hydroxypropylmethylcellulose by high-intensity ultrasound. *Food Hydrocolloids*, 23, 1089-1095.

Carraher, C. E. (2003). Seymour/Carraher's Polymer Chemistry, 6th ed., Marcel Dekker, pp

92-99.

Cellaa, R., Stefani, H. A. (2009). Ultrasound in heterocycles chemistry, *Tetrahedron*, 65, 2619-2641.

Chang, S. T., Miles, P. G. (1992). Mushroom biology: a new discipline. *Mycologist*, 6, 64-73.

Chemat, F., Tomao, V., Virot, M. (2008). Ultrasound-Assisted Extraction in Food Analysis, In: Handbook of food analysis instruments, pp. 85-103. CRC Press.

Chen, R. H., Chang, J. R., Shyur, J. S. (1997). Effect on ultrasound conditions and storages in acidic solutions on changes in molecular weight and polydispersity of treated chitosan. *Carbohydrate Research*, 299, 287-294.

Chen, S., Siu, K.C., Wang, W-Q., Liu, X-X., Wu, J.Y. (2013). Structure and antioxidant activity of a novel poly-N-acetylhexosamine produced by a medicinal fungus. *Carbohydrate Polymers*, 94, 332-338.

Chen, W., Wang, W. P., Zhang, H. S., Huang, Q. (2012). Optimization of ultrasonic-assisted extraction of water-soluble polysaccharides from Boletus edulis mycelia using response surface methodology, *Carbohydrate Polymers*, 87, 614-619.

Chen, X., Wang, W., Li, S., Xue, J., Fan, L., Sheng, Z., Chen, Y. (2010). Optimization of ultrasound-assisted extraction of Lingzhi polysaccharides using response surface methodology and its inhibitory effect on cervical cancer cells. *Carbohydrate Polymers*, 80, 944-948.

Cheung, Y. C., Siu, K. C., Liu, Y. S., & Wu, J. Y. (2012). Molecular properties and antioxidant activities of polysaccharide–protein complexes from selected mushrooms by ultrasound-assisted extraction. *Process Biochemistry*, 47, 892-895.

Cheung, Y. C., Siu, K. C., Wu, J.Y. (2013). Kinetic models for ultrasound-assisted extraction of water-soluble components and polysaccharides from medicinal fungi. *Food and Bioprocess Technology*. (DOI) 10.1007/s11947-012-0929-z.

Chihara, G. (1969). The antitumor polysaccharide lentinan: an overview. In T. Aoki, et al. (Eds.), Manipulation of host defense mechanism. *Nature*, 222, 687-694.

Chihara, G. (1992). Immunopharmacology of lentinan, a polysaccharide isolated from *Lentinus edodes*: its application as a host defense potentiator. *International Journal Oriental Medicine*, 17, 57-77.

Chihara, G., Hamuro, J., Maeda, Y. Y., Arai, Y., Fukuoka, F. (1970). Fractionation and purification of the polysaccharides with marked antitumor activity, especially lentinan, from lentinus edodes. *Cancer Research*, 30, 2776e2782.

Chuanyun, D., Bochu, W., Chuanren, D., Sakanishi, (2003). A. Low ultrasonic stimulates fermentation of riboflavin producing strain *Ecemothecium ashbyii*. *Colloids and Surfaces B: Biointerfaces*, 30, 37–41.

Chuanyun, D., Bochu, W., Huan, Z., Conglin, H., Chuanren, D., Wangqian, L. (2004). Effect of low frequency ultrasonic stimulation on the secretion of siboflavin produced by Ecemothecium ashbyii. *Colloids and Surfaces B: Biointerfaces*, 34, 7–11.

Coulson, J. M., & Richardson, J. F. (with Backhurst, J. R., & Harker, J. H.) (1991). Chemical engineering particle technology and separation processes, vol. 2, fourth ed. Pergamon Press, Oxford.

Cui, J. (2003). Polysaccharopeptides of *Coriolus versicolor*: physiological activity, uses, and production. *Biotechnology Advances*, 21, 109-122.

Cun, Z., Mizuno, T., Ito, H., Shimura, K., Sumiya, T., Kawade, M. (1994). Antitumor activity and immunological property of polysaccharides from the mycelium of liquid-cultured *Grifola frondosa*. *Journal of the Japanese Society for Food Science and Technology*, 41, 724-733.

Dahneke, B. E. (ed) (1983). Measurement of suspended particles by Quasi-elastic light scattering, Wiley.

Daraboina, N., Madras, G. (2009). Kinetics of the ultrasonic degradation of poly-(alkyl methacrylates), *Ultrasonics Sonochemistry*, 16, 273–279.

Decker, E. A., Welch, B. (1990). Role of ferritin as a lipid oxidation catalyst in muscle food. *Journal of Agricultural and Food Chemistry*, 38, 674-677.

Ebringerova, A., Hromadkova, Z. (2010). An overview on the application of ultrasound in

extraction, separation and purification of plant polysaccharides. *Central European Journal of Chemistry*, 8, 243-257.

Farzi, M., Saari, M. M., Emam-Djomeh, Z., Mohammadifar, M. A. (2011). Effect of ultrasonic treatment on the rheological properties and particle size of gum tragacanth dispersions from different species. *International Journal of Food Science and Technology*, 46, 849-854.

Flosdorf, E. W., Chambers, L. A. (1933). The chemical action of audible sound. *Journal of the American Chemical Society*, 55, 3051–3052.

Flosdorf, E. W., Chambers, L. A. (1935). An immunological study of the effects of intense sound vibrations on egg albumin. *Journal of Immunology*, 28, 297–310.

Futatsuyama, H., Yui, T., Ogawa, K. (1999). Viscometry of curdlan, a linear (1→3)-β-D-glucan, in DMSO or alkaline solutions. *Bioscience Biotechnology and Biochemistry*, 63, 1481–1483.

Gassen, M., Gross, A., Youdim, M. B. H. (1998). Apomorphine enantiomers protect cultured pheochromocytoma (PC12) cells from oxidative stress induced by H_2O_2 and 6-Hydroxydopamine. *Movement Disorders*, 13, 661-667.

Geciova, J, Bury, D, Jelen, P. (2002). Methods for disruption of microbial cells for potential use in the dairy industry-a review. *International Dairy Journal*, 12, 541–553.

Glisic, S. B., Ristic, M., Skala, D.U. (2011). The combined extraction of sage (*Salvia officinalis* L.): ultrasound followed by supercritical CO_2 extraction. *Ultrasonics Sonochemistry*, 18, 318–326.

Goodman, L. P., Dugan, Jr. L. R. (1970). The effect of sonication on lipase activity. *Lipids*, 5, 362–365.

Gordon, L., Pilosof, A. M. R. (2010). Application of high-intensity ultrasounds to control the size of whey proteins particles. *Food Biophysics*, 5, 203-210.

Grandpierre, C., Janssen, H.-G., Laroche, C., Michaud, P., Warrand, J. (2008). Enzymatic and chemical degradation of curdlan targeting the production of β-(1→3) oligoglucans, *Carbohydrate Polymers*, 71, 277-286.

Gronroos, A., Pentti, P., Hanna K. (2008). Ultrasonic degradation of aqueous carboxymethylcellulose: Effect of viscosity, molecular mass, and concentration. *Ultrasonics Sonochemistry*, 15, 644–648.

Güzey, D. (2002). Modification of protein structure and functionality using high-intensity ultrasound. Thesis, University of Tennessee, Knoxville.

Halpern, G. M. (1999). Cordyceps. China's Healing Mushroom. Avery Publishing Group, Garden City Park, N.Y.

Halpern, G. M. (2006). Healing Mushrooms. SquareOne Publishers, Garden City Park, NY.

Halpern, G.M. (2013). Fungal β-glucans. McGraw-Hill Yearbook of Science & Technology 2013. McGraw-Hill, New York, 170-173.

Herran N. S., Casas-Lopez J. L., Sanchez-Perez J. A., Chisti Y. (2008). Effects of ultrasound on culture of *Aspergillus terreus*. *Journal of Chemical Technology and Biotechnology*, 83, 593–600.

Hobbs, C. (2000). Medicinal value of *Lentinus edodes* (Berk.) Sing. (*Agaricomycetideae*). A literature review. *International Journal of Medicinal Mushrooms*, 2, 287-302.

Hromadkova, Z., Ebringerova, A., Valachovic, P. (1999). Comparison of classical and ultrasound-assisted extraction of polysaccharides from *Salvia officinalis* L. *Ultrasonics Sonochemistry*, 5(4), 163-168.

Huang, Q., Li, L., Fu, X. (2007). Ultrasound effects on the structure and chemical reactivity of cornstarch granules. *Starch*, 59, 371-378.

Iida, Y., Tuziuti, T., Yasui, K., Towata, A., Kozuka, T. (2008). Control of viscosity in starch and polysaccharide solutions with ultrasound after gelatinization. *Innovative Food Science & Emerging Technologies*, 9, 140-146.

Kardos, N., Luche, J. (2001) Sonochemistry in carbohydrate compounds. *Carbohydrate Research*, 332, 115-131.

Kashiwagi, Y., Norisuye, T., Fujita, H. (1981). Triple helix of *Schizophyllum commune*

polysaccharide in dilute solution. 4. Light scattering and viscosity in dilute aqueous sodium hydroxide. *Macromolecules*, 14, 1220-1225.

Kim, J.Y., Kim, C.L., Chung, C.H., 2002. Modeling of nuclide release from low-level radioactive paraffin waste: a comparison of simulated and real waste. *Journal of Hazardous Materials*, B94, 161-178.

Kitanović, S., Milenović, D., Veljković, V. B. (2008). Empirical kinetic models for the resinoid extraction from aerials parts of St. John's wort (Hypericum perforatum L.). *Biochemical Engineering Journal*, 41, 1-11.

Kuboi, R., Umakoshi, H., Takagi, N., Komasawa, I. (1995). Optimal disruption methods for the selective recovery of β-galactosidase from *E. coli*. *Journal of Fermentation and Bioengineering*, 79, 335-341.

Kwiatkowska, B., Bennett, J., Akunna, J., Walker, G.M., Bremner, D.H. (2011). Stimulation of bioprocesses by ultrasound, *Biotechnology Advances*, 29, 768-780.

Laemmli, U. K. (1970). Cleavage of structural proteins during assembly of head of bacteriophage-T4. *Nature*, 227, 680-685.

Leung, P. H., Zhang, Q. X., Wu, J. Y. (2006). Mycelium cultivation, chemical composition and antitumour activity of a *Tolypocladium* sp. fungus isolated from wild *Cordyceps sinensis*. *Journal of Applied Microbiology*, 101, 275–283.

Leung, P. H., Zhao, S. N., Ho, K. P., Wu., J. Y. (2009). Chemical properties and antioxidant activity of exopolysaccharides from mycelial culture of *Cordyceps sinensis* fungus Cs-HK1. *Food Chemistry*, 114, 1251-1256.

Li, H. Z., Pordesimo, L., Weiss, J. (2004). High Intensity ultrasound-assisted extraction of oil from soybeans, *Food Research International*, 37, 731-738.

Li, Q., Jean P. A., Tang, A., Chatel, A., Hoare, M. (2012). Use of focused acoustics for cell disruption to provide ultra-scale-down insights of microbial homogenization and its bioprocess impact—recovery of antibody fragments from rec E. coli, *Biotechnology and Bioengineering*, 109, 2059–2069.

Li, S. P., Tsim, K. W. K. (2004). The biological and pharmacological properties of *Cordyceps*

sinensis, a traditional Chinese medicine that has broad clinical applications. In: Packer, L., Ong, C. N., Halliwell, B. (Eds), Herbal and Traditional Medicine: Molecular Aspects of Health. Marcel Dekker, New York, pp. 657-683.

Li, S. P., Zhao, K. J., Ji, Z. N., Song, Z. H., Dong, T. T. X., Lo, C. K., Cheung, J. K. H., Zhu, S. Q., Tsim, K. W. K. (2003). A polysaccharide isolated from Cordyceps sinensis, a traditional Chinese medicine, protects PC12 cells against hydrogen peroxide-induced injury. *Life Sciences*, 73, 2503-2513.

Liu, H., Bao, J., Du, Y., Zhou, X., Kennedy, J. F. (2006). Effect of ultrasonic treatment on the biochemphysical properties of chitosan. *Carbohydrate Polymers*, 64, 553-559.

Lorimer, J. P., Mason, T. J., Cuthbert, T.C., Brookfield, E. A. (1995). Effect of ultrasound on degradation of aqueous native dextran. *Ultrasonics Sonochemitry*, 2, 55-57.

Lowery, O. H., Nira, J., Rosenbrough, A., Farr, L., Randall, R. J. (1951). Protein measurement with the Folin phenol reagent. *The Journal of Biological Chemistry*, 193 265-275.

Machova, E., Kvapilova, K., Kogan, G., Sˇandula J. (1999). Effect of ultrasonic treatment on the molecular weight of carboxymethylated chitin-glucan complex from *Aspergillus niger*, *Ultrasonics Sonochemistry*, 5, 169–172.

Malhotra, S.L. (1986). Ultrasonic solution degradations of poly (alkyl methacrylates). Journal of Macromolecular Science, Part A – Chemistry, 23, 729-748.

Mason, T. J., (1999). Sonochemistry, pp.8-60. Oxford University Press.

Mason, T. J., Lorimer, J. P. Bates, D. M. (1990). Quantifying sonochemistry: casting some light on a black art. *Ultrasonics*, 30, 40–48.

Mason, T. J., Lorimer, J. P. (2002). Applied Sonochemistry: The Uses of Power Ultrasound in Chemistry and Processing. Wiley-VCH, Weinheim.

Mason, T. J., Paniwnyk, L., Lorimer, J. P. (1996). The uses of ultrasound in food technology. *Ultrasonics Sonochemistry*, 3, S253–260.

Mason, T. J., Peters, D. (2002). Practical Sonochemsitry: Power ultrasound uses and

applications (2nd ed.), Horwood Publishing Series in Chemical Science.

Mason, T., Riera, E., Vercet, A., Lopez-Buesa, P. (2005). Application of ultrasound. In D. W. Sun (Ed.), Emerging technologies for food processing (pp. 323e350). California: Elsevier Academic Press.

Mclintock, I.S., (1967). The Elovich equation in chemisorption kinetics. *Nature*. 216, 1204 – 1205.

Meziane, S., Kadi, H. (2008). Kinetics and thermodynamics of oil extraction from olive cake. *Journal of the American Oil Chemists' Society*, 85, 391-396.

Middelberg, A. P. J. (1995). Process-scale disruption of microorganisms. Biotechnology Advances, 13(3), 491–551.

Milić, P. S., Rajković, K. M., Stamenković, O. S., Veljković, V. B. (2013). Kinetic modeling and optimization of maceration and ultrasound-extraction of resinoid from the aerial parts of white ladys bedstraw (Galium mollugo L.). *Ultrasonics Sonochemistry*. 20, 525-534.

Miyazaki, T., Nishijima, M. (1981). Studies on fungal polysaccharides. XXVII. Structural examination of a water-soluble, antitumor polysaccharide of *Ganoderma lucidum*. *Chemical & Pharmaceutical Bulletin*, 29, 3611-3625.

Mizuno, T. (1997). Anti-tumor mushrooms - *Ganoderma lucidum, Grifora frondosa, Lentinus edodes,* and *Agaricus blazei, Gendaishorin*. *Tokyo*, 188-193.

Mizuno, T., Zhuang, C. (1995). *Grifola frondosa*: pharmacological effects. *Food Research International*, 11, 135-149.

Mizuno, T., Saito, H., Nishitoba, T., Kawagashi, H. (1995). Antitumoractive substances from mushrooms. *Food Research International*, 11, 23-61.

Montalbo-Lomboy, M., Johnson, L., Khanal, S. K., Leeuwen, J., Grewell, D. (2010). Sonication of sugary-2 corn: A potential pretreatment to enhance sugar release. *Bioresource Technology*, 101, 351-358.

Nakata, M., Kawaguchi, T., Kodama, Y., and Konno, K. (1998). Characterization of curdlan in aqueous sodium hydroxide, *Polymer*, 39, 1475-1481.

Namanishi, S. I., Kiwjra, K., Kusur, S., Yaxiazau, E. (1974). Complex formation of gel-forming bacterial (1→3)-β-D-glucans (curdlan-type polysaccharides) with dyes in aqueous solution. *Carbohydrate Research*, 32, 47-51.

Nevell, T. P., Zeronian, S. H. (1985). Cellulose Chemistry and its applications, Ellis Horwood Limited.

Nguyen, T. M. P., Lee, Y. K., Zhou, W. B. (2009). Stimulating fermentative activities of bifidobacteria in milk by high intensity ultrasound. *International Dairy Journal*, 19, 410–416.

Ogawa, K., Hatano, M., (1978). Circular dichroism of the complex of a (1→3)-β-D-glucan with Congo Red. *Carbohydrate Research*, 67, 527–535.

Ogawa, K., Watanabe, T., Tsurugi, J., Ono, S. (1972). Conformational behavior of a gel-forming (1→3)-β-D-glucan in alkaline solution. *Carbohydrate Research*, 23, 399-405.

Okamura, K., Suzuki, M., Chihara, T., Fujiwara, A., Fukuda, T., Goto, S., et al. (1986). Clinical evaluation of Schizophyllan combined with irradiation in patients with cervical cancer. *Cancer*, 58, 865–872.

Okuyama, K., Otsubo, A., Fukuzawa, Y., Ozawa, M., Harada, T., Kasai, N. (1991). Single-helical structure of native curdlan and its aggregation state. *Carbohydrate chemistry*, 10, 645-656.

Pan, Z., Wenjuan, Q., Haile, M., Griffiths, G. A., Tara, H. M. (2011). Continuous and pulsed ultrasound-assisted extractions of antioxidants from pomegranate peel. *Ultrasonics Sonochemistry*, 18, 1249–1257.

Patist, A., Bates, D. (2008). Ultrasonic innovations in the food industry: From the laboratory to commercial production. *Innovative Food Science & Emerging Technologies*, 9, 147-154.

Peck, R., Devore, J.L. (2012). Statistics: The Exploration and Analysis of Data, 7th edition. Brooks/Cole, Cengage Learning.

Piyasena, P., Mohareb, E., McKellar, R. C. (2003). Inactivation of microbes using ultrasound: a review. *International Journal of Food Microbiology*, 87, 207-216.

Qi, H. M., Zhao, T. T., Zhang, Q. B., Li, Z., Zhao, Z. Q., Xing, R. (2005). Antioxidant activity of different molecular weight sulfated polysaccharides from *Ulva pertusa Kjellm* (Chlorophyta). *Journal of Applied Phycology*, 17, 527-534.

Radel S., McLoughlin A.J., Gherardini L., Doblhoff-Dier O., Benes E. (2000). Viability of yeast cells in well controlled propagating and standing ultrasonic plane waves. *Ultrasonics*, 38, 633–637.

Ramesh, H. P., Tharanathan, R. N. (1999). Water-extracted polysaccharides of selected cereals and influence of temperature on the extractability of polysaccharides in sorghum. *Food Chemistry*, 64, 345-350.

Re, R., Pellegrini, N., Proteggente, A., Pannala, A., Yang, M., Rice-Evans, C. (1999). Antioxidant activity applying an improved ABTS radical cation decolorization assay. *Free Radical Biology & Medicine*, 26, 1231-1237.

Rolz, C. (1986). Ultrasound effect on enzymatic saccharification. *Biotechnology Letters*, 8,131–136.

Saito, H., Yoshioka, Y., Yakoi, M., Yamada, J. (1990). Distinct gelation mechanism between linear and branched (1/3)-b-D-glucans as revealed by high-resolution solid-state carbon-13 NMR. *Biopolymers*, 29, 1689-1698.

Seshadri, R., Weiss, J., Hulbert, G. J., Mount, J. (2003). Ultrasonic processing influences rheological and optical properties of highmethoxyl pectin dispersions. *Food Hydrocolloids*, 17, 191-197.

Sinclair, G.W., Peppas N.A. (1984). Analysis of non-fickian transport in polymers using simplified exponential expressions. *Journal of Membrane Science*, 17, 329-331

Soria, A. C., Villamiel, M. (2010). Effect of ultrasound on the technological properties and bioactivity of food: a review. *Trends in Food Science & Technology*, 21, 323-331.

Stanisavljević, I.T., Lazić, M.L., Veljković, V.B. (2007). Ultrasonic extraction of oil from tobacco (*Nicotiana tabacum* L.) seeds. *Ultrasonics Sonochemistry*, 14, 646-652.

Staub, A. M. (1956). Removal of protein-Sevag method. *Methods in Carbohydrate Chemistry*, 5, 5–6.

Sulaiman, A. Z., Ajit, A., Yunus, R. M., Chisti, Y. (2011). Ultrasound-assisted fermentation enhances bioethanol productivity. *Biochemical Engineering Journal*, 54, 141-150.

Sun, Y. X., Li, T. B., Yan, J. W., Liu, J. C. (2010). Technology optimization for polysaccharides (POP) extraction from the fruitingbodies of *Pleurotus ostreatus* by Box–Behnken statistical design, *Carbohydrate Polymers*, 80, 242-247.

Sun, Y., Liu, D., Chen, J., Ye, X., Yu, D. (2011). Effects of different factors of ultrasound treatment on the extraction yield of the all-trans-β-carotene from citrus peels. *Ultrasonics Sonochemistry*, 18, 243-249.

Surenjav, U., Zhang, L., Xu, X., Zhang, X., Zeng, F. (2006). Effects of molecular structure on antitumor activities of $(1 \rightarrow 3)$- β -D-glucans from different *Lentinus edodes*. *Carbohydrate Polymers*, 63, 97–104.

Suslick, K. S. (1988). Homogeneous sonochemistry. In K. S. Suslick (Ed.), Ultrasound: Its chemical, physical, and biological effects (pp. 123-163). New York: VCH Publishers.

Taghizadeh, M. T., Asadpour, T. (2009). Effect of molecular weight on the ultrasonic degradation of poly(vinyl-pyrrolidone), *Ultrasonics Sonochemistry*, 16, 280–286.

Tao, Y., Zhang, L., Yan, F., Wu, X. (2007). Chain conformation of waterinsoluble hyperbranched polysaccharide from fungus. *Biomacromolecules*, 8, 2321–2328.

Thornycroft J., Barnaby S. W. (1895). Torpedo boat destroyers, Proc Institution of Civil Engineers, 122, 51

Toba, T., Hayasaka, I., Taguchi, S., Adachi, S. (1990). A new method for manufacture of lactosehydrolyzed fermented milk. *Journal of the Science of Food and Agriculture*, 52, 403–407.

Toma, M., Vinatoru, M., Paniwnyk, L., Mason, T. J. (2001). Investigation of the effects of ultrasound on vegetal tissues during solvent extraction. *Ultrasonics Sonochemistry*, 8, 137-142.

Tsuzuki, A., Ohno, N., Adachi, Y., Yadomae, T. (1999). Interleukin 8 production of human leukocytes stimulated by triple or single helical conformer of an antitumor (1→3)-β -D-glucan preparation, sonifilan. *Drug Development Research*, 48, 17–25.

Vankar, P.S., Srivastava, J., (2010). Ultrasound-assisted extraction in different solvents for phytochemical study of Canna indica. *International Journal of Food Engineering*, 6, article 6

Veličković, D. T., Milenović, D. M., Ristić, M. S., Veljković, V. B. (2006). Kinetics of ultrasonic extraction of extractive substances from garden (*Salvia officinalis* L.) and glutinous (*Salvia glutinosa* L.) sage. *Ultrasonics Sonochemistry*, 13, 150-156.

Vilkhu, K., Mawson, R., Simons, L., Bates, D. (2008). Applications and opportunities for ultrasound assisted extraction in the food industry — A review. *Innovative Food Science & Emerging Technologies*, 9, 161-169.

Villetti, M. A., Crespo, J. S., Soldi, M. S., Pires, A. T. N., Borsali, R., Soldi, V. (2002). Thermal degradation of natural polymers. *Journal of Thermal Analysis and Calorimetry*, 67, 295-303.

Vinatoru, M. (2001). An overview of the ultrasonically assisted extraction of bioactive principles from herbs. *Ultrasonics Sonochemistry*, 8, 303-313.

Vodenicˇarová, M., Drˇimalová, G., Hromádková, Z., Malovíková, A., Ebringerová, A. (2006). Xyloglucan degradation using different radiation sources: a comparative study. *Ultrasonics Sonochemistry*, 13, 157–164.

Wang, Z. M., Cheung, Y. C., Leung, P. H., Wu, J. Y. (2010). Ultrasonic treatment for improved solution properties of a high-molecular weight exopolysaccharide produced by a medicinal fungus. *Bioresource Technology*, 101, 5517-5522.

Wasser, S. P. (2002). Medicinal mushrooms as a source of antitumor and immunomodulating polysaccharides. *Applied Microbiology and Biotechnology*, 60, 258-274.

Wasser, S. P. (2010). Medicinal mushroom science, history, current status, future trends, and unsolved problems. *International Journal of Medicinal Mushrooms*, 12, 1-16.

Xia, E.Q., Ai, X.X., Zang, S.Y., Guan, T.T., Xu, X.R., Li, H.B., (2011). Ultrasound-assisted extraction of phillyrin from *Forsythia suspense*. *Ultrasonics Sonochemistry*, 18, 549-552.

Xing, R. E., Liu, S., Guo, Z. Y., Yu, H. H., Wang, P. B., Li, C. P., Li, Z., & Li, P. C. (2005). Relevance of molecular weight of chitosan and its derivatives and their antioxidant activities in vitro. *Bioorganic & Medicinal Chemistry*, 13, 1573-1577.

Yachmenev, V., Condon, B., Klasson, T., Lambert, A. (2009). Acceleration of the enzymatic hydrolysis of corn stover and sugar cane bagasse celluloses by low intensity uniform ultrasound. *Journal of Biobased Materials and Bioenergy*, 3, 25–31.

Yan, J. K., Li, L., Wang Z. M., Leung, P. H., Wang, W. Q., Wu, J. Y. (2009). Acidic degradation and enhanced antioxidant activities of exopolysaccharides from Cordyceps sinensis mycelial culture. *Food Chemistry*, 117, 641-646.

Yan, J. K., Li, L., Wang Z. M., Wu, J. Y. (2010). Structural elucidation of an exopolysaccharide from mycelial fermentation of a *Tolypocladium* sp. Fungus isolated from wild *Cordyceps sinensis*. *Carbohydrate Polymers*, 79, 125-130.

Yan, J. K., Wang, W. Q., Li, L., Wu, J. Y. (2011). Physiochemical properties and antitumor activities of two α-glucans isolated from hot water and alkaline extracts of Cordyceps (Cs-HK1) fungal mycelia. *Carbohydrate Polymers*, 85, 753-758.

Yang, L., Zhang, L. M. (2009). Chemical structural and chain conformational characterization of some bioactive polysaccharides isolated from natural sources. *Carbohydrate polymers*, 76, 349-361.

Yemm, E. W., Willis, A. J. (1954). The estimation of carbohydrates in plant extracts by Anthrone. *Biochemistry*, 57, 508-514.

Zhang , Y., Li, E., Wang , C., Li, Y., Liu, X. (2012). *Ophiocordyceps sinensis*, the flagship fungus of China: terminology, life strategy and ecology. *Mycology*, 3, 2–10.

Zhang, L., Li, X., Xu, X., Zeng, F. (2005). Correlation between antitumor activity, molecular weight, and conformation of Lentinan. *Carbohydrate Research*, 340, 1515–1521.

Zhang, M., Cui, S. W., Cheung, P. C. K., Wang, Q. (2007). Antitumor polysaccharides from mushrooms: a review on their isolation process, structural characteristics and antitumor

activity. *Trends in Food Science Technology*, 18(1), 4-19.

Zhao, J., Pispas, S., Zhang, G. (2009). Effect of sonication on polymeric aggregates formed by poly(ethylene oxide)-based amphiphilic block copolymers. *Macromolecular Chemistry and Physics*, 210, 1026-1032.

Zhao, L., Zhao, G., Chen, F., Wang, Z., Wu, J., Hu, X. (2006). Different effects of microwave and ultrasound on the stability of (all-E)-Astaxanthin. *Journal of Agricultural and Food Chemistry*, 54, 8346-8351.

Zheng, L., Sun, D.-W. (2006). Innovative applications of power ultrasound during food freezing processes—a review. *Trends in Food Science & Technology*, 17, 16-23.

Zhou, C., Ma, H. (2006). Ultrasonic Degradation of Polysaccharide from a Red Algae (*Porphyra yezoensis*), *Journal of Agricultural Food Chemistry*, 54, 2223-2228.

Zhou, X., Gong, Z., Su, Y., Lin, J. Tang, K. (2008). Cordyceps fungi: natural products, pharmacological functions and developmental products. *Journal of Pharmacy and Pharmacology*, 61, 279-291.

Zhou, X., Lin, Q., Dai, G., Ji, F. (1998). Ultrasonic degradation of polysilane polymers. *Polymer Degradation and Stability*, 60, 409-413.

Zhu, J. S., Halpern, G. M., Jones, K. (1998). The scientific rediscovery of an ancient Chinese herbal medicine: *Cordyceps sinensis. Journal of Alternative and Complementary Medicine*, 4, 289-303 (I); 429-457 (II).

Zhuang, C., Mizuno, T., I., H., Shimura, K., Sumiya, T., Kawade, M. (1994). Antitumor activity and immunological property of polysaccharides from the mycelium of liquid-cultured *Grifola frondosa*. *Nippon Shokuhin Kogyo Gakkaishi*, 41, 724-735.

Zhuang, C., Mizuno, T., Shimada, A., Ito, H., Suzuki, C., Mayuzumi, Y., et al. (1993). Antitumor protein-containing polysaccharides from a Chinese mushroom Fengweigu or Houbitake, *Pleurotus sajor-caju* (Fr.) Sing. *Bioscience, Biotechnology, and Biochemistry*, 57, 901-906.